Journal of the Anatomical Society of India

Print ISSN: 0003-2778

GENERAL INFORMATION

About the Journal

Journal of the Anatomical Society of India (ISSN: Print 0003-2778) is peer-reviewed journal. The journal is owned and run by Anatomical Society of India. The journal publishes research articles related to all aspects of Anatomy and allied medical/surgical sciences. Pre-Publication Peer Review and Post-Publication Peer Review Online Manuscript Submission System Selection of articles on the basis of MRS system Eminent academicians across the globe as the Editorial board members Electronic Table of Contents alerts Available in both online and print form. The journal is published quarterly in the months of January, April, July and October.

Scope of the Journal

The aim of the *Journal of the Anatomical Society of India* is to enhance and upgrade the research work in the field of anatomy and allied clinical subjects. It provides an integrative forum for anatomists across the globe to exchange their knowledge and views. It also helps to promote communication among fellow academicians and researchers worldwide. The Journal is devoted to publish recent original research work and recent advances in the field of Anatomical Sciences and allied clinical subjects. It provides an opportunity to academicians to disseminate their knowledge that is directly relevant to all domains of health sciences.

The Editorial Board comprises of academicians across the globe.

JASI is indexed in Scopus, available in Science Direct.

Abstracting and Indexing Information

The journal is registered with the following abstracting partners:

Baidu Scholar, CNKI (China National Knowledge Infrastructure), EBSCO Publishing's Electronic Databases, Ex Libris – Primo Central, Google Scholar, Hinari, Infotrieve, Netherlands ISSN center, ProQuest, TdNet, Wanfang Data

The journal is indexed with, or included in, the following:

SCOPUS, Science Citation Index Expanded, IndMed, MedInd, Scimago Journal Ranking, Emerging Sources Citation Index.

Impact Factor® as reported in the 2018 Journal Citation Reports® (Clarivate Analytics, 2019): 0.168

Information for Authors

Article processing and publication charges will be communicated by the editorial office. All manuscripts must be submitted online at www.journalonweb.com/jasi.

Subscription Information

Copies are sent for free of cost to the members of the Editorial Board. A subscription to JASI comprises 4 issues. Prices include postage. Annual Subscription Rate for non-members-

Rates of Membership (with effect from 1.1.2019)		
	India	**International**
Ordinary membership	INR 1500	US $ 100
Couple membership	INR 2250	
Life membership	INR 8000	US $ 900
Subscription Rates (till 31st August)		
Individual	INR 4500	US $ 600
Library/Institutional Trade discount of 10% for agencies only	INR 10000	US $ 900
Subscription Rates (after 31st August)		
Individual	INR 5000	
Library/Institutional	INR 10500	

The Journal of Anatomical Society of India (ISSN: 0003-2778) is published quarterly **Subscriptions** are accepted on a prepaid basis only and are entered on a calendar year basis. Issues are sent by standard mail Priority rates are available upon request.

Information to Members/Subscribers

All members and existing subscribers of the Anatomical Society of India are requested to send their membership/existing subscription fee for the current year to the Treasurer of the Society on the following address: Prof (Dr.) Punit Manik, Treasurer, ASI, Department of Anatomy, KGMU, Lucknow - 226003. Email: punitamanik@yahoo.co.in. All payments should be made through an account payee bank draft drawn in favor of the **Treasurer, Anatomical Society of India,** payable at **Lucknow** only, preferably for **Allahabad Bank, Medical College Branch, Lucknow.** Outstation cheques/drafts must include INR 70 extra as bank collection charges.

All complaints regarding non-receipt of journal issues should be addressed to the Editor-in-Chief, JASI at editorjasi@gmail.com. The new subscribers may, please contact subscriptions@medknow.com.

Requests of any general information like travel concession forms, venue of next annual conference, etc. should be addressed to the General Secretary of the Anatomical Society of India.

For mode of payment and other details, please visit www.medknow.com/subscribe.asp

Claims for missing issues will be serviced at no charge if received within 60 days of the cover date for domestic subscribers, and 3 months for subscribers outside India. Duplicate copies cannot be sent to replace issues not delivered because of failure to notify publisher of change of address. The journal is published and distributed by Wolters Kluwer India Pvt. Ltd. Copies are sent to subscribers directly from the publisher's address. It is illegal to acquire copies from any other source. If a copy is received for personal use as a member of the association/society, one cannot resale or give-away the copy for commercial or library use.

The copies of the journal to the subscribers are sent by ordinary post. The editorial board, association or publisher will not be responsible for non receipt of copies. If any subscriber wishes to receive the copies by registered post or courier, kindly contact the publisher's office. If a copy returns due to incomplete, incorrect or changed address of a subscriber on two consecutive occasions, the names of such subscribers will be deleted from the mailing list of the journal. Providing complete, correct and up-to-date address is the responsibility of the subscriber.

Nonmembers: Please send change of address information to subscriptions@medknow.com.

Advertising Policies

The journal accepts display and classified advertising. Frequency discounts and special positions are available. Inquiries about advertising should be sent to Wolters Kluwer India Pvt. Ltd, advertise@medknow. com.

The journal reserves the right to reject any advertisement considered unsuitable according to the set policies of the journal.

The appearance of advertising or product information in the various sections in the journal does not constitute an endorsement or approval by the journal and/or its publisher of the quality or value of the said product or of claims made for it by its manufacturer.

Addresses

Editorial Office

Dr. Vishram Singh, Editor-in-Chief, JASI
OC-5/103, 1st floor, Orange County Society,
Ahinsa Khand-I, Indirapuram, Ghaziabad,
Delhi, NCR- 201014.
Email: editorjasi@gmail.com

Published by

Wolters Kluwer India Pvt. Ltd
A-202, 2nd Floor, The Qube,
C.T.S. No.1498A/2 Village Marol, Andheri (East),
Mumbai - 400 059, India.
Phone: 91-22-66491818
Website: www.medknow.com

Printed at

Dhote Offset Tech. P. Ltd
Goregaon (E), Mumbai, India

Journal of the Anatomical Society of India

Print ISSN: 0003-2778

EDITORIAL BOARD

Journal of the Anatomical Society of India

Print ISSN: 0003-2778

EXECUTIVE COMMITTEE

Journal of the Anatomical Society of India

Volume 69 | Issue 1 | January-March 2020

CONTENTS

Journal of the Anatomical Society of India on Web

http://www.journalonweb.com/jasi

The Journal of the Anatomical Society of India now accepts articles electronically. It is easy, convenient and fast. Check following steps:

1 Registration

- Register from http://www.journalonweb.com/jasi as a new author (Signup as author)
- Two-step self-explanatory process

2 New article submission

- Read instructions on the journal website or download the same from manuscript management site
- Prepare your files (Article file, First page file and Images, Copyright form & Other forms, if any)
- Login as an author
- Click on 'Submit new article' under 'Submissions'
- Follow the steps (guidelines provided while submitting the article)
- On successful submission you will receive an acknowledgement quoting the manuscript ID

3 Tracking the progress

- Login as an author
- The report on the main page gives status of the articles and its due date to move to next phase
- More details can be obtained by clicking on the ManuscriptID
- Comments sent by the editor and reviewer will be available from these pages

4 Submitting a revised article

- Login as an author
- On the main page click on 'Articles for Revision'
- Click on the link "Click here to revise your article" against the required manuscript ID
- Follow the steps (guidelines provided while revising the article)
- Include the reviewers' comments along with the point to point clarifications at the beginning of the revised article file.
- Do not include authors' name in the article file.
- Upload the revised article file against New Article File - Browse, choose your file and then click "Upload" OR Click "Finish"
- On completion of revision process you will be able to check the latest file uploaded from Article Cycle (In Review Articles-> Click on manuscript id -> Latest file will have a number with 'R', for example XXXX_100_15R3.docx)

Facilities

- Submission of new articles with images
- Submission of revised articles
- Checking of proofs
- Track the progress of article until published

Advantages

- Any-time, any-where access
- Faster review
- Cost saving on postage
- No need for hard-copy submission
- Ability to track the progress
- Ease of contacting the journal

Requirements for usage

- Computer and internet connection
- Web-browser (Latest versions - IE, Chrome, Safari, FireFox, Opera)
- Cookies and javascript to be enabled in web-browser

Online submission checklist

- First Page File (rtf/doc/docx file) with title page, covering letter, acknowledgement, etc.
- Article File (rtf/doc/docx file) - text of the article, beginning from Title, Abstract till References (including tables). File size limit 4 MB. Do not include images in this file.
- Images (jpg/jpeg/png/gif/tif/tiff): Submit good quality colour images. Each image should be less than 10 MB) in size
- Upload copyright form in .doc / .docx / .pdf / .jpg / .png / .gif format, duly signed by all authors, during the time mentioned in the instructions.

Help

- Check Frequently Asked Questions (FAQs) on the site
- In case of any difficulty contact the editor

Original Article

A Pilot Study of MicroRNA Expression Profiles of the Spinal Neuron in Matrix Metalloproteinase-9 Knockout Mice

Jianpeng Li[1,2,*], Bin Jiang[1,2,*], Yidan Zhang[1], Ran Yao[3], Shijie Duan[3], Yikang Wang[3], Suijun Tong[1,2], Min Bi[1,2]

[1]Department of Neurology, The First Affiliated Hospital of Xiamen University, [3]Medical College of Xiamen University, Xiamen, [2]The First Clinical Medical College of Fujian Medical University, Fuzhou, Fujian, China

**These contributed equally to this manuscript*

Abstract

Introduction: Matrix metalloproteinase-9 (MMP9) plays a key role in blood–spinal cord barrier dysfunction. MMP9 blockade leads to improved injured locomotor recovery. However, it is still unknown whether MMP9 deficiency affects gene expression or signal transduction pathways in the spinal neuron. **Material and Methods:** In this study, we first screen the MMP9 knockdown mice with high superoxide dismutase (SOD) expression and low MMP9 expression by polymerase chain reaction analysis. Then, the gene microarrays were used to screen differentially expressed genes in the spinal neuron from MMP-9 knockout and wild-type mice. There were six groups in this experiment, including three negative control groups: SOD_1, SOD_2, and SOD_3, and three experiment groups: SOD_ MMP9_1, SOD_ MMP9_2, and SOD_ MMP9_3. The gene ontology terms were used to predict the potential functions of these differentially expressed genes, and the Kyoto Encyclopedia of Genes and Genomes was used to analyze the potential functions of these target genes in the pathways. **Results:** We found that the gene expression in the spinal neuron from MMP9 knockout mice was significantly altered compared to wild-type mice. FoxO signaling, axon guidance, ubiquitin-mediated proteolysis, regulation of actin cytoskeleton, and proteoglycans were changed. **Discussion and Conclusion:** In summary, MMP9 plays a role in spinal neuron signaling and the underlying mechanism may through affecting several signaling pathways.

Keywords: *Matrix metalloproteinase-9, microarray analysis, differentially expressed genes, spinal neuron*

Introduction

With an increasing number of traffic accidents, spinal cord injury becomes a serious common clinical disease with high morbidity. The tight junctions of capillaries, basement membrane, and blood-brain barrier were then destructed by matrix metalloproteinase-9 (MMP9).[1] After that, the vasogenic edema in the central nervous system is appearing. Under normal circumstances, MMP9 is expressed in microglia, astrocytes, and hippocampal neurons at a low constitutive level. Moreover, it can be induced in astrocytes, microglia/macrophages, and hippocampal cells in the central nervous system.[2-5] However, MMP9 increased rapidly in both inflammatory cells and endothelial cells after the spinal cord injury and reached a maximum at 24 h. It may be associated with the abnormal vascular permeability caused by hemorrhagic injury or inflammation.[6,7] In the past few years, MMP9 was confirmed to play a key role in blood–spinal cord barrier dysfunction.[8] MMP9 blockade leads to improved injured locomotor recovery. The above studies provided insight concerning the effect of MMP9 in the spinal neuron. In this study, to detect the effect of MMP9 on gene expression and signal transduction pathways in the spinal neuron, we chose the mice model with MMP9 knockdown. We first screen the MMP9 knockdown mice in the offspring. The polymerase chain reaction (PCR) analysis was performed on the tail genomic DNA, and the mice with high superoxide dismutase (SOD) expression and low MMP9 expression was chosen as the experiment groups. To identify whether gene expression would be affected by MMP9 deletion, in this study, we used spinal neurons from MMP9 knockout and wild-type mice, screened for differentially expressed genes using microarrays. The gene ontology (GO) terms were used to predict the potential functions of these differentially expressed genes and

How to cite this article: Li J, Jiang B, Zhang Y, Yao R, Duan S, Wang Y, *et al.* A pilot study of microRNA expression profiles of the spinal neuron in matrix metalloproteinase-9 knockout mice. J Anat Soc India 2020;69:1-8.

Article Info

Received: 14 June 2019
Accepted: 16 January 2020
Available online: 11 April 2020

Address for correspondence:
Dr. Suijun Tong,
Department of Neurology, The First Affiliated Hospital of Xiamen University, 55 Zhenhai Road, Xiamen, 361003 Fujian, China.
The First Clinical Medical College of Fujian Medical University, 20 Chazhong Road, Fuzhou, 350005 Fujian, China.
E-mail: suijuntongSJT@163.com
Dr. Min Bi,
Department of Neurology, The First Affiliated Hospital of Xiamen University, 55 Zhenhai Road, Xiamen, 361003 Fujian, China.
The First Clinical Medical College of Fujian Medical University, 20 Chazhong Road, Fuzhou, 350005 Fujian, China.
E-mail: c15010712956@163.com

Access this article online

Website: www.jasi.org.in
DOI: 10.4103/JASI.JASI_76_19
Quick Response Code:

the Kyoto Encyclopedia of Genes and Genomes (KEGG) was used to analyze the potential functions of these target genes in the pathways. Our results showed that the gene expression in the spinal neuron from MMP9 knockout mice was significantly altered and we predicted that MMP9 plays an important role through affecting several signaling pathways, including FoxO signaling, axon guidance, ubiquitin-mediated proteolysis, regulation of actin cytoskeleton, and proteoglycans.

Materials and Methods

Ethics approval and informed consent

All animals were obtained from The First Affiliated Hospital of Xiamen University (Fujian, China)

Preparation of EGE-LZX-010 knockout mice

EGE-LZX-010 gene is located on the positive strand of chromosome 2, with a total length of about 15.1 KB (NCBI ID: 17395). EGE-LZX-010 knockout mice were prepared using CRISPR/Cas9 (Beijing Biocytogen Co., Ltd). By analyzing the structure of the EGE-LZX-010 gene, two sgRNAs were used to knock out exon1–12 of ege-lzx-010 genes. To ensure the efficiency of the designed Cas9/sgRNA, the target sequences of C57BL/6 mouse tails were amplified by PCR and verified by sequencing, and the primers are shown in Figure 1a. Based on the design principle of sgRNA, a total of 14 sgRNA were designed, and the corresponding oligo sequences are shown in Figure 1b, and then the Cas9/sgRNA plasmid was constructed, meanwhile, the activity of sgRNA was detected by-UCA™. Finally, Cas9-sgRNA was injected embryos to construct the EGE-LZX-010 knockout mice. The injected embryos then developed into F0 generation mice, and the genotype of F0 generation mice was measured by PCR, the primers are shown in Figure 1c. F0 generation positive mice were mated with wild type to obtain F1 generation mice with stable genotype, and the genotype of F1 generation mice was also measured by PCR.

Sampling and DNA purification

Mouse genotypes were verified throughout the study by PCR performed on tail genomic DNA. First, 0.5–1 cm tissue from the tail of mice of each group was ground into powder using liquid nitrogen. The DNA was extracted from each sample using DNA extraction Kit (Generay, GK0121) according to the manufacturer's instructions. The concentration of DNA was determined by measuring the absorbance of each sample at A260/280 using Merinton SMA4000. The DNA with the ratio of A260/A280 between 1.8 and 2.2 was kept for the following the PCR analysis. Extracted DNA was stored in a freezer at 4°C or 20°C.

Polymerase chain reaction procedures

Two pairs of oligonucleotide primers were used to perform the PCR procedures: EGE-LZX-010-5, MSD-F: 5'TGGGGGTCCTGCCTGACTTG3', EGE-LZX-010-3, MSD-R: 5'CAGTCAGAACCTCTGCCCTCCTC3', SOD-F: 5' CAGTCAGAACCTCTGCCCTCCTC 3' and SOD-R: 5' CGC GAC TAA CAA TCA AAG TGA 3'. PCR were performed in a 96-well using a GeneAmp PCR kit (Applied Biosystems, Foster City. CA) in a -25 µL total reaction volumes containing 2.5 µL of PCR buffer 10X (50 mM KCl, 10 mM Tris-HCl [pH = 8.3], 0.1% Triton X-100), 1.0 µL genomic DNA, 1 µL of each primer, 2 µL dNTPs, and 0.5 µL (10U/µL) of Taq DNA polymerase (TaKaRa). GeneAmp PCR System 9700 was used to analyze the result.

a

Primer	Sequence (5'-3')	Product size (bp)	Tm(℃)
EGE-LZX-010-5'MSD-F	TGGGGGTCCTGCCTGACTTG	573	64
EGE-LZX-010-5'MSD-R	ACCCTTCGAAGCCGAACCCA		64
EGE-LZX-010-3'MSD-F	CTAGCGCCACTCTCCCGCAG	731	65
EGE-LZX-010-3'MSD-R	CAGTCAGAACCTCTGCCCTCCTC		64

b

5'Guide	score	sequence (5'-3')
Guide #1	92	CCACAAAAGTCGGCTGGCGC TGG
Guide #2	91	AAAGTCGGCTGGCGCTGGTA AGG
Guide #3	87	GGAAGACCACAAAAGTCGGC TGG
Guide #4	75	CTGCCAGCTGGGTGTCCGTG AGG
Guide #5	73	CGGTCCTCACCATGAGTCCC TGG
Guide #6	72	ATGGTGAGGACCGCAGCTTC TGG
Guide #7	69	CAGAGCTGCAGCCGAAAGCC AGG

5'Guide	score	sequence (5'-3')
Guide #8	90	GGACTCCCTCTCTTAGCGAC TGG
Guide #9	89	ATGCAAGCAATCCGGACCTT AGG
Guide #10	89	AGCAATCCGGACCTTAGGTC CGG
Guide #11	86	AACTAGCCAGTCGCTAAGAG AGG
Guide #12	85	GTTCACACAGCCCGGACCTA AGG
Guide #13	83	CACAGCCCGGACCTAAGGTC CGG
Guide #14	78	GCGTTCTCTACTGGAGTTCC CGG

c

Primer	Sequence (5'-3')	Tm (℃)	Product size (bp)
EGE-LZX-010-5'MSD-F	TGGGGGTCCTGCCTGACTTG	64	WT:573
EGE-LZX-010-5'MSD-R	ACCCTTCGAAGCCGAACCCA	64	
EGE-LZX-010-5'MSD-F	TGGGGGTCCTGCCTGACTTG	64	WT:6149
EGE-LZX-010-3'MSD-R	CAGTCAGAACCTCTGCCCTCCTC	64	Mut:~600

Figure 1: The sequences of primers in this study. (a) The primers to detect the target sequences. (b) The oligo sequences of 14 sgRNAs. (c) The primers to detect the genotype of mice

Target genes prediction, gene ontology enrichment, and Kyoto Encyclopedia of Genes and Genomes pathway analysis

Differentially expressed microRNAs (miRNAs) were screened with $P < 0.05$, and the potential target genes were predicted using TargetScan and MiRanda online software. The intersection elements of the two software were accepted as candidate target genes of the differential miRNA. The hierarchical clustering (HCL) was performed to determine the normalized expression level of each RNA type. The predicted target genes were input into the GO database (http://www.

geneontology.org/) to execute GO annotation and enrichment analysis from three ontologies: molecular function, cellular component, and biological process. The GO terms were significantly enriched in the predicted target gene candidates of the miRNA compared with the entire gene background. The GO terms with the $P \leq 0.01$ are defined as significantly enriched in the target gene candidates. Furthermore, the KEGG database (http://www.genome.ad.jp/kegg/) was used to analyze the potential functions of these target genes in the pathways. The genes with $P \leq 0.5$ were considered significantly enriched in target gene candidates.

Statistical analysis

The data were presented as the mean ± standard deviation and analyzed by the Student's *t*-test and variance (ANOVA) using SPSS 15.0 software (SPSS, Chicago, IL, USA). $P < 0.05$ was considered statistically significant.

Results

Preparation and identification of EGE-LZX-010 knockout mice

To prepare the EGE-LZX-010 knockout mice by CRISPR/Cas9 (Beijing Biocytogen Co., Ltd), the activities of 14 sgRNA were detected, and the results are shown in Figure 2a. Meanwhile, EGE-LZX-010-sgRNA5 and EGE-LZX-010-sgRNA9 were ligated into the T7 promoter plasmid to obtain microinjected RNA. The microinjected RNAs were identified by PCR assay, and the results are shown in Figure 2b. In addition, the EGE-LZX-010 knockout mice were obtained by injecting Cas9-sgRNA into embryos. The genotype of F0 generation mice was identified by PCR assay, and the results indicated that EX10-1, EX10-4, EX10-6, EX10-7, EX10-12, and EX10-14 were the positive mice [Figure 3a], and then the

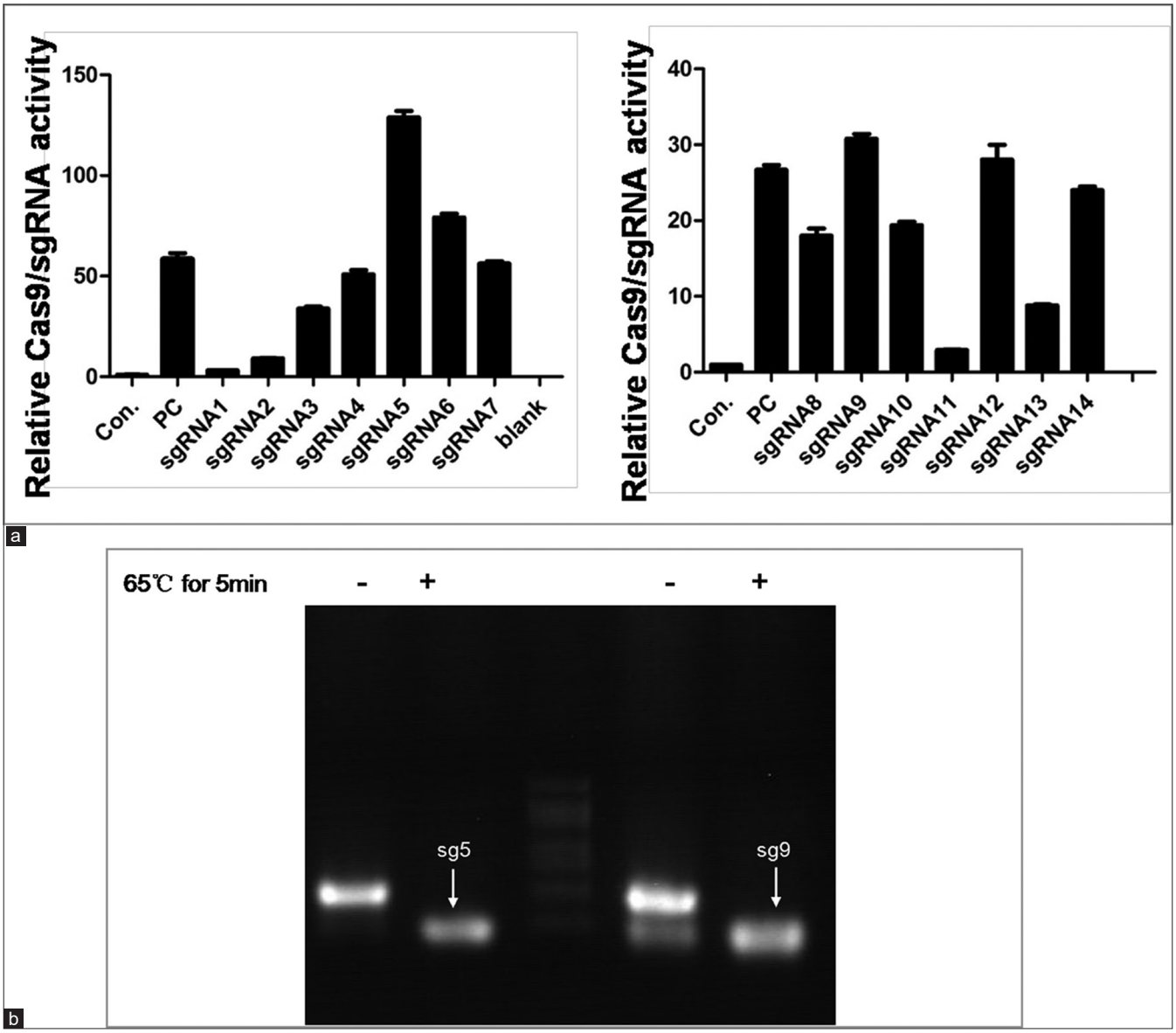

Figure 2: The activity identification of Cas9/sgRNA.(a) Cas9/sgRNA activity was measured by UCA™. (b) The microinjected RNAs were detected by polymerase chain reaction assay

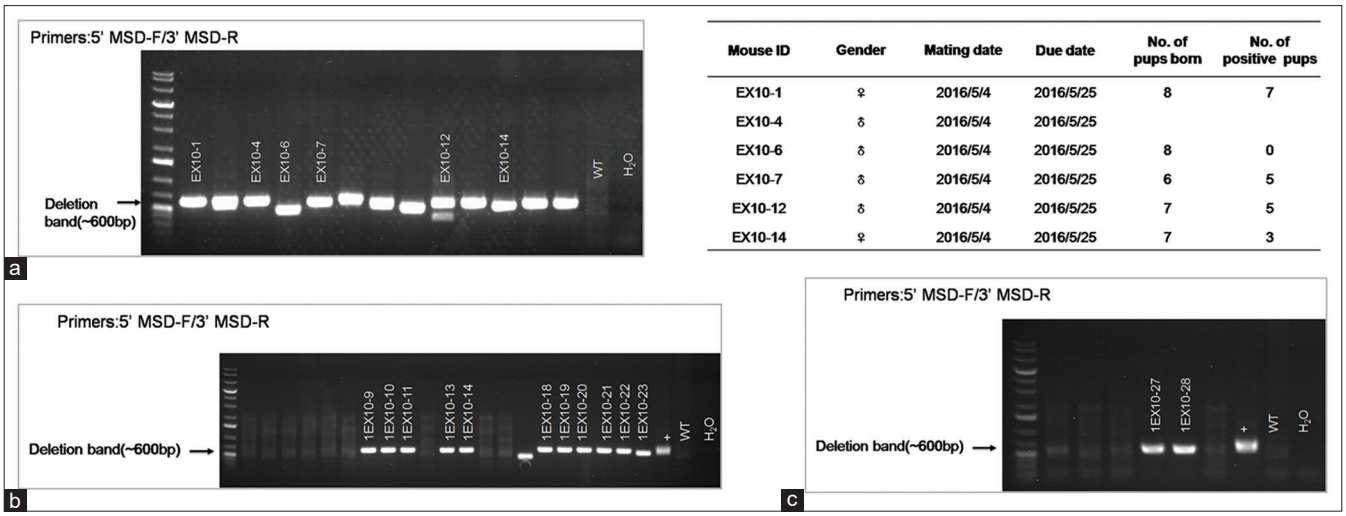

Mouse ID	Gender	Mating date	Due date	No. of pups born	No. of positive pups
EX10-1	♀	2016/5/4	2016/5/25	8	7
EX10-4	♂	2016/5/4	2016/5/25		
EX10-6	♂	2016/5/4	2016/5/25	8	0
EX10-7	♂	2016/5/4	2016/5/25	6	5
EX10-12	♂	2016/5/4	2016/5/25	7	5
EX10-14	♀	2016/5/4	2016/5/25	7	3

Figure 3: Detection of mice genotype. (a) The genotype of F0 generation mice was measured by polymerase chain reaction assay. (b) F0 generation positive mice were mated with wild type. (c) The genotype of F1 generation mice was measured by polymerase chain reaction assay

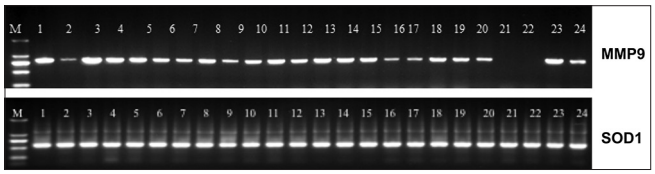

Figure 4: Screening mice with high superoxide dismutase expression and low matrix metalloproteinase-9 expression by polymerase chain reaction analysis. matrix metalloproteinase-9 and superoxide dismutase expressions in the progeny of matrix metalloproteinase-9 knockout mice were assessed by polymerase chain reaction assay with mouse tail genomic DNA and a specific primer pair designed from the matrix metalloproteinase-9 gene sequence (EGE-LZX-010). The polymerase chain reaction products were analyzed by 1.5% agarose gel electrophoresis

F1 generation mice were obtained by F0 generation positive mice mated with wild type [Figure 3b]. The genotype of F1 generation mice were also identified by PCR assay, and the results indicated that1EX10-9, 1EX10-10, 1EX10-11, 1EX10-13, 1EX10-14, 1EX10-18, 1EX10-19, 1EX10-20, 1EX10-21, 1EX10-22, 1EX10-23, 1EX10-27, and 1EX10-28 were positive heterozygous mice [Figure 3c].

Genotype

We detected the gene MMP9 and SOD expression in the progeny of MMP9 knockout mice by PCR performed on tail genomic DNA and screen mice with high SOD expression and low MMP9 expression. Using a primer pair spanning a sequence of MMP9 gene (EGE-LZX-010) that was knocked out in mice, a 236-bp fragment was generated, but the 600bp fragment was not in line 21 and line 22 [Figure 4]. The experiment was repeated six times, and the results were available in supplement Figure 1.

Differentially expressed genes in the spinal neuron of matrix metalloproteinase-9 knockout mice

In the present study, a total of 58,589 genes were annotated and available in supplement Table 1. After preliminary standardized analysis, 3,969 genes were screened

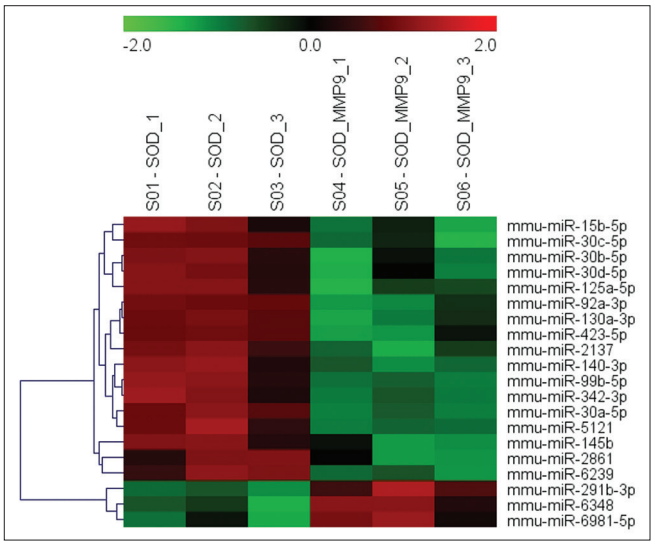

Figure 5: A hierarchical clustering analysis of differentially expressed miRNAs between the superoxide dismutase-expressed mice with and without matrix metalloproteinase-9 knockout. The heat map showed the expression levels of differentially expressed mouse miRNAs. Heat map colors represented the relative miRNA expression levels as indicated in the color key. The different color indicated different miRNA expression levels. Red indicates the high expression of miRNA and green indicates the low expression of miRNA

[Supplement Table 2]. A dendrogram of a hierarchical clustering analysis of differentially expressed miRNAs between the SOD mice with and without MMP9 knockout. The different expression of mouse miRNAs at the probe level was showed in the heat map. The expression profiles of 215 mature miRNAs were assessed using miRNA microarrays in SOD mice in the control groups and MMP9 knockout groups [Supplement Table 3]. Among these, 20 miRNAs were differential expression (17 down-regulated and 3 up-regulated) in the PMM9 knockout group compared to the control group [Figure 5]. Differentially expressed miRNA target gene prediction is listed in Table 1.

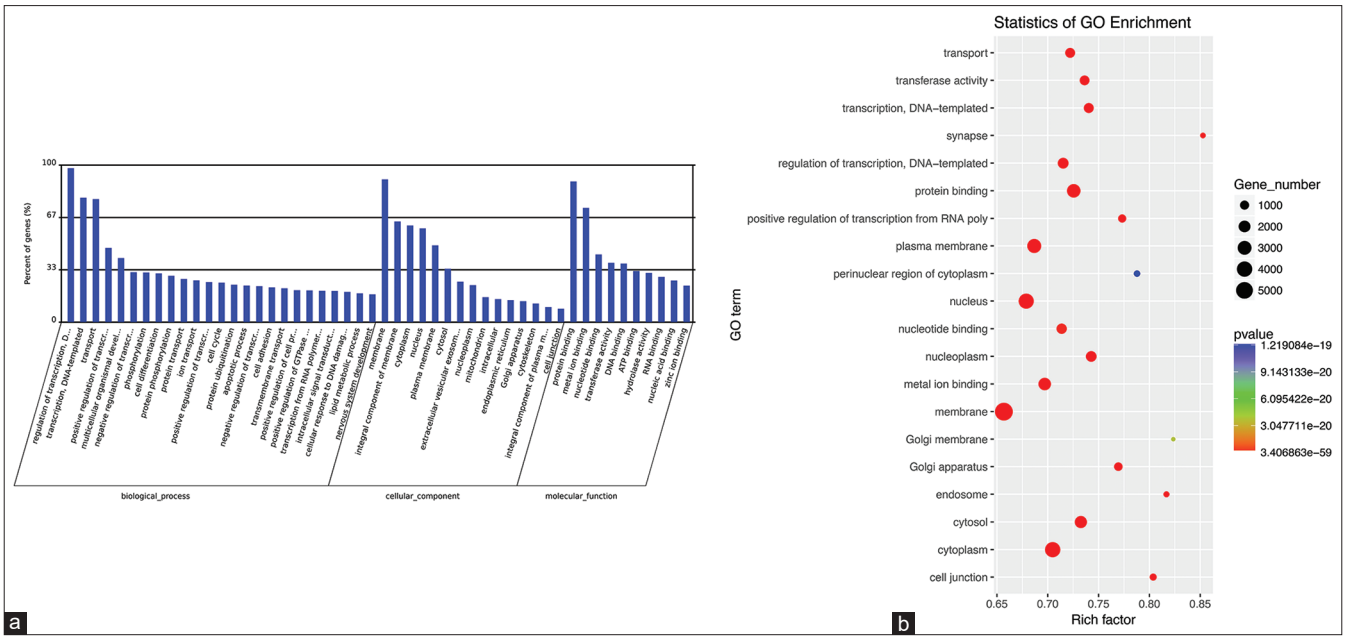

Figure 6: The statistics of gene ontology pathway enrichment. (a) The percent of genes in the gene ontology term was shown in the bar chart of biological processes, cellular components, and molecular functions. (b) Scatterplot of enriched terms showed the statistics of gene ontology enrichment in the spinal neuron of matrix metalloproteinase-9 knockout mice. The circular dots represented the numbers of annotated genes for different gene ontology terms. Different colors represented different levels of significance (*P* value). The rich factor was a ratio of the gene numbers of each term to the numbers of all genes with terms

Table 1: Differentially expressed microRNA target gene prediction (partial, $P \leq 0.05$)

Index	Reporter name	Target sequence (5' to 3')
1	mmu-miR-6239	UAGCGUUGGAUCACUCGGUG
2	mmu-miR-125a-5p	UCCCUGAGACCCUUUAACCUGUGA
3	mmu-miR-99b-5p	CACCCGUAGAACCGACCUUGCG
4	mmu-miR-30a-5p	UGUAAACAUCCUCGACUGGAAG
5	mmu-miR-2137	GCCGGCGGGAGCCCCAGGGAG
6	mmu-miR-92a-3p	UAUUGCACUUGUCCCGGCCUG
7	mmu-miR-6348	UCAGCCUUUAUAAGGUGUGUGU
8	mmu-miR-5121	AGCUUGUGAUGAGACAUCUCC
9	mmu-miR-130a-3p	CAGUGCAAUGUUAAAAGGGCAU
10	mmu-miR-291b-3p	AAAGUGCAUCCAUUUUGUUUGU
11	mmu-miR-140-3p	UACCACAGGGUAGAACCACGG
12	mmu-miR-15b-5p	UAGCAGCACAUCAUGGUUUACA
13	mmu-miR-342-3p	UCUCACACAGAAAUCGCACCCGU
14	mmu-miR-145b	GUCCAGUUUUCCCAGGAGACU
15	mmu-miR-30b-5p	UGUAAACAUCCUACACUCAGCU
16	mmu-miR-30c-5p	UGUAAACAUCCUACACUCUCAGC
17	mmu-miR-2861	GGGGCCUGGCGGCGGGCGG
18	mmu-miR-30d-5p	UGUAAACAUCCCCGACUGGAAG
19	mmu-miR-423-5p	UGAGGGGCAGAGAGCGAGACUUU
20	mmu-miR-6981-5p	GUGAGGAGAAGGAAGAGGCUGAAGGC
21	mmu-miR-7056-5p	UGUGGAGGAGGACAGAGAGGUU

Gene ontology annotations analysis of candidate target genes

To understand more about the roles of differentially expressed miRNAs between SOD and SOD_MMP9 groups mice, the differentially expressed genes were assigned to 565031 GO terms, including biological processes, cellular components, and molecular function terms [Supplement Table 4]. A total of 21754 putative target genes targeted by 13407 differentially expressed miRNAs were selected and submitted to GO enrichment. Among all GO terms, the biggest is GO: 0005737, annotated for 5699 candidate target genes. All candidate target genes

were distributed into 1188 GO terms [Supplement Table 5]. Typical enriched GO terms are shown in Figure 6a. We can see that the most enriched biological process term is "regulation of transcription," "transcription, DNA-templated," and "transport." The most enriched cellular component term is "membrane," "integral component of membrane," and "cytoplasm." The most enriched molecular function term is "protein binding," metal ion binding," and "nucleotide-biding." The statistics of the enriched GO categories for the target genes of differentially expressed miRNAs are shown in Figure 6b. We can see the most of the genes were located in the membrane and nucleus, related to transport, binding activity, transcription, and transferase activity and other biological functions.

Kyoto Encyclopedia of Genes and Genomes pathways analysis of candidate target genes

KEGG database is a collection of various pathways, representing the molecular interactions and reaction networks. To identify signaling pathways involved in the spinal neuron of MMP9 knockdown mice, 42459 differentially expressed genes were submitted to KEGG analysis [Supplement Table 6]. We found that the differentially expressed genes were significantly enriched in 124 KEGG pathways [Supplement Table 7]. The top 20 enriched pathways are shown in Figure 7. Differentially expressed genes were highly clustered in several signaling pathways, such as "FoxO signaling," "Axon guidance,"

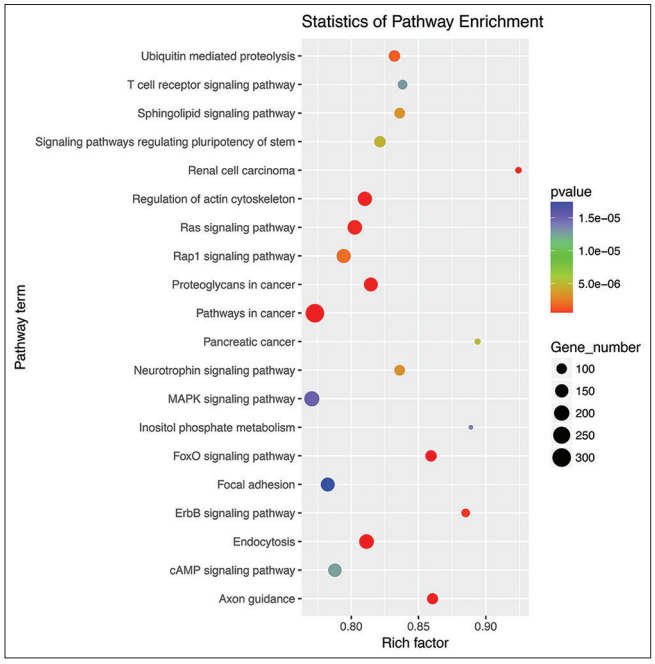

Figure 7: The selected top enriched pathway terms. Scatterplot of enriched Kyoto Encyclopedia of Genes and Genomes pathway showed the top 20 pathways enriched in the spinal neuron of matrix metalloproteinase-9 knockout mice. A rich factor was the ratio of the differentially expressed gene number to the total gene number in a certain pathway. The color and size of the dots represented the range of the *P* value and the number of genes to the indicated pathways, respectively. Top 20 enriched pathways were shown in the figure

"Ubiquitin-mediated proteolysis," "regulation of actin cytoskeleton," and "Proteoglycans in cancer," suggesting that MMP9 may perform its function through these pathways.

Discussion

The neurodegenerative disease is a kind of disease characterized by neuronal loss, neuronal dysfunction, and cell death.[9] For example, most motor neurons die in the progress of amyotrophic lateral sclerosis (ALS). SOD1 is a ubiquitously expressed cytosolic metalloenzyme which is closely related to the progressive motor neuron death and is implicated in inherited ALS.[10] Kaplan *et al.* have confirmed that the increment of SOD1 and reduction of MMP-9 function significantly delayed muscle denervation. Moreover, they suggested that MMP-9 may be a candidate therapeutic target for ALS.[11] In this study, we chose the mice with high SOD expression and low MMP9 expression in the offspring of MMP9 knockdown mice with the PCR analysis. As shown in Figure 1, a 236-bp fragment was generated, but the 600-bp fragment was not in line 21 and line 22.

MMP-9 is expressed normally in neurons, astrocytes, oligodendrocytes, microglial cells,[12-14] whereas MMP-9 can additionally be found in inflammatory cells such as macrophages, lymphocytes, neutrophils, and endothelial cells after a spinal cord injury.[15-18] The MMP-9 activation leads to the degradation of type IV collagenase and destruction of the extracellular matrix. As a result, the increase in microvascular basement membrane permeability, structural changes, blood–brain barrier, or blood-spinal cord barrier damage, edema, and hemorrhage following one by one.[19-21] The study performed by Noble *et al.* showed that MMP-9 played an important role in wound remodeling, cell migration, and neurite outgrowth after spinal cord injury.[13] The significantly upregulated expression of MMP-9 is correlated with the dysfunction in blood–spinal barrier integrity and inflammation. To support the pathogenic role for MMP-9 in SCI, MMP-9 null mice were used to the experiment and the result showed that a marked improvement in functional recovery in MMP9 null mice compared to wild-type controls.[13] The inhibition of MMP 9 activity improves recovery, highlighting the beneficial roles of MMP9 following SCI.[22] However, it is still unknown whether MMP9 deficiency affects gene expression or signal transduction pathways in the spinal neuron.

In the previous years, it has been realized that the expression of individual genes in an organism is the result of a network of regulatory genes. Whether MMP-9 inactivation might lead to changes in the expression of related genes in the spinal neuron has not been detected clearly. Because of the characteristics of broad detection range and accuracy, microarrays have been widely used to identify large numbers of differentially expressed

genes in the organism. Based on the above research, we confirmed that the microarray combined with knockout mice is an effective strategy to research the mechanism of different genes regulation. In the present study, using MMP 9 knockout mice and wild-type mice as a comparison, differentially expressed genes in the spinal neuron between MMP9 knockdown and SOD mice were identified using microarrays.

The GO and KEGG analyses were used to analyze the potential functions of these target genes in the pathways. It was found that altered expressions of genes included physiological functions such as ion transport, regulation of transcription, as well as those that regulate corresponding signal transduction pathways, such as different signaling pathways, pathways in cancers, biological, and cellular processes. In the previous studies, we know that as a kind of NF-KB-regulated gene, MMPs are closely associated with tumor invasion.[23,24] The study performed by Forsyth *et al.* showed that the MMP9 level was closely related to the increase of tumor progression in gliomas and was known as key enzymes for invasion.[25] In addition, Lakka *et al.* suggested that MMP-9 was also expressed when tumor cells migrate.[26] The data from the present study indicated that when MMP-9 is lost, global gene expression and protein function within the spinal neuron are affected.

Conclusion

The downregulation of MMP9 affected several signaling pathways in spinal neuron signaling, including FoxO signaling, axon guidance, ubiquitin-mediated proteolysis, regulation of actin cytoskeleton, and proteoglycans and these pathways may be underlying mechanism for MMP9 to function in the spinal neuron signaling.

Financial support and sponsorship

This work was financially supported by The Natural Science Foundation of Fujian Province of China (Grant Number: 2015J01547) and the Young and Middle-Aged Key Personnel Training Project of Fujian Province Health System of China (grant number: 2015-ZQN-JC-41).

Supplemental data

Available on: "link"

Conflicts of interest

There are no conflicts of interest.

References

1. Jang JW, Lee JK, Kim SH. Activation of matrix metalloproteinases-9 after photothrombotic spinal cord injury model in rats. J Korean Neurosurg Soc 2011;50:288-92.
2. Backstrom JR, Lim GP, Cullen MJ, Tökés ZA. Matrix metalloproteinase-9 (MMP-9) is synthesized in neurons of the human hippocampus and is capable of degrading the amyloid-beta peptide (1-40). J Neurosci 1996;16:7910-9.
3. Cuzner ML, Gveric D, Strand C, Loughlin AJ, Paemen L, Opdenakker G, *et al*. The expression of tissue-type plasminogen activator, matrix metalloproteases and endogenous inhibitors in the central nervous system in multiple sclerosis: Comparison of stages in lesion evolution. J Neuropathol Exp Neurol 1996;55:1194-204.
4. Liu Z, Shipley JM, Vu TH, Zhou X, Diaz LA, Werb Z, *et al*. Gelatinase B-deficient mice are resistant to experimental bullous pemphigoid. J Exp Med 1998;188:475-82.
5. Yong VW, Power C, Forsyth P, Edwards DR. Metalloproteinases in biology and pathology of the nervous system. Nat Rev Neurosci 2001;2:502-11.
6. Mun-Bryce S, Rosenberg GA. Gelatinase B modulates selective opening of the blood-brain barrier during inflammation. Am J Physiol 1998;274:R1203-11.
7. Rosenberg GA, Dencoff JE, McGuire PG, Liotta LA, Stetler-Stevenson WG. Injury-induced 92-kilodalton gelatinase and urokinase expression in rat brain. Lab Invest 1994;71:417-22.
8. Agrawal SM, Lau L, Yong VW. MMPs in the central nervous system: Where the good guys go bad. Semin Cell Dev Biol 2008;19:42-51.
9. Saxena S, Caroni P. Selective neuronal vulnerability in neurodegenerative diseases: From stressor thresholds to degeneration. Neuron 2011;71:35-48.
10. Turner BJ, Talbot K. Transgenics, toxicity and therapeutics in rodent models of mutant SOD1-mediated familial ALS. Prog Neurobiol 2008;85:94-134.
11. Kaplan A, Spiller KJ, Towne C, Kanning KC, Choe GT, Geber A, *et al*. Neuronal matrix metalloproteinase-9 is a determinant of selective neurodegeneration. Neuron 2014;81:333-48.
12. Lee SR, Tsuji K, Lee SR, Lo EH. Role of matrix metalloproteinases in delayed neuronal damage after transient global cerebral ischemia. J Neurosci 2004;24:671-8.
13. Noble LJ, Donovan F, Igarashi T, Goussev S, Werb Z. Matrix metalloproteinases limit functional recovery after spinal cord injury by modulation of early vascular events. J Neurosci 2002;22:7526-35.
14. Planas AM, Solé S, Justicia C. Expression and activation of matrix metalloproteinase-2 and -9 in rat brain after transient focal cerebral ischemia. Neurobiol Dis 2001;8:834-46.
15. Hibbs MS, Hoidal JR, Kang AH. Expression of a metalloproteinase that degrades native type V collagen and denatured collagens by cultured human alveolar macrophages. J Clin Invest 1987;80:1644-50.
16. Mainardi CL, Hibbs MS, Hasty KA, Seyer JM. Purification of a type V collagen degrading metalloproteinase from rabbit alveolar macrophages. Coll Relat Res 1984;4:479-92.
17. Murphy G, Ward R, Hembry RM, Reynolds JJ, Kühn K, Tryggvason K. Characterization of gelatinase from pig polymorphonuclear leucocytes. A metalloproteinase resembling tumour type IV collagenase. Biochem J 1989;258:463-72.
18. Wilhelm SM, Collier IE, Marmer BL, Eisen AZ, Grant GA, Goldberg GI. SV40-transformed human lung fibroblasts secrete a 92-kDa type IV collagenase which is identical to that secreted by normal human macrophages. J Biol Chem 1989;264:17213-21.
19. Winkler EA, Sengillo JD, Bell RD, Wang J, Zlokovic BV. Blood-spinal cord barrier pericyte reductions contribute to increased capillary permeability. J Cereb Blood Flow Metab 2012;32:1841-52.
20. Allen EA, Erhardt EB, Calhoun VD. Data visualization in the neurosciences: Overcoming the curse of dimensionality. Neuron 2012;74:603-8.
21. Hasturk A, Atalay B, Calisaneller T, Ozdemir O, Oruckaptan H, Altinors N. Analysis of serum pro-inflammatory cytokine levels after rat spinal cord ischemia/reperfusion injury and correlation

with tissue damage. Turk Neurosurg 2009;19:353-9.

22. Duchossoy Y, Horvat JC, Stettler O. MMP-related gelatinase activity is strongly induced in scar tissue of injured adult spinal cord and forms pathways for ingrowing neurites. Mol Cell Neurosci 2001;17:945-56.
23. Wu JT, Kral JG. The NF-kappaB/IkappaB signaling system: A molecular target in breast cancer therapy. J Surg Res 2005;123:158-69.
24. Rao JS. Molecular mechanisms of glioma invasiveness: The role of proteases. Nat Rev Cancer 2003;3:489-501.
25. Forsyth PA, Wong H, Laing TD, Rewcastle NB, Morris DG, Muzik H, *et al*. Gelatinase-A (MMP-2), gelatinase-B (MMP-9) and membrane type matrix metalloproteinase-1 (MT1-MMP) are involved in different aspects of the pathophysiology of malignant gliomas. Br J Cancer 1999;79:1828-35.
26. Lakka SS, Rajan M, Gondi C, Yanamandra N, Chandrasekar N, Jasti SL, *et al*. Adenovirus-mediated expression of antisense MMP-9 in glioma cells inhibits tumor growth and invasion. Oncogene 2002;21:8011-9.

Original Article

The Magnetic Resonance Imaging Evaluation of Morphometry of the Distal Femur and Proximal Tibia on Adult Anatolian Population

Abstract

Introduction: It is widely known that the production of knee prostheses is based on the morphometric parameters of the distal femur and proximal tibia. Although there have been studies on this subject in different populations in the literature, such a study has not been found in the Turkish population. It is aimed to establish an index and also compare it with previous results of different populations, in this study. **Material and Methods:** This study was conducted on 200 patients (78 females, 122 males) aged between 18 and 65 years who had magnetic resonance imaging retrospectively. People with previous fractures, dislocations or ruptures, tears, or tensions in the anterior cruciate ligament, history of knee surgery, and trauma were excluded from the study. Various measurements were conducted on images of the distal femur and proximal tibia morphometry. **Results:** Mean values of the measurements made on the distal femur and proximal tibia were calculated, it was determined that all parameters were higher in males than females. A statistically significant difference was found between the sexes in all the parameters evaluated except for the intercondylar notch height parameter ($P < 0.05$). According to the results of our study, the mean intercondylar notch width index (NWI) and intercondylar notch shape index (NSI) in the total population were calculated as 0.88 ± 0.18. There was no statistically significant difference between male and female values for NWI and NSI ($P > 0.05$). **Discussion and Conclusion:** In this study, finally, intercondylar notch classification was done. According to this, in 46.5% of cases, notch type, which defined as type A and 53.5% of the notches were identified as U type. None of the cases was classified as W type. Studies in which normal morphometric data are presented due to differences in races between skeletal structures have crucial importance. Therefore, the data obtained from our study are thought to be useful to produce specific knee prostheses.

Keywords: *Distal femur, intercondylar notch width index, knee morphometry, knee radiology, proximal tibia*

Paria Shojaolsadati, Neslihan Yüzbasioglu[1], Asrin Nalbant[2], Tugrul Ormeci[3], Soner Albay[4], Alpen Ortug[1], Bayram Ufuk Sakul[1]

Department of Anatomy, School of Medicine, Okan University, Departments of [1]Anatomy and [3]Radiology, School of Medicine, Istanbul Medipol University, Istanbul, [2]Department of Anatomy, School of Medicine, Bakircay University, Izmir, [4]Department of Anatomy, School of Medicine, Suleyman Demirel University, Isparta, Turkey

Introduction

The anatomic components forming the knee joint include the distal femur and the proximal tibia. Previous anthropometric studies were present in the literature for both on the distal femur and proximal tibia.[1-4]

For those patients for whom total knee arthroplasty (TKA) is planned, it is extremely important to ensure size matching of the components belonging to the distal femur and the proximal tibia to maximize the bony structure and the load transmission in the proximal tibia.[5,6] Ensuring this match during TKA will extend implant stability and life. During a TKA performance, a too small tibial component might lead to loosening due to an early relocation in the orthesis because of insufficient support by the distal bony compartment after resection.[7] Moreover in the case of a too large tibial component, soft-tissue irritation and pain might occur when the orthesis used protrudes over the distal bony compartment after resection. Studies about the distal femur also report that anatomic structures might be variable and that such variations might lead to certain pathologies.[8]

It is emphasized in recent anthropometric studies that the components involved in the formation of knee vary depending on races and that, therefore, the orthoses used in arthroplasty should be produced in consideration of racial differences.[9]

The systematic review study conducted in 2017 compares all the English articles in the literature, revealing results about the

How to cite this article: Shojaolsadati P, Yüzbasioglu N, Nalbant A, Ormeci T, Albay S, Ortug A, *et al.* The magnetic resonance imaging evaluation of morphometry of the distal femur and proximal tibia on adult anatolian population. J Anat Soc India 2020;69:9-14.

Article Info

Received: 15 July 2019
Accepted: 06 February 2020
Available online: 11 April 2020

Address for correspondence:
Dr. Alpen Ortug,
Department of Anatomy, School of Medicine, Istanbul Medipol University, Istanbul, Turkey.
E-mail: aortug@medipol.edu.tr

Access this article online

Website: www.jasi.org.in
DOI: 10.4103/JASI.JASI_93_19
Quick Response Code:

distal femur and proximal tibia. Accordingly, available information includes only white, Eastern Asian nations and Indians. There is still nocomparative index of the Middle Eastern and African populations.[10] The current study was planned because of a lack of morphometric data regarding the Turkish population that could be used for making prostheses for people of this region.

Magnetic resonance imaging (MRI) is noninvasive method that was utilized in previous studies for making such measurements and which enables distinguishing compartment boundaries in the clearest way possible and carrying out reliable measurements. For this reason, in our study as well, the measurements relating to the proximal tibia and the distal femur were made by MRI images retrospectively.

Material and Methods

Study group

The approval of this study was obtained before the commencement of work from the Non-Interventional Ethics Committee of Istanbul Medipol University. Two hundred Turkish patients were included in the study between 2016 and 2017 (122 males, 78 females; mean age: 35.37 ± 9.82) at Istanbul Medipol University Hospital Radiology Department. MRIs registered in picture archiving and communication systems (PACS) used for measurement and studied retrospectively. Those who had previous knee joint surgeries or had a knee trauma, fracture, dislocation, or a ruptured or torn anterior cruciate ligament (ACL) of any sprained ligament (sprain II and above) were not included in the study.

Imaging

The MRI was performed with the patient in the supine position and the knee in a relaxed position at a 5-degree external rotation by 3T (TR3029, TE 30) and 4-mm slice thickness. For image analysis, the archiving and measurement program PACS was utilized.

Measurements in each patient was based on two images; different longitudinal and angular parameters were measured on two different MRI sections including the section, in which the biepicondylar distance is visible in the widest aspect in the distal femur (first plane), and the section, in which the two condyles in the proximal tibia region are visible in the widest aspect (second plane). For standardization, the measurements were carried out by a single person by three repetitions, which were then averaged.

The parameters measured in the distal femur:

- Intercondylar notch height (NH); the longest vertical distance drawn between the postcondylar line and the notch on the first plane
- Intercondylar notch width (NW); the widest transverse distance of the notch on the first plane
- $\text{Femoral notch shape index (NSI)} = \dfrac{\text{notch width (NW)}}{\text{notch height (NH)}}$
- femoral mediolateral line (FML); longest line connecting the medial and the lateral dimensions of the distal femur on the first plane
- femoral medial condyle anteroposterior length (FMAP); the longest FMAP length on the first plane
- femoral lateral condyle anteroposterior length (FLAP); the longest FLAP length on the first plane
- Trochlear groove angle (TGA)
- The shape of femoral notch was classified as type A, type U and type W[1,11][Figure 1].

The parameters measured in the proximal tibia:

- Tibial mediolateral length (TML); the widest distance (or the widest transverse distance) of the bicondylar tibia in the axial MRI (second plane), the widest mediolateral diameter according to some references
- Tibial medial anteroposterior line (TMAP); the longest tibial medial condyle anteroposterior length on the second plane
- Tibial lateral condyle anteroposterior line (TLAP) [Figure 2]; the longest TLAP length on the second plane.

Statistics

The SPSS Version 17.0 for Windows; SPSS Inc, Chicago, Illinois, USA) was used for the analyses of all data. The Independent Student's *t*-test and Pearson's correlation test were performed for the analysis. Those with a value of $P < 0.05$ were considered to be statistically significant.

Results

The mean and standard deviation values of the parameters

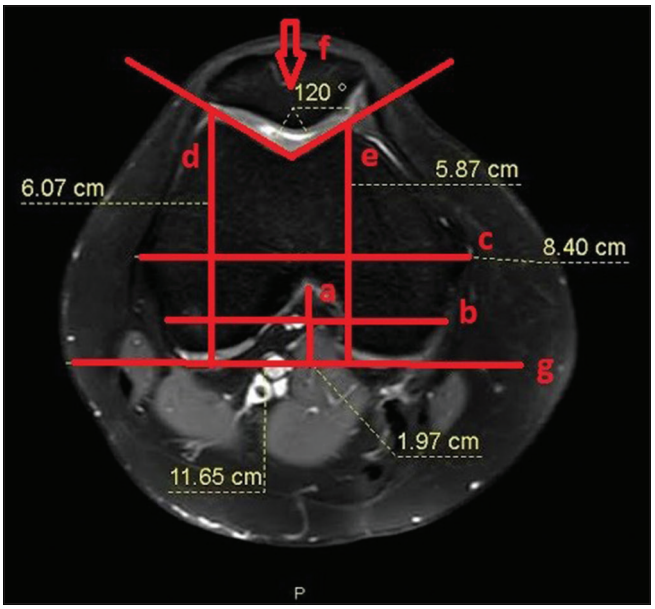

Figure 1: Axial magnetic resonance image of distal femur. a: NH, b: NW, c: FML, d: FLAP, e: FMAP, f: TGA, g: Reference line

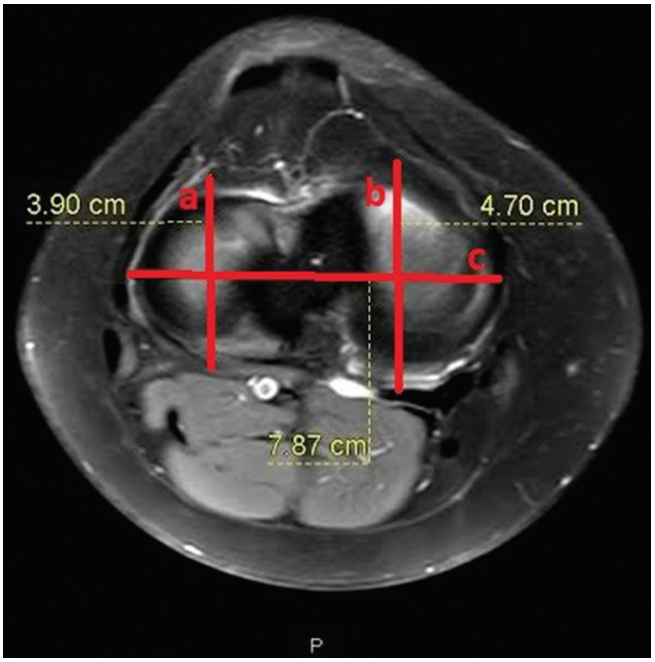

Figure 2: Axial magnetic resonance image of proximal tibia. a: TLAP, b: TMAP, c: TML

Table 1: Mean values and standard deviations of the measured parameters (mm)

	Mean±SD		
	Gender		Total
	Male (*n*=122)	Female (*n*=78)	
NH	2.30±0.37*	2.31±0.37*	2.30±0.37
NW	1.99±0.26	1.72±0.27	1.88±0.30
NSI	0.88±0.18	0.76±0.16	0.84±0.18
FML	8.58±0.51	7.60±0.52	8.20±0.70
FMAP	6.28±0.54	5.80±0.64	6.10±0.62
FLAP	5.88±0.46	5.45±0.47	5.71±0.51
TGA	130.31±5.33	128.56±5.08	129.63±5.29
TML	8.10±0.62	7.09±0.72	7.70±0.82
TMAP	4.83±0.52	4.51±0.78	4.71±0.65
TLAP	3.94±0.65	3.70±0.58	3.85±0.63
Age	39.20±12.93	35.21±12.91	37.65±13.04

*Difference not found between genders (P>0.05). SD: Standard deviation, NH: Notch height, NW: Notch width, NSI: Notch shape index, FML: Femoral mediolateral line, FMAP: Femoral medial condyle anteroposterior line, FLAP: Femoral lateral condyle anteroposterior line, TGA: Trochlear groove angle, TML: Tibial mediolateral length, TMAP: Tibial medial anteroposterior line, TLAP: Tibial lateral condyle anteroposterior line

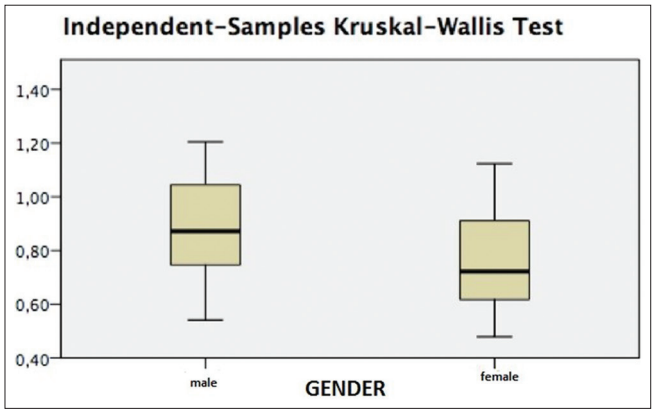

Figure 3: Distribution of the population according to notch shape index index

described the distal femur and the proximal tibia are shown separately for both total population and for sexes in Table 1. Accordingly, when an assessment is made between sexes, all parameters appear to be higher in males when compared with women except for NH.

When the obtained data were assessed statistically, a significant difference was found between sexes in all the parameters assessed except for NH ($P < 0.05$).

A statistically significant difference was determined between the mean NSI values of males and females. The mean NSI value in the total population was calculated to be 0.84 ± 0.18 [Figure 3].

In our study, an intercondylar notch classification was also made. Accordingly, two notch types A and U were defined in our study. Ninety-three of all knee specimens recorded as type A (46.5%), 107 recorded as type U (53.5%). A different type of intercondylar notch was not encountered except for A, U and W defined in previous studies.[1,11] The W type notch that was revealed in these previous studies was not encountered in our study. No relation was found in regard to notch type and sex.

Finally, in our study, the correlation between the parameters measured morphometrically was assessed by Pearson's correlation test [Table 2].

Discussion

Success in TKA highly depends on the proper sizing of the product. In this purpose, anthropological information about proximal tibia has a crucial effect. As a result of many different reasons such as altering gene pools because of migrations, anthropological differences, and lack of knowledge about different racial morphometry, data used for TKA and prosthetic production secondary to TKA is not very effective. Studies evaluating different groups of Asian subpopulations indicates that knee and body size difference of these populations result with the improper fit for western products.[12] In their study on three-dimensional knee morphology, Mahfouz *et al*.[13] revealed differences in the morphology of this region among races. Relevant morphological assessments of various populations have been made, but there is no clear information on the Turkish population. It is expected that this study will reveal the anatomical values of the knee in the Turkish population.

A previous study conducted in 1994, compared direct cadaveric notch measurements with radiographic and MRI

Table 2: Correlation between measured parameters correlation

	NH	FML	NW	FMAP	FLAP	TGA	TML	TMAP	TLAP
NH	1								
FML	−0.127	1							
NW	0.009	0.482**	1						
FMAP	0.077	0.502**	0.314**	1					
FLAP	0.078	0.658**	0.434**	0.714**	1			0.	
TGA	−0.205**	0.190**	0.072	−0.026	0.123	1			
TML	−0.088	0.748**	0.510**	0.081	0.488**	0.234**	1		
TMAP	0.166*	0.349**	0.161*	0.749**	0.475**	0.086	−0.004	1	
TLAP	0.163*	0.299**	0.036	0.674**	0.451**	0.029	−0.023	0.786**	1

*: P <0.001, **: P <0.01, r=1.00–0.76 very good correlation, r=0.75–0.51 good correlation, r=0.50–0.26 fair correlation, r=0.25–0.00 weak correlation. NW: Notch width, NH: Notch height, NW: Notch width, FML: Femoral mediolateral, FMAP: Femoral medial condyle anteroposterior, FLAP: Femoral lateral condyle anteroposterior, TGA: Trochlear groove angle, TML: Tibial mediolateral length, TMAP: Tibial medial anteroposterior line, TLAP: Tibial lateral condyle anteroposterior line

measurements and resulted in no direct difference between both measurement methods.[14] For this reason, we used MRI for our metric evaluations.

The morphometric knee values among Chinese, Koreans, Japanese, and Iranians were explored through different studies.[15-17] For the first time, we made a complete calculation of the bony components of the knee in Turkish people in a single study including both distal femur and proximal tibia measurements also with intercondylar notch type.

Significant differences between genders in terms of the distal femur and the proximal tibia values except for the NH were noted in our study. In their study on the distal femur morphology in 2007, Conley *et al.* determined a significant difference in the measurements of this region in men and women.[18] Previously, it is found 33.2 ± 2.8 for males and 29.0 ± 2.6 for females also in the Turkish population, similarly on 200 people without abnormal knee.[19] Our results are lesser than their value as 23.00 ± 0.37 for males and 23.10 ± 0.37 for females. The difference was statistically not significant between genders. However, the obtained results are interesting. Yet, the presence of such different values in the same population with similar age groups and similar sample size suggests that people vary even within themselves or that there may be also regional differences in the Anatolian population.

NW is commonly related to ACL injuries. It is stated that there is still a controversy as some authors claim that ACL injured groups have narrower NW; on the other hand, some authors report nonsignificance between each other.[20] Park *et al*.[20] compared this value with the ACL injured and control group. The result was found for 20.33 mm and 18.52 mm in the control group for males and females, respectively. Their results have shown a significant difference between the injured and control groups. Our results revealed 19.90 ± 0.26 for males and 17.20 ± 0.27 for females for the normal knee. For an accurate comparison, this value should be studied also in the ACL injured group in the Turkish population. Index of notch shape (NSI) served as a ratio between NW and NH. This ratio is related to ACL deformations. It is stated that this index might even be related to ACL ruptures.[1] In the presented study, the mean value for NW was found 1.88 cm and NH was found 2.30 cm for Turkish people. Hence that NSI was found (0.84 ± 0.18). Previous records indicate that this ratio was found in African as (0.60 ± 0.08) and (0.63 ± 0.09) in the European people.[21] According to Ouyang *et al.*[22] "The greater the ratio, the more rounded the intercondylar notch." Hence that according to this information, Turkish people have a more rounded notch with the highest NSI ratio.

According to the results of our study, the FML value was found to be 82 mm. The same value indicated in the White people as 73.5 mm, in the African-origin as 69.1 mm, in East Asia 71.4 mm and in the Indian as 65.4 mm. Interestingly, this value revealing width of the femur was found larger than all other populations in the Turkish people.[23-25] Hence that, the antropo-morphologic type of the knee in Turkish people found narrower at the sagittal axis but wider at the transverse axis.

FMAP and FLAP are the measurements indicating medial and lateral anteroposterior dimensions of the knee. Previously, the mean value for FMAP was 61.7 mm for White, 64.00 mm for African-origin and 58.00 mm for the East Asian populations and FLAP was 61.7 mm for White, 63.2 mm for African-origin and 58.7 mm for East Asian and 57.8 for Indian people.[10] Our study reveals that the mean value of FMAP for Turkish people is 61.00 ± 0.62 and FLAP 57.1 mm. As compared to all given populations, FMAP value is similar, but FLAP value for Turkish people is the smallest.[10,24-26] This is an interesting result, because Turkish people anthropologically considered as White-Caucasian like many central and Eastern European populations. Hence that, the femoral anteroposterior length smaller than East Asian people is a significant result.

TGA is related to dysplasia of the extensor mechanism.[27] It is stated that measurement of the angle is easy, quick, and

a reliable method for the prediction of severity.[27] Sulcus angle higher than 150° on an axial radiograph is considered to indicate femoral trochlear dysplasia.[28] Toms's comparative work for CT, MRI and ultrasound found similar results for all three methods on patients with patellar instability.[29] It is stated that previous studies revealing the sulcus for normal knee reported that the sulcus angle was 132° and the other was 138°.[30,31] Murshed *et al*. conducted a study on 100 people also in the Turkish population. They found 134.00° and 132.20° for males and females, respectively. This angles are slightly larger than our results which is 130.31°, 128.56°, and 129.63° for males, females, and mean, respectively. The difference may be because of the sample size which is 200 people in our study.

TMAP, TLAP, and TML are the dimensions for the measurement of anteroposterior and transverse dimensions of the proximal tibia. The value of TMAP was found 47.1 mm in the Turkish population which was 49.8 mm in White people, 49 mm in East Asian, and 47.5 mm in Indian.[23,24] TLAP was found to be 44.3 mm in Whites, 44.4 mm in East Asia, and 43.8 mm in Indians. Our result for the Turkish people was 38.5 mm.[23] In comparison to numerical TMAP and TLAP values, results for Turkish people were found lower than all other races. The TML value was found 77 mm in the Turkish population, 74.3 mm in White, 73.2 mm in African-origin 72.8 mm in East Asian, and 72.8 mm in Indian people. The numerical value of TML compared with the other race and in Turkish people was found to be higher than all other populations.[23,24] These results reveal that morphologically proximal tibia of the Turkish population is narrower in sagittal axis and wider in the transverse axis similar to the distal femur.

Intercondylar notch shape is divided into three as A, U, and W.[32] Even though, association between the shape and ACL injury risk is not commonly clear, some of the researchers suggest A type should be more vulnerable because of its narrow shape.[1] Similarly, Al-Saeed found 73% of the patients with ACL tear with A type.[1] Presented study of ours, revealed 46.5% of the cases as type A and 53.5% of the cases as type U with no type W, on normal knee. In order to find the answer of "Does these results mean that nearly half of the Turkish population is more vulnerable for ACL injury?" question, a larger sample group of both normal and ACL ruptured patients should be compared.

Conclusion

According to the results of this study in Turkish people, the distal femur shape has the slightly larger mediolateral diameter and smaller or medium size anteroposterior diameter compared to all other populations. Accordingly, two femoral notch types as A and U were defined in our study. 93 of all knee specimens recorded as Type A (46.5% of total), 107 recorded as Type U (53.5% of total). The W type notch that was revealed in previous studies was not encountered in our study.

In addition, our results revealed a wider mediolateral diameter and smaller anteroposterior diameter than other races at the proximal tibia. This study will have crucial clinical impact on the production of the specific prostheses belong to the Turkish population and populations with similar anthropologic tibial shape.

Acknowledgment

Preliminary data of this article were presented as poster at 17th National Congress of Anatomy, September 5-9, 2016, Eskişehir, Turkey.

Financial support and sponsorship

Nil.

Conflicts of interest

There are no conflicts of interest.

References

1. Al-Saeed O, Brown M, Athyal R, Sheikh M. Association of femoral intercondylar notch morphology, width index and the risk of anterior cruciate ligament injury. Knee Surg Sports Traumatol Arthrosc 2013;21:678-82.
2. Balcarek P, Walde TA, Frosch S, Schüttrumpf JP, Wachowski MM, Stürmer KM, *et al*. Patellar dislocations in children, adolescents and adults: A comparative MRI study of medial patellofemoral ligament injury patterns and trochlear groove anatomy. Eur J Radiol 2011;79:415-20.
3. Ewe T, Ang H, Chee E, Ng W. An analysis of the relationship between the morphometry of the distal femur, and total knee arthroplasty implant design. Malay 2009;3:24-8.
4. Havet E, Gabrion A, Leiber-Wackenheim F, Vernois J, Olory B, Mertl P. Radiological study of the knee joint line position measured from the fibular head and proximal tibial landmarks. Surg Radiol Anat 2007;29:285-9.
5. Berend ME, Small SR, Ritter MA, Buckley CA. The effects of bone resection depth and malalignment on strain in the proximal tibia after total knee arthroplasty. J Arthroplasty 2010;25:314-8.
6. Innocenti B, Truyens E, Labey L, Wong P, Victor J, Bellemans J. Can medio-lateral baseplate position and load sharing induce asymptomatic local bone resorption of the proximal tibia? A finite element study. J Orthop Surg Res 2009;4:26.
7. Cheng FB, Ji XF, Zheng WX, Lai Y, Cheng KL, Feng JC, *et al*. Use of anthropometric data from the medial tibial and femoral condyles to design unicondylar knee prostheses in the Chinese population. Knee Surg Sports Traumatol Arthrosc 2010;18:352-8.
8. Urabe K, Mahoney OM, Mabuchi K, Itoman M. Morphologic differences of the distal femur between Caucasian and Japanese women. J Orthop Surg (Hong Kong) 2008;16:312-5.
9. Surendran S, Kwak DS, Lee UY, Park SE, Gopinathan P, Han SH, *et al*. Anthropometry of the medial tibial condyle to design the tibial component for unicondylar knee arthroplasty for the Korean population. Knee Surg Sports Traumatol Arthrosc 2007;15:436-42.
10. Kim TK, Phillips M, Bhandari M, Watson J, Malhotra R. What differences in morphologic features of the knee exist among patients of various races? A systematic review. Clin Orthop Relat Res 2017;475:170-82.

11. Chen C, Ma Y, Geng B, Tan X, Zhang B, Jayswal CK, *et al*. Intercondylar notch stenosis of knee osteoarthritis and relationship between stenosis and osteoarthritis complicated with anterior cruciate ligament injury: A study in MRI. Medicine (Baltimore) 2016;95:e3439.
12. Kwak DS, Surendran S, Pengatteeri YH, Park SE, Choi KN, Gopinathan P, *et al*. Morphometry of the proximal tibia to design the tibial component of total knee arthroplasty for the Korean population. Knee 2007;14:295-300.
13. Mahfouz M, Abdel Fatah EE, Bowers LS, Scuderi G. Three-dimensional morphology of the knee reveals ethnic differences. Clin Orthop Relat Res 2012;470:172-85.
14. Herzog RJ, Silliman JF, Hutton K, Rodkey WG, Steadman JR. Measurements of the intercondylar notch by plain film radiography and magnetic resonance imaging. Am J Sports Med 1994;22:204-10.
15. Hosaka K, Saito S, Ishii T, Mori S, Sumino T, Tokuhashi Y. Asian-specific total knee system: 5-14 year follow-up study. BMC Musculoskelet Disord 2011;12:251.
16. Hovinga KR, Lerner AL. Anatomic variations between Japanese and Caucasian populations in the healthy young adult knee joint. J Orthop Res 2009;27:1191-6.
17. Uehara K, Kadoya Y, Kobayashi A, Ohashi H, Yamano Y. Anthropometry of the proximal tibia to design a total knee prosthesis for the Japanese population. J Arthroplasty 2002;17:1028-32.
18. Conley S, Rosenberg A, Crowninshield R. The female knee: Anatomic variations. J Am Acad Orthop Surg 2007;15 Suppl 1:S31-6.
19. Murshed KA, Ciçekcibaşi AE, Karabacakoğlu A, Seker M, Ziylan T. Distal femur morphometry: A gender and bilateral comparative study using magnetic resonance imaging. Surg Radiol Anat 2005;27:108-12.
20. Park JS, Nam DC, Kim DH, Kim HK, Hwang SC. Measurement of knee morphometrics using MRI: A comparative study between ACL-injured and non-injured knees. Knee Surg Relat Res 2012;24:180-5.
21. Tillman MD, Smith KR, Bauer JA, Cauraugh JH, Falsetti AB, Pattishall JL. Differences in three intercondylar notch geometry indices between males and females: A cadaver study. Knee 2002;9:41-6.
22. Ouyang X, Wang YH, Wang J, Hong SD, Xin F, Wang L, *et al*. MRI measurement on intercondylar notch after anterior cruciate ligament rupture and its correlation. Exp Ther Med 2016;11:1275-8.
23. Lim HC, Bae JH, Yoon JY, Kim SJ, Kim JG, Lee JM. Gender differences of the morphology of the distal femur and proximal tibia in a Korean population. Knee 2013;20:26-30.
24. Chaichankul C, Tanavalee A, Itiravivong P. Anthropometric measurements of knee joints in Thai population: Correlation to the sizing of current knee prostheses. Knee 2011;18:5-10.
25. van den Heever DJ, Scheffer C, Erasmus P, Dillon E. Classification of gender and race in the distal femur using self organising maps. Knee 2012;19:488-92.
26. Terzidis I, Totlis T, Papathanasiou E, Sideridis A, Vlasis K, Natsis K. Gender and side-to-side differences of femoral condyles morphology: Osteometric data from 360 caucasian dried femori. Anat Res Int 2012;2012:679658.
27. Davies AP, Costa ML, Shepstone L, Glasgow MM, Donell S. The sulcus angle and malalignment of the extensor mechanism of the knee. J Bone Joint Surg Br 2000;82:1162-6.
28. Chhabra A, Subhawong TK, Carrino JA. A systematised MRI approach to evaluating the patellofemoral joint. Skeletal Radiol 2011;40:375-87.
29. Toms AP, Cahir J, Swift L, Donell ST. Imaging the femoral sulcus with ultrasound, CT, and MRI: Reliability and generalizability in patients with patellar instability. Skeletal Radiol 2009;38:329-38.
30. Murshed KA, Çiçekcibaşi AE, Ziylan T, Karabacakoğlu A. Femoral sulcus angle measurements: An anatomical study of magnetic resonance images and dry bones. Turk J Med Sci 2004;34:165-9.
31. Merchant A. Patellofemoral disorders: Biomechanics, diagnosis and nonoperative treatment. Operative Arthroscopy. New York: Raven Press; 1991. p. 261-75.
32. van Eck CF, Martins CA, Vyas SM, Celentano U, van Dijk CN, Fu FH. Femoral intercondylar notch shape and dimensions in ACL-injured patients. Knee Surg Sports Traumatol Arthrosc 2010;18:1257-62.

Original Article

MTHFR C677T Polymorphism and Risk of Nonsyndromic Cleft in Craniofacial Region in a South Indian Population

Betty Anna Jose, Varsha Mokhasi, Subramani Arumugam Subramani[1], Mahendrakar Shashirekha

Departments of Anatomy and [1]Plastic Surgery, Vydehi Institute of Medical Sciences and Research Centre, Whitefield, Bengaluru, Karnataka, India

Abstract

Introduction: Methylenetetrahydrofolate reductase (MTHFR) C677T polymorphism was found associated with cleft palate (CP) and cleft lip with or without CP in different populations and only very few studies were conducted in the Indian population. The aim of this case–control study is to detect whether there is any association of C677T MTHFR gene polymorphism with clefts in the craniofacial region, especially with Nonsyndromic cleft lip with cleft palate (NSCLP) in the South Indian population. **Material and Methods:** The study was conducted on 179 nonsyndromic cleft cases and 130 healthy individuals without cleft were included as controls. To detect the polymorphism, polymerase chain reaction–restriction fragment length polymorphism method was carried out, and the result was analyzed using Chi-square test and binary logistic regression model. **Results:** Among the cleft cases, 120 were NSCLP and it showed 6.67% CT genotype and 18.33% TT genotype, while in controls, it was 18.46% and 1.54%, respectively. The TT genotype increased the risk of NSCLP (odds ratio [OR] =0.079, 95% confidence interval [CI]: 0.02–0.34, P = 0.0007) and CT genotype decreased the risk (OR = 2.59, 95% CI: 1.11–6.06, P = 0.028). However, CT + TT model had no association with NSCLP when compared to CC genotype. No significant difference was found between other 59 clefts and polymorphism. **Discussion and Conclusion:** The association of MTHFR C677T polymorphism with NSCLP varies from population to population. Our study found an association between the polymorphism and NSCLP. The TT genotype increased the risk of NSCLP and CT genotype reduced the risk.

Keywords: *Cleft lip/palate, methylenetetrahydrofolate reductase C677T, nonsyndromic, polymorphism*

Introduction

Nonsyndromic cleft in the lip and palate has a multifactorial etiology. Several putative genes were studied and specific genes in single or combined with other genes were identified in syndromic and nonsyndromic clefts in various populations. It was found that maternal folic acid intake during the periconceptional period reduces the risk of clefts and it enlightened that the enzymes and coding genes involved in the folate metabolism might be associated with the congenital clefts. Methylenetetrahydrofolate reductase (MTHFR) is one of the important enzymes involved in the folate metabolism, coded by the MTHFR gene.

Folate and MTHFR enzymes are very much required for DNA synthesis and methylation which, in turn, is essential for normal cell division and gene expression during the embryonic period.[1] In the folate cycle, folic acid is reduced to tetrahydrofolate, its active form. Folate is its natural form and folic acid is the synthetic form. For the conversion of 5,10-methylenetetrahydrofolate to 5-methyl tetrahydrofolate, the MTHFR enzyme is required and the methyl group thus formed is used up for the conversion of homocysteine to methionine. Methionine is an essential amino acid. If this conversion is not occurring, the serum homocysteine level increases which has a teratogenic effect in the embryonic life.[2]

The C677T variant in exon 4 is a common functional mutation identified in the MTHFR gene.[3] In C677T polymorphism, C is substituted by T and it changes the amino acid alanine to valine at 222 position. This change in the amino acid results in the thermolabile MTHFR enzyme.[4] Hypofunctional MTHFR leads to hypomethylation and the thermolabile form

How to cite this article: Jose BA, Mokhasi V, Subramani SA, Shashirekha M. MTHFR C677T Polymorphism and risk of nonsyndromic cleft in craniofacial region in a South Indian Population. J Anat Soc India 2020;69:15-20.

Article Info

Received: 26 August 2019
Accepted: 04 February 2020
Available online: 11 April 2020

Address for correspondence:
Dr. Betty Anna Jose, Department of Anatomy, Vydehi Institute of Medical Sciences and Research Centre, Whitefield, Bengaluru - 560 066, Karnataka, India.
E-mail: bettyannacj@gmail.com

Access this article online

Website: www.jasi.org.in
DOI: 10.4103/JASI.JASI_114_19
Quick Response Code:

causes a reduction in the activity of MTHFR enzyme and increased level of plasma homocysteine.[5]

To identify the association between MTHFR gene polymorphism and nonsyndromic orofacial clefts, many studies were conducted in different populations and showed conflicting results[6-11] and very few studies were conducted in the Indian population. No specific gene is identified as a common causative factor of clefting. In different populations, different polymorphisms were identified as the causative factor. Therefore, we conducted a retrospective study to detect the significance of C677T MTHFR gene polymorphism in cases with nonsyndromic clefts in the craniofacial region, especially with nonsyndromic cleft lip palate (NSCLP) in the South Indian population.

Materials and Methods

Study population

The sample size comprised 309 unrelated subjects which included 157 males and 152 females aged between 9 months and 30 years of the South Indian origin. The study was conducted on 179 nonsyndromic cleft cases from the plastic surgery department and 130 healthy individuals without cleft were included as controls. Among the cases, 8 were cranial clefts, 7 with facial clefts, 22 with cleft lip (CL), 22 with isolated cleft palate (CP), and 120 cases with CL palate. The participants were clinically examined, verified their medical records, and interviewed their parents. Informed written consent was obtained from the participants and from their parents in case of minor. Approval of Institutional Ethics Committee was obtained at the beginning of the study.

Genotyping

The peripheral venous blood samples of 3–5 ml were collected in BD lithium heparinized EDTA vacutainer for the DNA extraction. DNA was extracted by phenol–chloroform extraction method with isopropanol precipitation and stored at −20°C for further procedure. At the time of analysis, samples were thawed and processed for polymerase chain reaction (PCR) amplification. The primers for PCR amplification were designed using Primer 3Plus (Sigma Corporation USA) software and the designed oligonucleotides were synthesized in Sigma Corporation USA. The sequence of primers was 5'GTG AAC TAC TGT GGC CTG GAG3' and 5' ACG TCC TTG ATC TCC TGT GG3'. The PCR conditions were as follows: initial denaturation at 95°C for 5 min, annealing at 52°C for 30 s, extension at 72°C for 1 min, for 30 cycles, and final extension at 72°C for 5 min. PCR yielded a 500 bp product that was digested with restriction endonuclease enzyme Hae III (Merck, India) and loaded in 3% agarose gel electrophoresis and visualized by ethidium bromide staining. The C677T mutation caused Hae III restriction site resulting in the cleavage of 500bp fragment into 350bp and 150bp fragments. The digested products were visualized under UV Transilluminator (Bio Bee, India). The PCR–restriction fragment length polymorphism analysis for the genotyping was according to the method followed previously.[12]

Statistical analysis

Allele frequency was determined by direct counting of alleles. Goodness-of-fit Chi-squared test was used to assess the allele and genotype frequencies. Based on the genotype frequency, Hardy–Weinberg Equilibrium (HWE) was tested in case and control groups. The association was analyzed using Chi-square test and binary logistic regression model using SPSS statistical software version 21.0 (IBM Corp., Chicago, USA).

Results

Among 179 cases, the distribution of clefts was as follows: 4.5% craniofacial clefts [Figure 1], 3.9% facial clefts [Figure 2], 67% CL palate [Figure 3], 12.3% CL [Figure 4], and 12.3% isolated CP [Figure 5]. The male preponderance was 54.7% and females were 45.3%. The most common laterality was left sided (44.7%) followed by bilateral (22.4%), right (18.4%), and median (14.5%). The C677T MTHFR, TT genotype, was identified only in CL palate cases and not in other cleft types. Among the 120 cases of NSCLP, 30 cases were identified with C677T polymorphism. Among the 30 NSCLP cases with C677T polymorphism, the left laterality was found in 22 subjects in which 18 with TT genotype and 4 with CT genotype and the bilateral cases were 8 where 4 were TT genotype and other 4 with CT genotype. No right laterality was found and the left laterality was more in males than the females in these 30 NSCLP cases with polymorphism. However, this difference in

Figure 1: Craniofacial clefts in midline

Figure 2: Facial cleft on left side

Figure 4: Cleft lip: Unilateral cleft lip on left side

the laterality and polymorphism did not show any significance.

The remaining 59 clefts belonged to craniofacial clefts, facial clefts, CL, and isolated CP with a genotype of CC (71.2%) and CT (28.8%), and its difference with controls was not statistically significant (odds ratio [OR] = 0.57, 95% confidence interval [CI]: 0.278–1.168, $P = 0.12$). The 59 cases of other clefts was following the HWE (HWp = 0.196, $\chi^2 = 1.67$) and the allele frequency was 0.86 and 0.14 for C and T allele, respectively. The OR of CC versus CT was OR = 0.57 (95% CI: 0.28–1.17,

Figure 3: Cleft lip palate: Unilateral left side cleft lip with cleft palate

Figure 5: Isolated cleft palate in the posterior aspect

$P = 0.12$) and CC versus CT + TT was OR = 0.617 (95% CI: 0.30–1.25, $P = 0.18$).

The distribution of MTHFR gene variant in the control group was in HWE, but the 120 cases of NSCLP deviated from the HWE. Among the NSCLP cases, the minor allele frequency was 0.22 in cases, while it was 0.11 in controls.

Table 1: Allelic and genotypic frequencies of methylenetetrahydrofolate reductase C677T polymorphism in nonsyndromic cleft lip palate cases and control groups

	NSCLP cases, *n* (%) 120	Controls, *n* (%) 130	OR (95% CI)	*P*
C allele frequency	0.78	0.89	χ^2=11.027	0.0009
T allele frequency	0.22	0.11		
CC genotype	90 (75)	104 (80)	Reference	
CT genotype	8 (6.67)	24 (18.46)	2.59 (1.11-6.06)	0.028
TT genotype	22 (18.33)	2 (1.54)	0.079 (0.02-0.34)	0.0007
CT + TT	30 (25)	26 (20)	0.75 (0.41-1.36)	0.344
CT versus TT			0.03 (0.006-0.158)	<0.0001
HW p*	<0.01	0.653		

*HW p- *P* value of HWE. NSCLP=Nonsyndromic cleft lip palate, OR=Odds ratio, CI=Confidence interval, HWE=Hardy Weinberg Equilibrium

The CT genotype was found more common in controls, and TT genotype of MTHFR C677T polymorphism was more frequent in NSCLP cases. The presence of TT genotype in NSCLP cases (18.33%) and controls (1.54%) showed a statistically significant difference [Table 1].

Discussion

The present study revealed the distribution of MTHFR C677T polymorphism in cleft cases and controls of South Indian origin. It also showed that the differences in the allele frequency (*P* = 0.0009) and MTHFR C677T frequency were statistically significant between the NSCLP cases and controls. The CT genotype was higher in controls (18.46%) than in NSCLP cases (6.67%) and it revealed that T-allele in the heterozygote was associated with NSCLP to lower the risk (OR = 2.59, 95% CI: 1.11–6.06). A similar result was observed in a study of MTHFR polymorphism and gene–environment interaction.[13] The possible mechanism of the protective effect of T-allele and the risk of NSCLP can be explained with the changes in folate metabolism. The reduced enzymatic activity of MTHFR might increase the 5,10-methylenetetrahydrofolate which, in turn, increases the conversion of deoxyuridine monophosphate to deoxythymidine monophosphate (dTMP). The dTMP forms deoxythymidine triphosphate and involves in DNA synthesis. Thus, misincorporation of uracil into DNA is reduced.[14] A study from the Indian subcontinent showed that CT genotype was predominant in cases than the controls and was associated with nonsyndromic CL with or without CP,[9] but the result was different in South Indian population, in which increased CT genotype frequency was found in controls.[15] This is in accordance with our study where CT genotype in controls was three times more than the NSCLP cases. This varied difference among the Indian studies might be due to the heterogeneity in the Indian population.[15] This shows that the association of MTHFR C677T polymorphism with NSCLP varies from population to population.

Furthermore, the present study showed that the frequency of TT genotype was 18.33% in NSCLP cases, while it was very low in controls (1.54%), and this difference (OR = 0.079, 95% CI: 0.02–0.34) revealed that there is an association between MTHFR C677T polymorphism in homozygous TT and NSCLP and it increased the risk of NSCLP. A similar result was found in a Chinese study where the TT genotype caused an increased risk of NSCL/P in Northern China, but no association found in the samples from Southern China.[16] This shows the genetic heterogeneity and influence of MTHFR C677T polymorphism. The T-allele frequency was comparatively lower in Indians when compared to Europeans and Americans and the TT genotype was seen in approximately 1% Indian population.[17] The Southern Chinese population showed that MTHFR C677T polymorphism in CT and TT genotypes increased the risk of NSCL/P and CT genotype contributed to the increased risk of CL only.[18] Our study also found an association between the polymorphism and NSCLP but not with CL. No polymorphism was found in CL cases. In our study, we found that the TT genotype increased the risk of NSCLP and CT genotype reduced the risk. A meta-analysis found that CT and TT genotype of the infant increased the risk of NSCLP among Asians.[19]

In humans, any disruption by genetic or environmental factors during the period of 14th–60th day of postconception may predispose to a cleft in the craniofacial region. The gene expression, cell migration, cell transformation, and apoptosis occur in a sequential series during this period.[20] Increased embryonic homocysteine or hyperhomocysteinemia[5] causes apoptosis due to the oxidative stress which may disturb the normal development of the palate.[21] The function of thermolabile MTHFR enzyme is reduced from 30% to70% in CT and TT genotypes, respectively, at 37°C[22] and further lowered to 65% at 46°C or more.[23] This shows that enzyme activity is 30% in TT genotype and 70% in CT genotype. The TT genotype showed lower serum folate and higher homocysteine concentration than the CC genotype and the CT genotype subjects. The maternal homocysteine enters the fetus through the amniotic fluid and induces apoptosis in palatal mesenchyme and prevents the fusion of palatal shelves.[21] Reduced methionine synthesis due to hyperhomocysteinemia may reduce the cell proliferation as methionine is an essential amino acid required for DNA synthesis and cell growth. The study on murine models showed that the silencing of MTHFR gene expression can prevent growth and induce apoptosis in palatal mesenchyme.[11]

The proper folate supplementation during early pregnancy can compensate the decreased enzymatic activity of

MTHFR[8] and mask the effect of polymorphism. In such cases, despite the presence of polymorphism, the cleft does not happen. However, all mothers might not be aware of their pregnancy in the early stage. The upper lip formation or fusion of two maxillary swellings with intermaxillary segment is completed by 40th–48th day, and the fusion of palatal shelves is completed by the 60th day of intrauterine life.[20] Hence, the intake of folic acid in the first 60 days of pregnancy has paramount importance. The conditions such as maternal malnutrition, absence of fortification, and no folate intake neither in natural or synthetic form could not mask the effect of C677T polymorphism and may lead to the risk of NSCLP. Different theories were put forward to explain the pathogenesis of craniofacial clefting.[24] The theory of failure of ectodermal fusion states that at the time of fusion, the epithelial cells must disappear in the area of fusion of processes to facilitate the mesoderm to fuse. The absence of the ossification centers and the developmental arrest can cause the cleft. The failure of mesodermal migration, the arrest of neural crest cell migration, and imbalance in the cell formation and apoptosis are the other theories. The premature involution of embryonic arteries is also pointed out as an embryonic change that causes cleft. The stapedial artery derived from the second pharyngeal arch is present only during 33–40 days of fetal development and its absence results in ischemia which may cause facial clefting.[25]

In our study, the other 59 clefts in the craniofacial region had CC and CT genotypes 71.2% and 28.8%, respectively, and it did not show any significant difference with the CT genotype of the control group (18.46%). The TT genotype was not present among the 59 clefts. MTHFR TT genotype was associated with an increased risk of isolated CP in the Ireland population.[26] However, the present study did not show any association between clefts in the craniofacial region other than NSCLP and MTHFR C677T polymorphism. The fusion of palatal shelves occurs initially in the mid-portion and slowly it is continued towards the anterior or primary palate and posterior directions. When the fusion toward the anterior direction is not occurring completely and if the upper lip is not fused, the condition leads to the CL palate. The event of fusion happens only after disrupting the epithelial seam of palatal shelves which lead to the mesenchymal merging of two shelves.[20] In case of CT genotype, the teratogenic effect may be less and it may cause cleft in a small range like CL or CP. However, in TT genotype, the impact may be more and the cleft is extended from the palate to the upper lip could be the reason for the presence of TT genotype in NSCLP cases and the same was not found in other 59 clefts in our study.

A recent study in the Moroccan population revealed a low association between C677T polymorphism and risk of NSCL/P (OR = 0.24; 95% CI; 0.105–0.536).[27] MTHFR C677T polymorphism showed an increased risk of NSCL/P in the Indian population.[9] However, a study by Murthy *et al*. could not find any association between NSCL/P with MTHFR C677T polymorphism in the South Indian population.[15] The present study revealed that CT genotype reduced the risk and TT genotype increased the risk of NSCLP. According to Tolarova *et al*., TT genotype is three times more frequent in CL/P patients than in controls.[28] In our study, this frequency was much higher, 18.33% in patients and only 1.54% in controls. Moreover, the TT genotype showed a significant association with increased risk of NSCLP. In NSCLP cases, the CT genotype was very less than the TT genotype and CT genotype was three times lesser when compared to the controls [Table 1]. However, this difference did not contribute to any significant association. This may be due to the fact that the NSCLP case group was not in HWE. In our study, the CC genotype with CT and TT genotypes did not show a significant difference, but the difference was significant in CT genotype with TT genotype [Table 1]. A recent meta-analysis on 22 studies in the overall population showed that MTHFR C677T polymorphism was significantly associated with nonsyndromic orofacial cleft and contributed to the increased risk of NSCL/P.[3]

In our study among the 30 cases of NSCLP who showed polymorphism, 22 were with left laterality and the remaining 8 with a bilateral cleft in lip and palate. No right laterality was found in cases with polymorphism. The presence of polymorphism in the bilateral clefts might be because of the presence of left laterality in those cases. It hints at the association of polymorphism with left laterality. In our study, we could not find any association of polymorphism with laterality. However, interestingly, all cases with polymorphism had left laterality. Further studies should be conducted in a large sample to find out the association between NSCLP and laterality.

Previous studies were dealing with the cleft in palate or CL with or without CP. The present study included various clefts in the craniofacial region and it is grouped into craniofacial clefts, facial clefts, CL palate, CL, and CP. The NSCLP cases were more in our study and its predominance might have caused more study on its etiology in varied populations. To date, very few studies have correlated the laterality with polymorphism despite there was no significance found in our study.

Conclusion

The MTHFR C677T polymorphism is associated with the risk of NSCLP but not with other clefts in the craniofacial region. The TT genotype increased the risk of NSCLP and CT genotype showed a decrease in the risk. All the cases with polymorphism had left laterality. Further studies should be conducted to identify whether any association exists between the polymorphism and laterality of cleft.

Declaration of patient consent

The authors certify that they have obtained all appropriate

patient consent forms. In the form, the patients' parents have given their consent for their images and other clinical information to be reported in the journal. The patients' parents understand that their names and initials will not be published and due efforts will be made to conceal their identity, but anonymity cannot be guaranteed.

Financial support and sponsorship

Nil.

Conflicts of interest

There are no conflicts of interest.

References

1. Murray JC, Wehby GL, Ferreira M, Felix T, Costa A, Padovani C. Oral cleft prevention programme. BMC Pediatr 2012;12:184.
2. Greene ND, Dunlevy LE, Copp AJ. Homocysteine is embryotoxic but does not cause neural tube defects in mouse embryos. Anat Embryol (Berl) 2003;206:185-91.
3. Rai V. Strong association of C677T polymorphism of methylenetetrahydrofolate reductase gene with nosyndromic cleft lip/palate (nsCL/P). Indian J Clin Biochem 2018;33:5-15.
4. Kang SS, Wong PW, Susmano A, Sora J, Norusis M, Ruggie N. Thermolabile methylenetetrahydrofolate reductase: An inherited risk factor for coronary artery disease. Am J Hum Genet 1991;48:536-45.
5. Jacques PF, Bostom AG, Williams RR, Ellison RC, Eckfeldt JH, Rosenberg IH, *et al*. Relation between folate status, a common mutation in methylenetetrahydrofolate reductase, and plasma homocysteine concentrations. Circulation 1996;93:7-9.
6. Prescott NJ, Winter RM, Malcolm S. Maternal MTHFR genotype contributes to the risk of non-syndromic cleft lip and palate. J Med Genet 2002;39:368-9.
7. van Rooij IA, Vermeij-Keers C, Kluijtmans LA, Ocké MC, Zielhuis GA, Goorhuis-Brouwer SM, *et al*. Does the interaction between maternal folate intake and the methylenetetrahydrofolate reductase polymorphisms affect the risk of cleft lip with or without cleft palate? Am J Epidemiol 2003;157:583-91.
8. Pezzetti F, Martinelli M, Scapoli L, Carinci F, Palmieri A, Marchesini J, *et al*. Maternal MTHFR variant forms increase the risk in offspring of isolated nonsyndromic cleft lip with or without cleft palate. Hum Mutat 2004;24:104-5.
9. Ali A, Singh SK, Raman R. MTHFR 677TT alone and IRF6 820GG together with MTHFR 677CT, but not MTHFR A1298C, are risks for nonsyndromic cleft lip with or without cleft palate in an Indian population. Genet Test Mol Biomarkers 2009;13:355-60.
10. Boyles AL, Wilcox AJ, Taylor JA, Meyer K, Fredriksen A, Ueland PM, *et al*. Folate and one-carbon metabolism gene polymorphisms and their associations with oral facial clefts. Am J Med Genet A 2008;146A: 440-9.
11. Xiao WL, Wu M, Shi B. Folic acid rivals methylenetetrahydrofolate reductase (MTHFR) gene-silencing effect on MEPM cell proliferation and apoptosis. Mol Cell Biochem 2006;292:145-54.
12. Zappacosta B, Romano L, Persichilli S. Genotype prevalence and allele frequencies of 5,10-methylenetetrahydrofolate reductase (MTHFR) C677T and A1298C polymorphisms in Italian newborns. Laboratory Med 2009;12:732-6.
13. Estandia-Ortega B, Velázquez-Aragón JA, Alcántara-Ortigoza MA, Reyna-Fabian ME, Villagómez-Martínez S, González-Del Angel A. 5,10-methylenetetrahydrofolate reductase single nucleotide polymorphisms and gene-environment interaction analysis in non-syndromic cleft lip/palate. Eur J Oral Sci 2014;122:109-13.
14. Ma J, Stampfer MJ, Giovannucci E, Artigas C, Hunter DJ, Fuchs C, *et al*. Methylenetetrahydrofolate reductase polymorphism, dietary interactions, and risk of colorectal cancer. Cancer Res 1997;57:1098-102.
15. Murthy J, Gurramkonda VB, Karthik N, Lakkakula BV. MTHFR C677T and A1298C polymorphisms and risk of nonsyndromic orofacial clefts in a south Indian population. Int J Pediatr Otorhinolaryngol 2014;78:339-42.
16. Zhu J, Ren A, Hao L, Pei L, Liu J, Zhu H, *et al*. Variable contribution of the MTHFR C677T polymorphism to non-syndromic cleft lip and palate risk in China. Am J Med Genet A 2006;140:551-7.
17. Singh K, Singh SK, Sah R, Singh I, Raman R. Mutation C677T in the methylenetetrahydrofolate reductase gene is associated with male infertility in an Indian population. Int J Androl 2005;28:115-9.
18. Han Y, Pan Y, Du Y, Tong N, Wang M, Zhang Z, *et al*. Methylenetetrahydrofolate reductase C677T and A1298C polymorphisms and nonsyndromic orofacial clefts susceptibility in a southern Chinese population. DNA Cell Biol 2011;30:1063-8.
19. Pan Y, Zhang W, Ma J, Du Y, Li D, Cai Q, *et al*. Infants' MTHFR polymorphisms and nonsyndromic orofacial clefts susceptibility: A meta-analysis based on 17 case-control studies. Am J Med Genet A 2012;158A: 2162-9.
20. Sperber GH. Formation of the primary palate. In: Wyszynski DF, editor. Cleft Lip and Palate: From Origin to Treatment. NY: Oxford University Press; 2002. p. 5-13.
21. Knott L, Hartridge T, Brown NL, Mansell JP, Sandy JR. Homocysteine oxidation and apoptosis: A potential cause of cleft palate. *In vitro* Cell Dev Biol Anim 2003;39:98-105.
22. Frosst P, Blom HJ, Milos R, Goyette P, Sheppard CA, Matthews RG, *et al*. A candidate genetic risk factor for vascular disease: A common mutation in methylenetetrahydrofolate reductase. Nat Genet 1995;10:111-3.
23. Bhaskar LV, Murthy J, Venkatesh Babu G. Polymorphisms in genes involved in folate metabolism and orofacial clefts. Arch Oral Biol 2011;56:723-37.
24. Rare Cranio-Facial Clefts. Available from: http://www.cpmundi.org/adjuntos/manuales/es/rare_cranio-facial_clefts. [Last Accessed on 2019 Aug 20].
25. Braithwaite F, Watson J. A report on three unusual cleft lips. Br J Plast Surg 1949;2:38-49.
26. Mills JL, Kirke PN, Molloy AM, Burke H, Conley MR, Lee YJ, *et al*. Methylenetetrahydrofolate reductase thermolabile variant and oral clefts. Am J Med Genet 1999;86:71-4.
27. Rafik A, Rachad L, Kone AS, Nadifi S. MTHFR C677T polymorphism and risk of nonsyndromic cleft lip with or without cleft palate in the Moroccan population. Appl Clin Genet 2019;12:51-4.
28. Tolarova MM, Van der Pul NMJ, Goldberg AC, Hol F. A common mutation in the MTHFR gene as a risk factor for nonsyndromic cleft lip and or palate anomalies. Am J Hum Genet 1998;63:A27.

Original Article

Study on Mandibular Parameters of Forensic Significance

D. Sreelekha, D. Madhavi[1], S. Swayam Jothi[2], A. Vijayalakshmi Devi[3], K. Srinidhi[4]

Department of Anatomy, Sree Balaji Medical College and Hospital, Chrompet,Chennai, [2]Department of Anatomy, Shri Sathya Sai Medical College, Kanchipuram, Tamil Nadu, [1]Department of Anatomy, Guntur Medical College, Guntur, [3]Department of Anatomy, Siddhartha Medical College, [4]Housesurgeon, NRI Medical College, Vijayawada, Andhra Pradesh, India

Abstract

Introduction: Bones often survive the process of decay and therefore provide the major evidence of human age and sex after death. The identification of human skeletal remains is a critical problem and is very important in medico-legal and anthropological works. The determination of sex of an individual is important and necessary both in the living and dead for medico-legal purposes. The aim of this study is to measure and analyze the various parameters of the mandible and to assess the reliability of the above parameters in terms of percentage accuracy in sex determination. **Material and Methods:** A total of 106 whole-adult human mandibles of unknown sex, between the age group of 18–60 years, were collected and studied at the Department of Anatomy and Forensic Medicine, Guntur Medical College, Guntur from 2014 to 2015. The following parameters studied were symphyseal height, mandibular body length, bicondylar diameter, bigonial diameter, inter incisor width, and mandibular angle. **Results:** Of the six parameters studied, highly significant (statistically) difference in sex was observed in bigonial diameter (82.15% accuracy) and mandibular angle (81.5% accuracy). **Discussion and Conclusion:** The inference of the study is that no single parameter gives 100% accuracy in the determination of the sex of the individual. Hence, a judicious consideration of the highly significant parameters of the mandible may be taken into account in the determination of the sex of the individual.

Keywords: *Mandible, morphometry, sexual dimorphism*

Introduction

The mandible is a single bone forming the caudal part of the facial skull.[1]

The only bone in the skull with the exception of the tympanic ossicles that is capable of separate movement. It is composed of a thick outer shell of dense bone, with a small amount of cancellous tissue contained within it, and hence that its body is cut with difficulty by bone forceps. It resists decay longer than the other parts of the skeleton, which accounts for the fact that it is often the sole representative of the bones of the face in specimens from strata of past geological periods.[2] Sex can be more accurately determined after the attainment of puberty. The differences are well marked in the bony pelvis and skull. Mandible next to the pelvis in human remains will help us in the identification of age, sex, and race.[3] When the entire skeleton is available, sex can be determined up to 100% accuracy but in cases of mass disasters where usually fragmented bones are found, sex differentiation with 100% accuracy is not possible.[4,5] Recognizable sex differences do not appear until after puberty except in the pelvis, and the accuracy from this bone is about 75% to 80%.

In the skull, features are modified by senility. According to Krogman, the degree of accuracy in sexing adult skeletal remains in the entire skeleton is 100%, pelvis alone is 95%, skull alone is 90%, pelvis plus skull is 98%, and long bones alone 80%.[6]

Sex determination based only on characteristics of teeth and their supporting structures had been a difficult task, whereas X-ray examination of the mandible gives definitive information about the sex. The mandibular condyles are smaller in females. By radiological examination, sex determination of skull is possible to the extent of 88%.[7]

Aim

The aim is to measure and analyze the various parameters of the mandible under study and to assess the reliability of the above parameters in terms of percentage accuracy in sex determination.

How to cite this article: Sreelekha D, Madhavi D, Jothi SS, Devi AV, Srinidhi K. Study on mandibular parameters of forensic significance. J Anat Soc India 2020;69:21-4.

Article Info

Received: 31 May 2019
Accepted: 13 January 2020
Available online: 11 April 2020

Address for correspondence:
Dr. D. Madhavi, Department of Anatomy, Guntur Medical College, Guntur, Andhra Pradesh, India.
E-mail: madhavikondepudi@gmail.com

Access this article online

Website: www.jasi.org.in
DOI: 10.4103/JASI.JASI_52_19
Quick Response Code:

Material and Methods

After obtaining institutional ethical committee clearance, 106 whole-adult human mandibles of unknown sex, between the age group of 18–60 years were collected and studied at the Department of Anatomy and Forensic Medicine Guntur Medical College, Guntur.

Based on morphological features, the mandibles were first categorized as male and female. The mandibles with prominent bony markings and everted mandibular angle were categorized as male and those with relatively smooth and less prominent markings with inverted or straight mandibular angle were categorized as female mandibles. The following parameters were carefully measured and studied using measuring scale, Vernier callipers, and goniometer [Figure 1]:

- symphyseal height
- mandibular body length
- bicondylar diameter
- bigonial diameter
- inter incisor width
- mandibular angle.

Symphyseal height or chin height

The straight distance between the infradentale and gnathion.[8] Infradentale is the highest anterior point of the alveolar process of mandible between the two central incisors in the midline. Gnathion is the most anterior and inferior point of the bony chin.[9] Instrument used – sliding caliper [Figure 2] determined by known statistical standards.

Mandibular body length

From the most anterior point on the symphysis menti to an imaginary point formed by the posterior margin of the ramus and the anteroposterior axis of the body and measured parallel to the axis.[10] Instrument used-sliding caliper [Figure 2].

Bicondylar breadth

It measures the straight distance between two condylia laterale.[8] Condylia laterale is the lateral most point of the head of the condyle of the mandible.[9] Instrument used – sliding caliper [Figure 2].

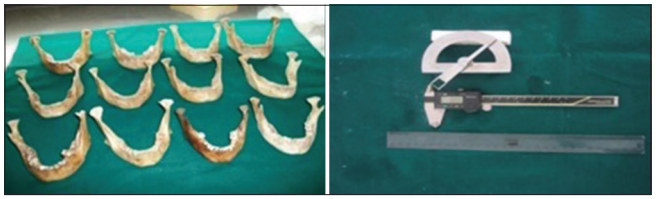

Figure 1: Sample and instruments used for measurement of parameters

Bigonial breadth

It measures the straight distance between two gonia. Instrument used – sliding caliper.[8] Gonion is the intersection of the lines tangent to the posterior margin of the ascending ramus and the mandibular base [Figure 2].[9]

Inter incisor width

The width of the dental arch measured between the points of contact between the lateral incisor and canine on each side.[10] Instrument used – sliding caliper [Figure 2].

Mandibular angle

Measures the angle made by ramus with the body when placed on the surface.[8] Instrument used – goniometer [Figure 2].

Observation

The 106 mandibles chosen for the study were classified based on morphological features into 84 males and 22 females. The range, mean, and standard deviation (SD) for each of the six parameters for male and female mandibles was calculated [Table 1].

Data management and statistical analysis

All the six parameters were accurately measured and tabulated, and the 106 mandibles were classified as males (84) and females (22) based on morphological features. The range, mean, and SD of each of the parameters for the male and female mandibles were calculated, as shown in Table 1. Independent sample *t*-test was applied and the *P* value of significance is noted, as shown in Table 2. For the parameters that showed significance, using mean and SD, a "calculated range" was arrived at by the formula "Mean ± 3SD." A calculated range for male (*p* and *q*) and for female (*r* and *s*) was obtained. From these

Figure 2: Measurement of all the parameters

values, the minimum in male range and the maximum in the female range were taken as "demarking points," and the limiting point was determined by known statistical standards. According to the standard methods followed by previous workers, the limiting point is an absolute value found within the range of the demarking points [Table 3]. The limiting point was so chosen that the vast number of male mandibles showed values greater than it and the bulk of female mandibles showed values lesser than the chosen limiting point. Based on the limiting point for each parameter, the percentage accuracy [Table 4] of the sex was calculated by taking the mandibles whose values were more than the limiting factor as males and those values less than the limiting factor as females.

Results

Of the six parameters studied, highly significant (statistically) difference in sex was observed in bigonial diameter (82.15% accuracy) and mandibular angle (81.5% accuracy).

Table 1: Range, mean±standard deviation of all the six parameters for male and female mandibles

Parameters	Sex	Range	Mean±SD
Symphyseal height	Male	38-24	29.98±3.132
	Female	35-22	28.32±2.784
Mandibular body length	Male	99-75	87.67±5.213
	Female	95-76	84±4.539
Bicondylar diameter	Male	125-96	112.34±6.393
	Female	117-87	105±7.94
Bigonial diameter	Male	108-76	89.38±6.907
	Female	89-70	77.8±5.17
Inter incisor width	Male	23-11	17.19±2.33
	Female	19-15	17±2.069
Mandibular angle	Male	118-96	106.8±5.052
	Female	126-105	116.36±5.534

SD: Standard deviation

Table 2: *T* value and *P* value

Mandibular parameters	*T*	*P*	Significance
Symphyseal height	2.421	0.0078	Highly significant
Mandibular body length	3.269	0.000	Very highly significant
Bicondylar diameter	4.009	0.000	Very highly significant
Bigonial diameter	8.676	0.000	Very highly significant
Inter incisor width	1.591	0.055	Not significant
Mandibular angle	7.371	0.000	Very highly significant

Discussion

Bigonial diameter

In the present study, the mean bigonial diameter for males was 89.33 mm and for females was 77.8 mm with a $P = 0.000$, which was very highly significant.

Flossie and Sayee in 2000, on the south Indian population, studied that the bigonial diameter in males were higher than females with a very highly significant $P = 0.001$.[11] Ongkana and Sudwan in 2009 and Sivaprakash in 2012 observed similar results with a highly significant *P* value.[12,13] Datta *et al*. in a study on 50 bones, found the mean bigonial breadth to be 9.6 cm and 8.9 cm in males and females, respectively.[14]

The results of the present study were in accordance with the previous studies.

Mandibular angle

In the present study, the average male mandibular angle was 106.8° and in females was 116.36° with a $P = 0.000$, which was very highly significant. The female value was found to be higher than in males.

- In earlier studies by Prakash and Abdi in 1987, it was observed that the mean mandibular angle was more in females 123° than males 118.6°.[15] Mbajiorgu in 2005 and Sivaprakash in 2012 also arrived at similar findings.[13,16] Ranganath *et al*. found that the mean mandibular angle in males was 110.68° and for females was 114.53°.[17]
- The values of our study were similar to the results of Ranganath *et al*. Similar to the earlier works; it showed a higher female value than males and a very highly statistically significant difference.

Percentage accuracy

- In the present study, the two variables, bigonial diameter, and mandibular angle showed the highest percentage accuracy of 82.15% and 81.50%, respectively, in determining the sex of the mandible
- Hanihara working on Japanese mandibles, was able to classify the sex of 85.6% mandibles using four mandibular parameters.[18] In a study done by Giles on American

Table 3: Determination of limiting factor

Significant parameters	Demarking points, mean±3SD				Limiting factor
	Male		Female		
	Mean−3SD (*P*)	Mean+3SD (*q*)	Mean−3SD (*r*)	Mean+3SD (*s*)	
Symphyseal height	20.58	39.37	19.98	36.66	29
Mandibular body length	72.04	103.3	70.41	97.59	85
Bicondylar diameter	102.17	131.51	81.8	128.82	113
Bigonial diameter	68.68	110.08	61.49	92.51	81
Mandibular angle	91.65	121.95	99.77	132.95	112

SD: Standard deviation

Table 4: Percentage accuracy of mandibular parameters

Parameters	Percentage accuracy	Average (%)
Symphyseal height	Male - 65.5	66.80
	Female - 68.2	
Mandibular body length	Male - 72.6	68
	Female - 63.6	
Bicondylar diameter	Male - 48.8	67.50
	Female - 86.3	
Bigonial diameter	Male - 91.6	82.15
	Female - 72.7	
Mandibular angle	Male - 85.7	81.50
	Female - 77.3	

mandibles, he was able to classify the sex of mandibles in 83.2% of the cases by using three variables and 84.1% of the cases by using five variables.[19] In a study done by Sivaprakash in South Indian mandibles, he was able to sex the mandible in 83% of cases by using ten variables and 85.5% of the cases using three variables.[13]

Conclusion

The identification of gender from skeletal remains is of paramount importance in anthropological and medico-legal aspects and can be done based on morphological features or parametrical analysis or as a judicious combination of both as in the present study.

- All the parameters measured were higher in male mandibles compared to female mandibles except for mandibular angle, which showed higher female values
- Statistically significant differences were observed in five parameters, i.e., symphyseal height, mandibular body length, bicondylar diameter, bigonial diameter, and mandibular angle
- Every parameter, independent of the other parameters, provides a certain percentage of certainty about the sex of the mandible. Hence, the percentage accuracy of the above five significant parameters was calculated precisely by methods followed by earlier workers. The results were that symphyseal height gave a percentage accuracy of 66.8%, mandibular body length of 68%, bicondylar diameter of 67.5% bigonial diameter of 82.15%, and mandibular angle of 81.5% accuracy
- However, since no single parameter can provide certainty of the sex of the mandible, and as suggested by earlier workers also, a combination of factors is to be considered in determining the gender
- The two variables, bigonial diameter, and mandibular angle showed higher percentage accuracy in determining the sex of the mandible.

Limitation of the study

As the sample size of female mandibles is small, further studies with a larger or equal male and female sample size may be done to arrive at a more accurate conclusion of the significant parameters. Furthermore, in the present study as no single parameter provides certainty of the sex of the mandible, a combination of parameters needs to be considered in determining the gender.

Financial support and sponsorship

Nil.

Conflicts of interest

There are no conflicts of interest.

References

1. William George Dismore Upjohn. Elementary osteology. Melbourne: Queen City Printers: George Robertson and Co; 1888. p. 67.
2. Frazer JE. Anatomy of Human Skeleton. 5th ed. London: JA Churchill Limited; 1958. p. 222-8.
3. Kumar MP, Lokanadham S. Sex determination and morphometric parameters of Human mandible. Int J Res Med Sci 2017;1:93-6.
4. Saini V, Srivastava R, Rai RK, Shamal SN, Singh TB, Tripathi SK. Mandibular ramus: An indicator for sex in fragmentary mandible. J Forensic Sci 2011;56 Suppl 1:S13-6.
5. Scheuer L. Application of osteology to forensic medicine. Clin Anat 2002;15:297-312.
6. Reddy KSN, Murthy OP. Essentials of Forensic Medicine and Toxicology. 33rd Ed. Jaypee Brothers Medical Publishers (P) Ltd, New Delhi. 2014. p. 65.
7. Tedeshi. Radiological examination and sex determination of skull. Forensic Med J 1977;2:1119-23.
8. Singh IP, Bhasin MK. A laboratory manual of Biological anthropology. New Delhi: Kamlaraj Enterprises; 1989. p. 194, 195, 198, 205.
9. Phullari BS. Orthodontics Principles and Practice. 1st ed. Ch. 15, Sec. 4. Jaypee Brothers Medical Publishers (P) Ltd, New Delhi; 2011. p. 184-5.
10. Jayachandra Pillai T. Some Studies on Human Mandible. Andhra Pradesh: Diss Submitted to Dr. NTR Univ.; 2002. p. 1, 18-20, 26-32.
11. Flossie J, Sayee R. Sexing of the mandible. Anat karnataka 2000;1:11-6.
12. Ongkana N, Sudwan P. Gender difference in Thai mandibles using metric analysis. Chiang Mai Med J 2009;48:43-8.
13. Sivaprakash S. Biometric Study of Human Mandible for Determination of Sex. Mangalore: Diss Submitted to Manipal Univ KMC; 2012. p. 60, 70.
14. Datta A, Siddappa SC, Gowda VK, Channabasappa SR, Shivalingappa SB, Srijit, *et al*. A study of sex determination from humen mandible using various morphometrical parameters. Indian J Forensic Community Med 2015;2:158-66.
15. Prakash M. Sexual dimorphism measurements. J Anat Soc India 1987;36:45.
16. Mbajiorgu FE, Zivanovic S, Asala SA, Mawera G. A pilot study of the mandibular angle in black Zimbabweans. Cent Afr J Med 1996;42:285-7.
17. Ranganath vallabhajosyula, Yogitha Ravindranath, Roopa Ravindranath. Sexual dimorphism in mandibular morphology: a study on South Indian sample. South Asian Anthropologist 2008; 8:9-11.
18. Hanihara K. Sex diagnosis of Japanese skulls and scapulae by means of discriminant function. J Anthropol Society of Nippon 1959;67:191-7.
19. Giles E. Sex determination by discriminant function analysis of the mandible. Am J Phys Anthropol 1964;22:129-35.

Original Article

Morphometric Study of Nasal Parameters in Adult Jaunsari Tribe Population of Dehradun District of Uttarakhand

Mukesh Singla, Kumar Satish Ravi, Mohd Salahuddin Ansari

Department of Anatomy, AIIMS, Rishikesh, Uttarakhand, India

Abstract

Introduction: Physical anthropometry has been helpful in clinical diagnosis, forensic medicine, orthodontics, plastic, and reconstructive surgery. The Jaunsari tribe is a unique tribal community of Uttarakhand. There is lack of anthropometric study on them. Hence, it was planned to study facial anthropometric parameters specially that of the nose, in adult Jaunsari tribe of district Dehradun, Uttarakhand. With objectives (1) To study the nasal anthropometric parameters of adult males and females. (2) To analyze the sex differences, if any. (3) and its statistical significance. **Material and Methods:** The study was carried on 100 adult males and 100 adult females of >18 years of age, belonging to Jaunsari tribe, after due approval from the Institutional Ethical Committee and informed consent. The methodology adopted for the anthropometric measurements was of Singh and Bhasin, and concerned measurements were taken and appropriate statistical tests were applied. **Results:** Nasal index, parameters related to it and total facial height are statistically significantly different among males and females. Sagittal Naso-facial Index and Elevation of Nose Index are 44.93 ± 3.79, 44.22 ± 3.18 and 69.23 ± 17.13, 65.70 ± 8.73 in females and males, respectively, which mean relatively elevated and shorter nose. **Discussion and Conclusion:** The most common nose type in females is leptorhinae (60%), whereas in males both leptorhinae and mesorrhine type of nose are equally (47%) prevalent. Predominant nasal breadth in male (69%) and in female (68%) is above medium type, whereas predominant nasal height in male (42%) and in female (50%) is above medium type and below medium type, respectively.

Keywords: *Adult, anthropometry, face, female, male, nose*

Introduction

The only constant thing in human life is change. The change is taking place within the individual as well as outside the individual. These changes are inducing changes in individual's physical morphology. The physical dimensions of the human body are greatly influenced by factors such as age, sex, race, geographical location, and ecology.[1,2] Physical anthropometry has provided techniques for evaluation and measurement of dimensions of the human body.[3,4] Cephalometry is one of the important branches of physical anthropometry which deals with measurement of dimensions of the head and face.[5-7] It has been helpful in clinical diagnosis, forensic medicine, orthodontics, and plastic and reconstructive surgery.[5,8,9] The nasal dimensions are one of the important cephalometric dimensions which are used for description of racial and sexual differences.[4,10-12]

Three anatomical facial prominences play an important role in the characterization of the profile of an individual because of this, these three, lips, nose, and chin have been the great source of attention.[13] Beauty and attractiveness of the face is dependent on reciprocal proportion and esthetic harmony between these parameters which constitute the aesthetic facial triads.[14] As all the anatomical factors mentioned are important, but nose occupies the central position for esthetic characterization.[15] Anatomically, nose consists of external and internal part, of which external part is the most studied one.[16] The nose is made up of bones and cartilages which maintain its pyramidal shape. Cosmetically, external nose is of great importance because of its role in enhancing individual's personality and beauty.[17]

Physical anthropology mainly deals with external measurements and descriptions of the human body.[18] Nasal index ratio which is the ratio of nasal width to nasal

How to cite this article: Singla M, Ravi KS, Ansari MS. Morphometric study of nasal parameters in adult jaunsari tribe population of dehradun district of Uttarakhand. J Anat Soc India 2020;69:25-30.

Article Info

Received: 31 May 2019
Accepted: 09 September 2019
Available online: 11 April 2020

Address for correspondence:
Dr. Mohd Salahuddin Ansari, Department of Anatomy, AIIMS, Veerbhadra Marg, Rishikesh - 249 203, Uttarakhand, India.
E-mail: msalahuddin.ansari12@gmail.com

Access this article online

Website: www.jasi.org.in
DOI: 10.4103/JASI.JASI_62_19
Quick Response Code:

height multiplied by 100, has aided in the classification of nasal index into three different nose types: 69.9 and below leptorrhine or long-nosed, 70–84.9 mesorrhine or medium-nosed and 85 and above platyrrhine or broad-nosed.[19]

The Jaunsari tribe is the largest tribe of Uttarakhand. They have got the body features resembling that of both the Mongols as well as Indo-Aryan groups who have settled in the Himalayan provinces.[20] Because of being relatively isolated from the population of rest of the country for a longer period, this tribal community may have retained their unique physical features, culture, and traditions.

This study will provide the facial anthropometric parameter of adult male and female population of Jaunsari tribe of Dehradun. These facial anthropometric parameters can be used as the standard for future reference for the Jaunsari population. Hence, the study was planned to study facial anthropometric parameters, especially that of nose, in adult Jaunsari tribe of district Dehradun, Uttarakhand. With objectives (1) To study the nasal anthropometric parameters of adult male and female population of Jaunsari tribe of Dehradun district in Uttarakhand. (2) To analyse the sex difference in the nasal anthropometric parameters of Jaunsari tribe if any. (3) and its statistical significance.

Material and Methods

This is a cross-sectional type of study, carried over 200 adult population of Jaunsari tribe consisting of 100 male and 100 female individuals of >18 years of age, after due ethical clearance and their informed consent.

Two tehsils-Chakrata and Kalsi were selected, out of six tehsils of Dehradun district for this study, because Jaunsari tribes are mainly inhabiting these two tehsils of district Dehradun. Equal numbers of randomly selected male and female individuals were taken from randomly selected villages of Chakrata (Lakhwar and Hartar) and Kalsi (Jari and Koti). The individual selection was based on the voter list available at the tehsil office of Chakrata and Kalsi.

The methodology for anthropometric measurements was adopted from Singh and Bhasin.[21] Individuals were asked to sit on a low stool of about 40 cm height for taking head and face measurements. The landmarks were marked on the body by skin marking pencil [Figures 1 and 2]. The head of subject was rested without any strain, in the eye-ear plane or (Frankfurt-Horizontal Plane), i.e., tragion and the infraorbital must lie in the same horizontal plane. The subject was advised not to change his position while measurements were taken. The observer was standing on the right side of the subject while taking the various measurements of the face. Keeping left hand on the head of subject and holding the tips of the upper arm of the caliper with thumb and index finger on the desired landmark, lower arm of the caliper was slided upward to the extent that the tip touches the landmark. The tip of the lower arm must only touch the different landmarks [Figures 3-7]. The facial muscles were relaxed,

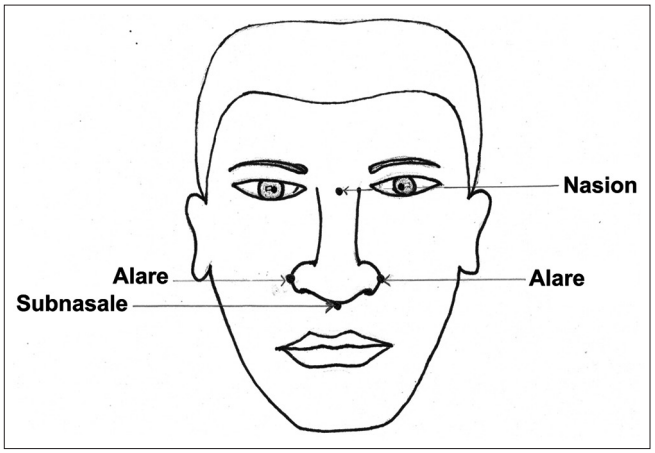

Figure 1: Somato-metric landmarks

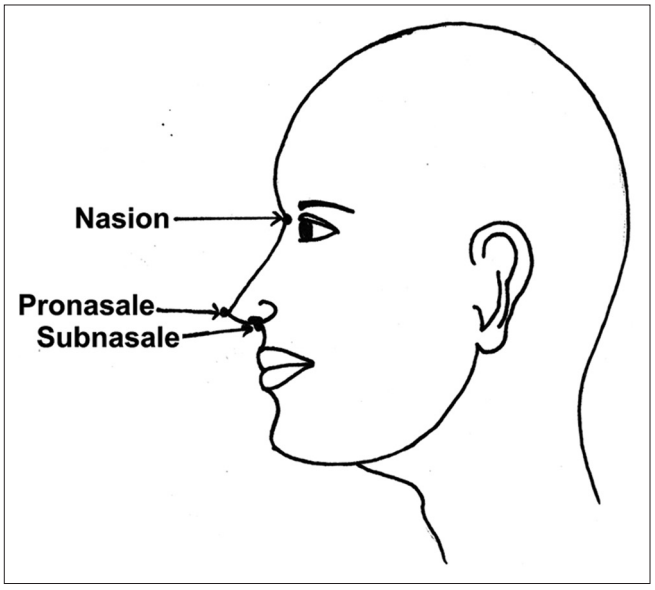

Figure 2: Somato-metric landmarks

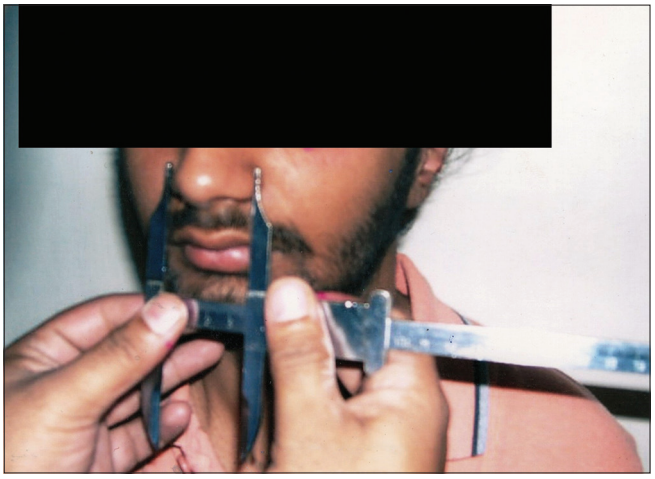

Figure 3: Measurement of nasal breadth

and the jaw was kept closed during the measurement. Following somatometric landmarks and measurement were taken by using digital sliding caliper with flat arms.

Somatometric landmarks

1. Nasion (n) – It is the point of the nasal root intersected by mid-sagittal plane. The nasal root is not depression of the nose but at the nasofrontal suture which can be felt by slightly probing the root of the nose [Figure 1]
2. Gnathion (gn) – It is the lowest point on the lower margin of the lower jaw intersected by the mid-sagittal plane. This point can be palpated on the lower jaw from behind and slightly anterior to chin [Figure 2]
3. Alare (al) – It is the most laterally placed point on the nasal wing [Figure 1]
4. Pronasale (prn) – It is the most anterior place point on the tip of the nose when the head is held in mid-sagittal plane [Figure 1]
5. Subnasale (sn) – It is the point where the lower margin of the nasal septum meets the integument of the upper lip. This point should be sought where the tangent drawn to the nasal septum meets the upper lip [Figure 2].

Somatometric measurements

1. Nasal breadth (al-al): It measures the straight distance between the two alarae (al) i.e., the most laterally placed points on the nasal wings [Figure 3]
2. Nasal height (n-sn): It measures the straight distance between nasion and subnasale (sn) [Figure 4]
3. Nasal depth: It measures the projective distance between the tip of the nose and hind most point on the nasal septum. This measurement is taken by fixing the movable arm of the sliding caliper on the reverse side [Figure 5]
4. Nasal length (n-prn): It measure the straight distance between nasion (n) and pronasale (prn) [Figure 6]
5. Morphological facial height or total facial height (n-gn): It measures the straight distance between nasion (n) and gnathion (gn) [Figure 7].

Indices

1. Sagittal Naso Facial Index: $\frac{\text{Nasal height} \times 100}{\text{Morphological facial height}}$
2. Nasal Index: $\frac{\text{Nasal breadth} \times 100}{\text{Nasal height}}$
3. Elevation of Nose Index: $\frac{\text{Nasal depth} \times 100}{\text{Nasal breadth}}$

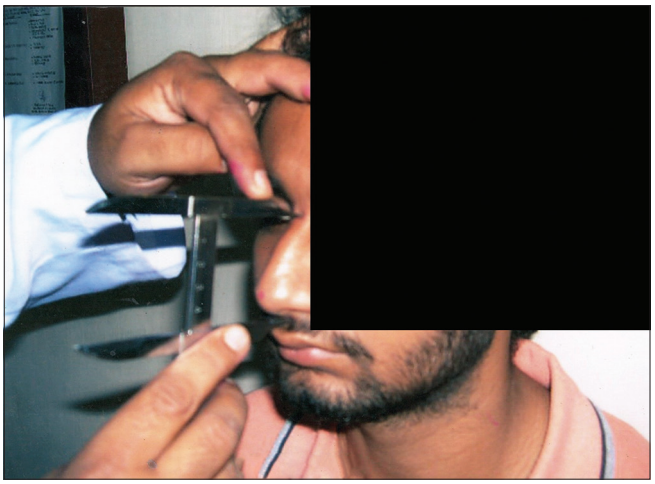

Figure 4: Measurement of nasal height

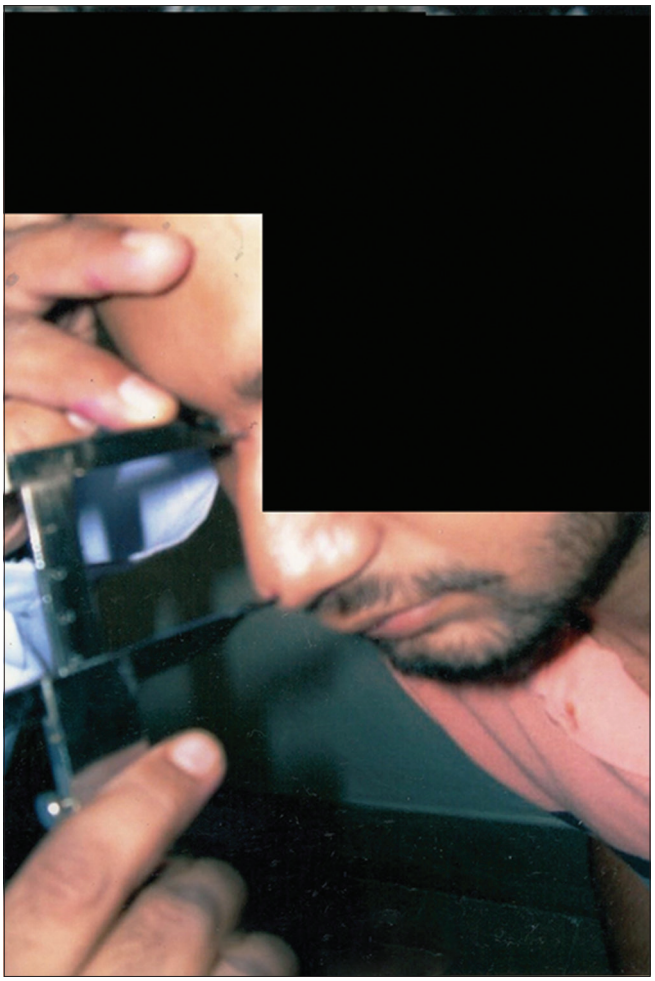

Figure 5: Masurement of nasal length

Results

After the completion of our study, collected data of all the desired morphometric parameters mentioned in the material and method were subjected to appropriate statistical tests (mean, standard deviation, range-value) by using the SPSS software (IBM). Results are presented in the form of table [Figures 1-5]. It is evident from Table 1 that Nasal Index, parameters related to it and total facial height are statistically significantly different among male and female Jaunsari population. Sagittal Naso-facial Index and Elevation of Nose Index were found to be 44.93 ± 3.79, 44.22 ± 3.18 and 69.23 ± 17.13, 65.70 ± 8.73 in female and male Jaunsari population, respectively. It means

Table 1: Comparison of facial parameters of male and female Jaunsari population

Parameters	Mean±SD		Range of parameters				*P*
	Female	Male	Female		Male		
			Minimum	Maximum	Minimum	Maximum	
Nasal breadth (mm)	33.32±2.56	36.814±2.65	30	44	28.00	41.00	<0.001
Total facial height (mm)	111.67±9.14	118.09±6.66	101	140	96.00	140.00	<0.001
Nasal height (mm)	50.14±5.83	52.22±4.69	41	65	42.00	82.80	0.006
Nasal depth (mm)	22.94±5.34	24.08±2.85	17	31	16.00	48.00	0.06
Nasal length (mm)	46.87±7.02	48.46±4.76	34	60	31.10	75.10	0.06
Sagittal Naso facial Index	44.93±3.79	44.22±3.18	36.28	54.62	30.00	60.48	0.2
Nasal Index	67.21±8.47	71.03±8.18	57.25	102.32	35.02	88.64	0.001
Elevation of Nose Index	69.23±17.13	65.70±8.73	47.22	93.33	48.48	151.03	0.07

SD: Standard deviation

Table 2: Nasal breadth range variation according to schaginhaufen[21]

Class	Range	Male (%)	Female (%)
Short	≤-24	0	0
Below medium	25-29	0	6
Medium	30-34	18	68
Above medium	35-39	69	25
Large	40-≤	13	1

Table 3: Range-variation of nasal height according to Martin[21]

Class	Range (mm)	Male (%)	Female (%)
Below medium	45-49	29	50
Above medium	50-54	42	41
large	55-59	22	4
Very large	>60	7	3

Table 4: Range-variation of Nasal Index according to Martin and Saller[21]

Class	Range (mm)	Male (%)	Female (%)
Hyperleptorhinae	≤-54.9	0	6
Leptorhinae	55.0-69.9	47	60
Mesorhinae	70.0-84.9	47	32
Chamaerhine	85.0-99.9	5	2
Hyerchamaerhinae	100.0-x	1	0

Jaunsari population has in general, nose, which is relatively shorter in length and elevated. From Table 2, it can be seen that predominant nasal breadth in male (69%) and in female (68%) are above medium type and medium type, respectively. From Table 3, it can be seen that predominant nasal height in male (42%) and in female (50%) are above medium type and below medium type, respectively. From Table 4, further it can be seen that equal percentage of male population are having leptorhinae (47%) and mesorrhine (47%) type of nose, whereas in female predominant type of nose is leptorhinae (60%) type.

Discussion

Different authors have studied nasal index in different races and in various locations. Nasal index of Indo-Aryans and Indian Negroids was studied by Risley.[22] Nasal indexes of Lebanon (63.30), Alawite (62.74), Damascus (63.26), Armenians (63.80), Greeks (68.49), and Arabic (74.48) were reported by Daniel.[23] Different studies by different group of authors on different ethnic groups of Nigeria have reported significant sexual dimorphism and platyrrhine type of nose in them.[24,25] Some authors reported nasal index of south Indian population predominantly to be mesorrhine type based on their study of south Indian skull.[26] A comparative analysis can be seen in Table 5. In the present study, we found that nasal index, nasal breadth, nasal height, and total facial height are statistically significantly different among male and female Jaunsari population [Table 1]. It can also be seen that predominant nasal height in male (42%) and in female (50%) are above medium type and below medium type respectively [Table 3]. Although we have not focused on the factors which might be responsible for this morphometric presentation, it seems to be because of their specific geographical location and climatic condition which warrants a further study. The present study has provided values of different important morphometric parameters related to the nose (nasal breadth, total facial height, nasal height, nasal depth, nasal length, Sagittal Naso-facial Index, nasal index, Elevation of Nose Index) and predominant types of nose based on

Figure 6: Measurement of morphological upper facial length

Table 5: Comparison of the present study with other studies on the basis of Nasal Index

Authors	Race/Population	Nasal Index	
		Male	Female
Heirnaux & Hartono[27]	Western Europeans	69.90	
	Bantus	85.00	
Franciscus & Long[10]	Onges	72.3-97.7	70.5-97.4
	Sudroid	89.80	
	Aryans	83.00	
Nichang[28]	German	71.00	
Oladipo *et al*.[29]	Igbo	95.80	90.80
	Yoruba	90.00	88.10
Oladipo *et al*.[30]	Ogani	106.10	90.90
Oladipo *et al*.[31]	Ijaws	96.37	
	Yorubas	89.20	
	Igbos	94.10	
Oladipo, Fawehinmi *et al*.[32]	Yoruba	90.02	83.58
Nurul Syamimi binti Mohd Azlan Sunil1 and K. Yuvaraj Babu.[26]	South Indian	77.30	
Present study	Jaunsari Population (Uttarakhand)	71.03	67.21

Figure 7: Measurement of nasal depth

these parametric values [Tables 1-4]. These will be of great help in dealing with different forensic conditions, clinical diagnosis, planning of orthodontics, plastic, and reconstructive surgeries on the Jaunsari population.

Limitations of the study

1. As it represents a local geographic population, it cannot be generalized
2. It has not focused on the factors which might be responsible for this type of presentation of nasal parameters
3. There is no comparison between Jaunsari tribe and rest of the population of state of Uttarakhand.

Future recommendation

For future studies, it is recommended that study should be designed taking into account of people of both Kumaon and Garhwal region of state of Uttarakhand, and hence that comparison and generalization can be made.

Conclusion

Hence, we concluded that

1. Nasal index, nasal breadth, nasal height, and total facial height are statistically significantly different among male and female Jaunsari population
2. In general nose of the Jaunsari population, is relatively shorter in length and elevated
3. Equal percentage of male population are having leptorhinae (47%) and mesorrhine (47%) type of nose, whereas in female predominant type of the nose is leptorhinae (60%)
4. Predominant nasal breadth in male (69%) and in female (68%) are above medium type and medium type, respectively, and
5. Predominant nasal height in male (42%) and in female (50%) is above medium type and below medium type, respectively.

Declaration of patient consent

The authors certify that they have obtained all appropriate patient consent forms. In the form the patient(s) has/have given his/her/their consent for his/her/their images and other clinical information to be reported in the journal. The patients understand that their names and initials will not be published and due efforts will be made to conceal their identity, but anonymity cannot be guaranteed.

Acknowledgment

We are grateful to Dr. Vartika Saxena, Professor, Dr. Ranjeeta Kumari, Additional Professor Department of Family Medicine and Dr. Nilotpal Choudhary, Additional Professor, Department of Pathology, AIIMS, Rishikesh for their valuable contribution to this project.

Financial support and sponsorship

Nil.

Conflicts of interest

There are no conflicts of interest.

References

1. Golalipour MJ, Haidari K, Jahanshahi M, Farahani RM. The shapes of head and face in normal male newborns in South – East of Capsian Sea (Iran-Gogan). J Anat Soc India 2003;52:28-31.
2. Golalipour MJ, Vakilli MA, Ahamadpour M. Height and weight of newborns in relation with mother age, race and parity. J Qazvin Univ Med Sci 2001;16:58-64.
3. Chamella M. Biological Anthropology. Translated to Persian (Farsi) by Nadri A. 1st ed. Tehran: Gostar Publisher; 1997. p. 75.
4. Heidari Z, Sagheb HM, Mugahi MN. Morphological evaluation of head and face in 18 – 25 years old women in South East of Iran. J Med Sci 2006;6:400-4.
5. Heidari Z, Mahmoudzadeh-Sagheb H, Mohamadi M, Noori Mugahi MH, Arab A. Cephalic and proscopic indices: Comparison in one-day newborn boys in Zahedan. J Fac Med 2004;62:156-65.
6. Will MJ, Ester MS, Ramirez SG, Tiner BD, McAnear JT, Epstein L, *et al.* Comparison of cephalometric analysis with ethnicity in obstructive sleep apnea syndrome. Sleep 1995;18:873-5.
7. Jahanshahi M, Golalipour MJ, Heidari K. The effect of ethnicity on facial anthropometry in Northern Iran. Singapore Med J 2008;49:940-3.
8. Williams PL, Bannister LH, Berry MM, Collins P, Dyson M, Dussak JE, *et al*. Gray's Anatomy: Skeletal System. 38th ed. Philadelphia: Churchill Livingstone; 1995. p. 607-12.
9. Meibodi EM, Mastari FR. Study of normal range of anatomical dimensions of one day old newborns by cephalometry. J Med Council Islamic Republic Iran 1996;14:1-8.
10. Franciscus RG, Long JC. Variation in human nasal height and breadth. Am J Phys Anthropol 1991;85:419-27.
11. Zhang XT, Wang SK, Zhang W, Wang XF. Measurement and study of the nose and face and their correlations in the young adult of Han nationality. Plast Reconstr Surg 1990;85:532-6.
12. Porter JP, Olson KL. Analysis of the african american female nose. Plast Reconstr Surg 2003;111:620-6.
13. Perez DA. Influence of Facial Prominence in the Aesthetic Appreciation of Facial Profile. Thesis for the title: Dentist University of Talca Chile; 2004.
14. Canut JA. Dentofacial aesthetic analysis. Rev Esp Ortod 1996;26:13-30.
15. Iida N, Ogwa T, Tsutsumi K, Tonegawa M, Yokaro K. An examination of the external nose reconstruction methods used in our department. Jpn J Plast Reconstr Surg 2002;45:3542.
16. Hochman B, Casticho HT, Ferreira LM. Photographic and morphometric standardization in the computerized photogrammetry of the nose. Acta Cir Bras 2002;17:25866.
17. Harzrika P, Nayak DR, Balakrishna R. The Textbook for Ear, Nose, Throat and Head and Neck Surgery. 1st ed. Dariya Ganj, New Delhi: CBS Publishers and Distributors; 2007. p. 24950.
18. Alex FR, Steven B, Timothy GL. Human Body Composition. 4th ed. Champaign, IL: Human Kinetics Publishers; 1996. p. 16772.
19. Ukoha UU, Egwu OA, Ndukwe GU, Akudu LS, Umeasalugo KE. Anthropometric study of the nose in a student population. Ann Bioanthropol 2016;4:8-11.
20. Anitha S, Vasukuttan KA. Book Reviews Published in Mathrubhoomi Weekly for the Period of 1960–70 Study.
21. Singh IR, Bhasin MK. Somatometry. A Laboratory Manual on Biological Anthropology. 1st ed. Delhi: Kamla-Raj Enterprises; 1968. p. 149-93.
22. Risley HH. Appendix IV, Indo-Aryan Type In: Crook W, editor. The People of India. 2nd ed. Delhi: Orient Books; 1969. p. 389-395.
23. Daniel B. Racial Anthropology and Genetics of the Lebanese; 2002. p. 12.
24. Akpa AO, Ugwu C, Maliki AO, Maliki SO. Morphometric study of nasal parameters in Nigerian Igbos. J Exp Clin Anat 2003;2:245.
25. Oladipo GS, Coker T, Anugweje KC, Abidoye AO. Study of some anthropometric parameters of Itsekiri and Okpe ethnic groups of Delta state, SouthSouth Nigeria. Int J Community Res 2013;2:7780.
26. Sunil NS, Babu KY. The nasal index of South Indian skulls. Int J Adv Res 2017;5:1816-9.
27. Hiernaux J, Boedhi Hartono D. Physical measurements of the adult Hadza of Tanzania. Ann Hum Biol 1980;7:339-46.
28. Nichani JR, Willatt DJ. Dimensional analysis – Its role in our preoperative surgical planning of rhinoplasty. Clin Otolaryngol Allied Sci 2004;29:518-21.
29. Oladipo GS, Gwunireama IU, Asawa OD. Anthropometric comparison of nasal indices between the Igbos and Yorubas in Nigeria. Global J Med Sci 2006;5:37-40.
30. Oladipo GS, Olotu JE, Didia BC. Anthropometric study of Nasal parameters of the Ogonis in Nigeria. Sci Afr 2007;6:69-71.
31. Oladipo GS, Olabiyi AO, Oremosu AA, Noronha CC. Nasal indices among major ethnic groups in Southern Nigeria. Sci Res Essays 2007;2:20-2.
32. Oladipo GS, Eroje MA, Fawehinmi HB. Anthropometric comparison of the nasal indices between the Adoni and Okrika ethnis groups of Rivers state, Nigeria. Int J Med Med Sci 2009;1:135-7.

Original Article

Morphometric Evaluation of Trigeminal Nerve and Meckel Cave with 3.0 Magnetic Resonance Imaging

Selva Sen, Sabriye Sennur Bilgin[1], Alper Atasever

Department of Anatomy, School of Medicine, Istanbul Medipol University, [1]Department of Radiology, Istanbul Medipol University Hospital, Istanbul, Turkey

Abstract

Introduction: This study aimed to investigate morphometric features of the trigeminal nerve in healthy people on magnetic resonance images. The alterations in the size of the trigeminal nerve in the cisternal region along with aging and asymmetry between the right and left trigeminal nerves were also assessed. The knowledge of normal morphometric properties of the trigeminal nerve may be useful in evaluating patients having trigeminal neuralgia. **Material and Methods:** This retrospective study included 120 (62 males, 58 female) healthy individuals over 20 years old who had no previous or current cranial pathology. According to age ranges, individuals were evaluated in four groups as 20–29 years, 30–39 years, 40–49 years, and 50 years and older. Besides the long- and short-axis lengths of the trigeminal nerve, long- and short-axis lengths of Meckel cave, as well as the trigeminal-pons angle, were measured using three-dimensional balance fast-field echo sequence with 3T magnetic resonance imaging on the right and left sides. **Results:** It was observed that the lengths of trigeminal nerve were shorter on the right side in comparison to the left side (mean long axis 0,79 ± 0,20 cm on the right, 0,86 ± 0,28 cm on the left, P <0,05; and mean short-axis: 0,36 ± 0,10 cm on the right and 0,41 ± 0,17 cm on the left, P <0,05). Moreover, in males, the long-axis length of the Meckel cave was higher on both the right and left sides compared to females (P < 0.05). **Discussion and Conclusion:** This study shows that, both the width and length of the right trigeminal nerve are shorter compared to left in healthily population. In addition, long axis of Meckel Cave, that is posterolateral to anteromedial extend, was longer on both the right and left sides in males compared to females.

Keywords: *Aging, morphometry, trigeminal ganglion, trigeminal nerve, trigeminal neuralgia*

Introduction

The trigeminal nerve is the thickest cranial nerve which provides sensitive innervation of the head and face region, as well as the motor innervation of the masticatory muscles besides some other small muscles.[1]

The trigeminal nerve emerges from the anterolateral surface of the pons with two roots: the smaller being one is the motor and the bigger one is the sensory root. These two roots penetrate the pontocerebellar cistern (prepontine cistern), a large cavity containing cerebrospinal fluid, and extend to the apex of the petrous part of the temporal bone. At the apex of the petrous part, it enters the Meckel cave which is a sac formed by dura mater. In this sac, there is the trigeminal ganglion, where the cell bodies of the sensory axons in the trigeminal nerve are located. Distal to the ganglion, the three main branches of the trigeminal nerve arise: ophthalmic nerve, maxillary nerve, and mandibular nerve. Spreading to the head and face, these branches carry pain-temperature, pressure-touch, and vibration senses to the central nervous system. Motor root also enters the Meckel cave and joins the mandibular branch as it passes through the oval foramen.[2,3]

Magnetic resonance imaging (MRI) is a noninvasive method to image the intracranial portion of the trigeminal nerve.[4,5] Daniels *et al*. demonstrated that the magnetic resonance (MR) images of the intracranial portion of the trigeminal nerve matched the photos obtained from the anatomical sections of the same cadaver and concluded that the MRI images could be used to evaluate the cisternal part of the trigeminal nerve.[4]

Lesions involving the cisternal segment of the trigeminal nerve typically present with trigeminal neuralgia (TN).[6] TN is more common in females and on the right

How to cite this article: Sen S, Bilgin SS, Atasever A. Morphometric evaluation of trigeminal nerve and meckel cave with 3.0 magnetic resonance imaging. J Anat Soc India 2020;69:31-6.

Article Info

Received: 12 April 2019
Accepted: 05 February 2020
Available online: 11 April 2020

Address for correspondence:
Ms. Selva Sen,
Department of Anatomy, School of Medicine, İstanbul Medipol University, Kavacık Kavşağı, Atatürk Caddesi No. 19 34000, Kavacık, Beykoz İstanbul, Turkey.
E-mail: selvasen@medipol.edu.tr

Access this article online

Website: www.jasi.org.in
DOI: 10.4103/JASI.JASI_38_19
Quick Response Code:

side. Incidence increases with age and usually observed after the fifth decade.[7,8] Although theories exist, the exact mechanism (s) underlying the idiopathic (primary) TN is not yet understood. Previous studies have described atrophy and size differences of the affected trigeminal nerve relative to the unaffected side or control group.[9-12] The nerve may also be impinged upon by various lesions involving this area. The knowledge of the normal morphometric properties of the trigeminal nerve may be useful for better evaluation of such pathological conditions.

There are only a few studies evaluated the length of trigeminal nerves and branches on cadavers; however, the information obtained from the cadaver may differ from that of a living human due to the applied fixation and manipulation methods.[13-15] To our knowledge, there is no previous study reporting the morphometric characteristics of the cisternal portion of the trigeminal nerve in healthy individuals using MRI, as well as comparison of trigeminal nerve morphometry in terms of lateralization, age, and gender.

This study aimed to investigate morphometric features of the trigeminal nerve in healthy people on MR images. We have also assessed alterations in the size of the trigeminal nerve in the cisternal region along with aging and evaluate the asymmetry between the right and left trigeminal nerves.

Material and Methods

This study was conducted in the Istanbul Medipol Universty Hospital Radiology Department with the approval of the Ethics Committee of Medipol University. In this retrospective study, we included MR images of 120 (62 male, 58 female) individuals who were admitted with various complaints but proven to have no intracranial pathology and no history of TN. Cases were divided into four age groups: 20–29 years, 30–39 years, 40–49 years, and 50 years and older.

All MR examinations were performed on a whole-body 3T unit (Intera Achieva; Philips, Best, the Netherlands) using an 8-channel sensitivity-encoding head coil. Three-dimensional balance fast-feld echo sequences were performed in addition to the routine Magnetic Rezonans sequences. All images were transferred to Philips IntelliSpace workstation, sagittal and coronal reconstruction was utilized on the workstation, For standardization, the measurements were carried out by a single person with the supervision of an experienced neuroradiologist by three repetitions, which were then averaged.

The following anatomical parameters of the trigeminal nerve were measured on both sides:

1. The length of the long axis of the trigeminal nerve in the cisternal region (trigeminal long axis): In axial images, the length of the trigeminal nerve between its origins from the pons to the entrance of the Meckel cavity was measured in the prepontine cistern [Figure 1A]

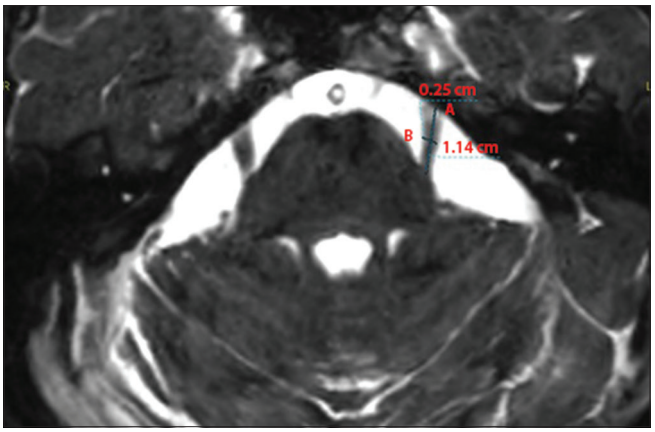

Figure 1: A: Trigeminal long axis, B: trigeminal short axis

2. The length of the short axis of the trigeminal nerve in the cisternal region (trigeminal short axis): The thickness of the mid-point of the trigeminal long-axis length was measured [Figure 1B]
3. The length of the long axis of the Meckel cave (Meckel long axis): The longest distance of the Meckel cave in axial images was measured [Figure 2A]
4. The length of the short axis of the Meckel cave (Meckel short axis): The thickness at the mid-point of the Meckel long axis was measured [Figure 2B]
5. Trigeminal-pons angle (pons angle): The angle between the medial margin of the trigeminal nerve and the anterior surface of the pons at the root entry zone was measured on axial images [Figure 3].

Statistical analysis

Statistical analyses were performed using the SPSS 15.0 for Windows statistical software (SPSS Inc., Chicago, IL, USA). The normal distribution suitability of the variables was tested with one-sample Kolmogorov–Smirnov test. Variables with normal distribution were shown by mean and standard error averages (mean ± standard deviation [SD]). Chi-square, Student's t independent, one-way analysis of variance (ANOVA), and correlation analysis (Pearson and Spearman) tests were used for statistical analysis. The homogeneity of the variances was tested with the Levene test. Two-tailed *post hoc* comparisons were performed using Tukey's honestly significant difference test for groups with significant ANOVA outcome. For statistical significance, $P < 0.05$ was accepted.

Results

The long and short axes of the trigeminal nerve, trigeminal diameter, long and short axes at the Meckel cave, and pons angle were measured on both sides. Measurements of the right and left sides, as well as gender and age group differences, were compared.

The mean values and SDs of the measurements are shown in Table 1 according to gender and laterality. Among genders, none of the measurements showed any statistically

significant difference except the Meckel long axis. The long axis of the Meckel cave was higher in males on both the right and left sides. When the right- and left-side measurements are compared in all cases, trigeminal long and the short axes were longer on the left side. Trigeminal diameter, as well as the Meckel long and short-axis measurements of the right and left sides, showed no significant difference.

Comparisons of measurements among age groups did not show any significant difference [Table 2].

Discussion

The trigeminal nerve is the thickest cranial nerve that receives general sensation from the head region. It also innerves muscles of mastication and some small muscles in the head region. Changes in the structure of the trigeminal nerve may cause clinical problems such as neuralgia and sensory and motor loss. Knowing the morphometric characteristics of the trigeminal nerve and its ganglion in MR images is important in the evaluation of patients with problems involving the trigeminal nerve and its ganglion.[14]

Histologic studies on the anatomy of the trigeminal nerve mostly deal with the axon count and lengths of its branches. Songur *et al*. studied tissue samples of the intracranial portion of trigeminal nerves obtained from forty cadavers. The mean length of the trigeminal nerve was calculated as 25.32 ± 2.90 mm and trigeminal ganglion width as 13.5 ± 1.2 mm.[13] Ajayi *et al*. have investigated the anatomy of the nerve. They calculated the mean length and width of trigeminal ganglion as 18.3 mm and 7.9 mm, respectively.[14] Ziyal *et al*. studied six trigeminal nerves obtained from cadavers and reported the length of the trigeminal nerve ranging from 28 to 31 mm.[15] These values are considerably lower than the values obtained in our study, which we think might be due to the used chemicals in cadaver studies and the differences in the measurement method.

Yıldız *et al*. studied the volumes of the cisternal portions of trigeminal nerves on both sides in 100 healthy individuals with MRI and compared the differences between genders and the differences between the right and left sides. They reported no significant difference between the left and right trigeminal nerve volumes and also no difference among genders. However, volume differences between the left and right sides in the healthy individuals were low (4.6% ±3.6%) compared to reported differences in TN patients. They stated that the difference in trigeminal nerve volume between normal and symptomatic sides might be an important finding in suspected cases of TN, though it is not clear whether trigeminal nerve atrophy is a cause or consequence of TN.[16]

Taarnhøj and Olivecrona suggest that the elongation of the brainstem with atrophy in the elderly leads to stretching of the trigeminal nerve.[17,18] Kakizawa *et al*. evaluated 110 healthy individuals and found that the long axis of the trigeminal nerve in the cisternal segment at the sagittal oblique plane MRI was significantly longer in healthy elderly individuals and suggested that this was due to brain stem atrophy.[19]

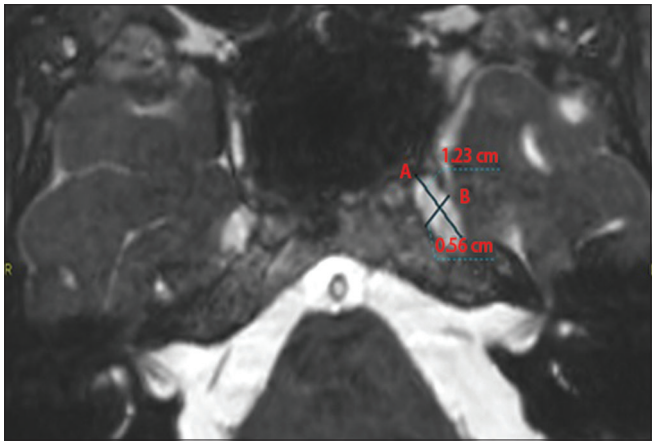

Figure 2: A: Meckel long axis, B: Meckel short axis

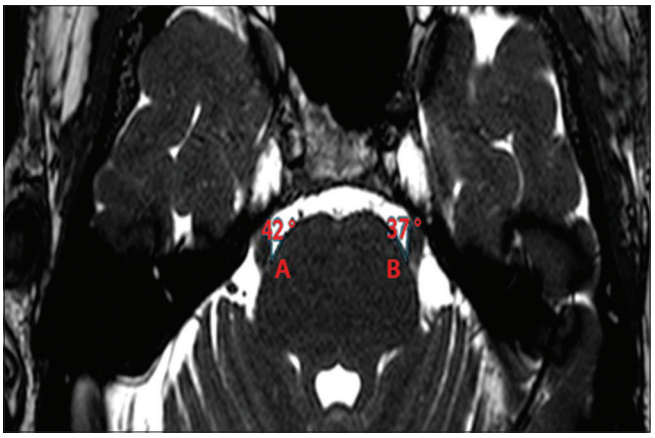

Figure 3: Pons angle

Table 1: The mean values and standard deviations of measurements by gender and laterality

	Female		Male		Total		*P*	
	Right	Left	Right	Left	Right	Left	Right	Left
Trigeminal long axis	0.77±0.22	0.84±0.26	0.81±0.19	0.88±0.26	0.79±0.20	0.86±0.28	0.23	0.44
Trigeminal short axis	0.37±0.14	0.39±0.14	0.36±0.07	0.42±0.19	0.36±0.10	0.41±0.17	0.5	0.29
Meckel long axis	1.19±0.26	1.21±0.20	1.29±0.24	1.30±0.19	1.25±0.25	1.26±0.20	0.03	0.02
Meckel short axis	0.50±0.10	0.49±0.10	0.52±0.11	0.52±0.12	0.51±0.10	0.50±0.11	0.25	0.17
Pons angle	38.95±13.94	32.74±12.26	39.31±14.04	36.95±11.20	39.13±13.93	34.92±11.86	0.89	0.05

Table 2: The compression of measurements by age group

	20-29		30-39		40-49		50 and over		*P*	
	Right	Left	Right	Left	Right	Left	Right	Left	Right	Left
Trigeminal long axis	0.81±0.18	0.89±0.24	0.74±0.19	0.81±0.29	0.78±0.21	0.8±0.28	0.84±0.24	0.93±0.32	0.26	0.22
Trigeminal short axis	0.35±0.07	0.35±0.07	0.37±0.13	0.43±0.16	0.39±0.08	0.46±0.20	0.35±0.13	0.4±0.21	0.39	0.06
Meckel long axis	1.28±0.22	1.28±0.14	1.25±0.22	1.17±0.19	1.21±0.31	1.29±0.24	1.25±0.25	1.28±0.21	0.72	0.05
Meckel short axis	0.5±0.10	0.49±0.09	0.5±0.12	0.48±0.10	0.49±0.10	0.49±0.13	0.54±0.09	0.55±0.11	0.3	0.08
Pons angle	37.20±13.28	34.80±12.93	37.50±13.61	31.43±11.64	38.00±14.81	34.53±11.70	43.83±13.61	38.9±10.42	0.2	0.11

Rasche *et al*. suggested that cisternal volume should be higher due to brainstem atrophy in the elderly, and therefore, the position of the superior cerebellar artery is changed as the cerebellar tentorium is displaced caudally. This displacement may increase trigeminal nerve compression by blood vessels. With the above reasoning, they suggested that the length of the trigeminal nerve in the cisternal segment and the angle of emergence from the pons might be important in TN etiology.[20] In our study, there was no significant statistical difference in the variance analysis of long- and short-axis length of the trigeminal nerve, Meckel cave, and trigeminal-pons angle among the age groups. We could not find any other studies dealing with the in-depth analysis of the morphological characteristics of the trigeminal nerve with aging.

In our study, the average length of the long axis of the trigeminal nerve was 0.79 ± 0.20 cm on the right and 0.86 ± 0.28 cm on the left side, and the average length of the short axis was 0.36 ± 0.10 cm on the right and 0.41 ± 0.17 cm on the left side. The trigeminal long-axis length values were little higher than the findings of Parise *et al*. (6.33 ± 2.19 mm) and similar with those of Cheng *et al*. (8.3 ± 2.2 mm) with the measurements obtained from TN patients.[9,21] Ha *et al*. measured the short-axis length of 3.46 mm in 30 healthy individuals. Ha *et al*. reported that there was no significant difference in the length of the short and long axes of the trigeminal nerve between the right and left sides in healthy individuals and only in TN patients between the affected and unaffected sides.[22] Other than this study, we could not found any studies assessing the trigeminal short-axis length in the literature. Interestingly, in our study, both short- and long-axis lengths were significantly shorter on the right side, where TN was frequently seen.

Park *et al*. analyzed the relationship between the morphometric characteristics of the trigeminal nerve and pontine cisternal volume on TN patients. On the affected side, they observed the smaller the pontine cisternal volume is, the shorter is the trigeminal nerve becomes. Smaller pontine cistern and shorter trigeminal nerve might be more prone to be compressed by vessels.[23]

Cheng *et al*. measured the length of the cisternal segment of the trigeminal nerve in 60 TN patients and 30 healthy individuals. They observed that there were no significant difference between the right and left sides in healthy people and no difference also between the affected and unaffected sides in TN patients.[9]

Parise *et al*. suggested that anatomic factors such as the volume of the posterior cranial fossa may affect the proximity between the vascular structures and the trigeminal nerve. They measured the volume of the cisternal region and the length of the trigeminal nerve in 18 healthy individuals and 26 TN patients. They reported that in the TN group, the cisternal length of the trigeminal nerve was shorter on the affected side. Furthermore, the cisternal length of the trigeminal nerve in all TN patients was shorter than healthy individuals, though the difference was not statistically significant.[21] Shorter cisternal region and the length of the nerve may predispose to compression in terms of closer proximity with the surrounding structures. However, if the brainstem atrophy and caudal sagging occur with age, these findings are inconsistent, as one would expect that the length of the trigeminal nerve should be greater on the affected side.

Bjerrum and Thornval, *et al*. suggested that mechanical factors altering the shape of the skull could cause neuralgia by stretching the trigeminal nerve.[24] Gardner stated that asymmetrically petrous apex is higher on one side, causing trigeminal nerve stretching and resulting TN. He observed that elevation of the petrous apex is more common on the right side even in healthy people.[25] Smith and Mumford suggested that the angle of the petrous part of the temporal bone was considerably variable and it might have a role in the etiology of TN.[26] Bjerrum and Thornval reported that petrous apex was higher on the affected side in TN cases.[24] Our findings are inconsistent as one would expect that the length of the trigeminal nerve should be greater on the right side due to the elevation of the petrous apex, where TN was frequently seen. Rothman and Wepsic determined that a high position of the petrous apex was a poor risk factor for TN and did not correlate with the greater presence of neuralgia on the right side.[27] Brinzeu *et al*. measured the angle of the petrous ridge and angle of the nerve on passing over the ridge in 42 TN patients. They found that the bony angle of the petrous ridge was more acute on the affected side in TN patients and also significantly more acute compared to the controls.[28] Hence, the trigeminal nerve may be stretched by the petrous bone in TN.

Pons angle

Ha *et al*. suggested that the decrease of pons angle on the affected side in patients with TN may increase microvascular compression at the medial margin of the trigeminal nerve.[22] In their study, evaluating 30 TN patients, they found the mean pons angle as 40.17° on the affected side, 51.39° on the unaffected side, and 52.02° in healthy individuals. There was no difference in the right and left sides in healthy individuals.

Cheng *et al*. measured the mean pons angle as 42.4° on the affected side, 47.6° on the nonaffected side, and 46.0° in the control group.[9] Cheng *et al*. and Ha *et al*. found that the pons angle on the affected side is smaller than the nonaffected side in patients with TN. Therefore, they suggested that a small angle may increase the possibility of neurovascular compression.[22,29]

In our study, the mean trigeminal-pons angle was measured as 39.13 °±13.93° on the right side and 34.92° ±11.86° o n the left side. The mean trigeminal-pons angle values were found to be higher on the right side, but this difference was not statistically significant. Furthermore, there was no statistically significant difference between gender and age groups. The pons angle values in our study were found to be less than those mentioned above, which might be due to racial differences.

Meckel cave

Rasche *et al*. suggested that prepontine cistern and Meckel cave should be smaller in patients with TN as a consequence of the more caudal displacement of the cerebellar tentorium.[20]

Ha *et al*. measured Meckel cave volume on axial MRI and found no significant difference between healthy individuals and TN patients.[22]

In our study, the long axis of the Meckel cave was found to be longer on both sides in males than females. This might be due to the bigger skull size in males. The short axis of the Meckel cave did not show any difference among all compared groups.

Conclusion

We have not found any change in the morphometric properties of the trigeminal nerve and the Meckel cave with aging. Short- and long-axis lengths of the trigeminal nerve were shorter on the right side, and the right pons angle was larger than the left side. It needs further studies to evaluate whether the shorter length and larger pons angle of the trigeminal nerve play a role in the etiology of TN and more frequent occurrence on the right side.

In this study, only healthy individuals were evaluated. For more accurate investigations of the etiology of TN, our findings should be compared with MR images obtained from TN patients.

Financial support and sponsorship

Nil.

Conflicts of interest

There are no conflicts of interest.

References

1. Maria AP, Leslie PG. Cranial nerves. In: A Textbook of Neuroanatomy. 1st ed. New Jersey: Wiley; 2013. p. 325-32.
2. Kaplan A, Alaiitin E. Anatomi. 5th ed. Ankara: Günes Kitapevi; 2014. p. 2, 199-201.
3. Duane EH, Brainstem. Standring S, editor. Gray's Anatomy: The Anatomical Basis of Clinical Practice, 41nd ed. Churchill Livingstone: Elsevier; 2016. p. 309-21.
4. Daniels DL, Pech P, Pojunas KW, Kilgore DP, Williams AL, Haughton VM. Trigeminal nerve: Anatomic correlation with MR imaging. Radiology 1986;159:577-83.
5. Yousry I, Moriggl B, Schmid UD, Naidich TP, Yousry TA. Trigeminal ganglion and its divisions: Detailed anatomic MR imaging with contrast-enhanced 3D constructive interference in the steady state sequences. AJNR Am J Neuroradiol 2005;26:1128-35.
6. Bathla G, Hegde AN. The trigeminal nerve: An illustrated review of its imaging anatomy and pathology. Clin Radiol 2013;68:203-13.
7. Sathasivam HP, Ismail S, Ahmad AR, Basri NN, Muhamad H, Mohd Tahir NF, *et al*. Trigeminal neuralgia: A retrospective multicentre study of 320 Asian patients. Oral Surg Oral Med Oral Pathol Oral Radiol 2017;123:51-7.
8. Watson P. Postherpetic neuralgia. Am Fam Physician 2011;84:690-2.
9. Cheng J, Meng J, Liu W, Zhang H, Hui X, Lei D. Nerve atrophy in trigeminal neuralgia due to neurovascular compression and its association with surgical outcomes after microvascular decompression. Acta Neurochir (Wien) 2017;159:1699-705.
10. Duan Y, Sweet J, Munyon C, Miller J. Degree of distal trigeminal nerve atrophy predicts outcome after microvascular decompression for Type 1a trigeminal neuralgia. J Neurosurg 2015;123:1512-8.
11. Wilcox SL, Gustin SM, Eykman EN, Fowler G, Peck CC, Murray GM, *et al*. Trigeminal nerve anatomy in neuropathic and non-neuropathic orofacial pain patients. J Pain 2013;14:865-72.
12. Yousry I, Moriggl B, Schmid UD, Naidich TP, Yousry TA. Trigeminal ganglion and its divisions: Detailed anatomic MR imaging with contrast-enhanced 3D constructive interference in the steady state sequences. AJNR Am J Neuroradiol 2005;26:1128-35.
13. Songur A, Acar T, Özen O, Baş O, Şahin Ö, Küçüker H, *et al*. The Investigation of the Course of Trigeminal Nerve in the Cranial Base and Histological Analysis. Fırat Tıp Derg 2008;13:171-5.
14. Ajayi NO, Lazarus L, Satyapal KS. Trigeminal cave and ganglion: An anatomical review. Int J Morphol 2013;31:1444-8.
15. Ziyal IM, Sekhar LN, Ozgen T, Söylemezoğlu F, Alper M, Beşer M. The trigeminal nerve and ganglion: An anatomical, histological, and radiological study addressing the transtrigeminal approach. Surg Neurol 2004;61:564-73.
16. Yildiz E, Dincer A, Yolcu S, Peker S. Volume of the cisternal portion of the trigeminal nerve: A study with 3.0-tesla constructive-interference-in-steady-state imaging of healthy subjects. J Neurol Sci 2015;32:106-14.
17. Taarnhøj P. Decompression of the trigeminal root and the

posterior part of the ganglion as treatment in trigeminal neuralgia; preliminary communication. J Neurosurg 1952;9:288-90.
18. Olivecrona H. Trigeminal neuralgia and its treatment (article in German). Nervenarzt 1941;14:49-57.
19. Kakizawa Y, Seguchi T, Kodama K, Ogiwara T, Sasaki T, Goto T, *et al*. Anatomical study of the trigeminal and facial cranial nerves with the aid of 3.0-tesla magnetic resonance imaging. J Neurosurg 2008;108:483-90.
20. Rasche D, Kress B, Stippich C, Nennig E, Sartor K, Tronnier VM. Volumetric measurement of the pontomesencephalic cistern in patients with trigeminal neuralgia and healthy controls. Neurosurgery 2006;59:614-20.
21. Parise M, Acioly MA, Ribeiro CT, Vincent M, Gasparetto EL. The role of the cerebellopontine angle cistern area and trigeminal nerve length in the pathogenesis of trigeminal neuralgia: A prospective case-control study. Acta Neurochir (Wien) 2013;155:863-8.
22. Ha SM, Kim SH, Yoo EH, Han IB, Shin DA, Cho KG, *et al*. Patients with idiopathic trigeminal neuralgia have a sharper-than-normal trigeminal-pontine angle and trigeminal nerve atrophy. Acta Neurochir (Wien) 2012;154:1627-33.
23. Park SH, Hwang SK, Lee SH, Park J, Hwang JH, Hamm IS. Nerve atrophy and a small cerebellopontine angle cistern in patients with trigeminal neuralgia. J Neurosurg 2009;110:633-7.
24. Bjerrum J, Thornval G. Roentgenographic findings in trigeminal neuralgia. Acta radiol 1959;51:289-96.
25. Gardner WJ, Todd EM, Pinto JP. Roentgenographic findings in trigeminal neuralgia. Am J Roentgenol Radium Ther Nucl Med 1956;76:346-50.
26. Smith DG, Mumford JM. Petrous angle and trigeminal neuralgia. Pain 1980;8:269-77.
27. Rothman KJ, Wepsic JG. Side of facial pain in trigeminal neuralgia. J Neurosurg 1974;40:514-23.
28. Brinzeu A, Dumot C, Sindou M. Role of the petrous ridge and angulation of the trigeminal nerve in the pathogenesis of trigeminal neuralgia, with implications for microvascular decompression. Acta Neurochir (Wien) 2018;160:971-6.
29. Cheng J, Meng J, Liu W, Zhang H, Lei D, Hui X. Nerve atrophy and a small trigeminal pontine angle in primary trigeminal neuralgia: A morphometric magnetic resonance imaging study. World Neurosurg 2017;104:575-80.

Original Article

Gene Alterations after Human Adipose-Derived Stem Cell-Derived Exosome Injection in Monosodium Iodoacetate-Induced Osteoarthritis Rats by Microarray Analysis

Jae Chul Lee[1,2], Soo Young Choe[3]

[1]Department of Plastic and Reconstructive Surgery, Seoul National University College of Medicine, Seoul National University Bundang Hospital, Seongnam, [2]Department of Obstetrics and Gynecology, University of Ulsan College of Medicine, Asan Medical Center, Seoul, [3]Department of Biology, School of Life Sciences, Chungbuk National University, Cheongju, Korea

Abstract

Introduction: Exosome (exo) is a small extracellular vesicles containing cell-derived factors, and serve to mediate the paracrine effect of cells. Despite the therapeutic potential of human adipose-derived stem cells (hADSCs)-derived exo-related treatment modalities, the molecular parameters needed to define the "paracrine effect" remain largely unknown. **Material and Methods:** Using high-density oligonucleotide RNA sequencing, the differential gene expression profiles between a fraction of exo (derived from hADSCs) and its mesenchymal stem cells subpopulation were obtained. **Results:** Of particular interest was a subset of 66 genes preferentially expressed at fivefold or higher in the group treated with exo derived from hADSCs. This subset contained numerous genes involved in the angiogenesis, inflammatory response, immune response, cell cycle, cell death, cell differentiation, cell proliferation, DNA repair, RNA splicing, and secretion functions. In addition, six protein networks were constructed. The interaction network consisted of 57 proteins encoded by upregulated genes. However, the interaction network also consisted of 69 proteins encoded by downregulated genes. **Discussion and Conclusion:** Our results provide a basis for more reproducible and reliable quality control using genotypic analysis for the definition of hADSCs-exo. Therefore, these results will serve to provide a basis for studies of the molecular mechanisms which control the core properties of hADSCs-exo. Understanding the processes driving hADSCs-exo recruitment could prove invaluable in the development of novel, targeted therapies to selectively inhibit pathological responses in OA.

Keywords: *Adipose-derived stem cell, exosome, microarray, monosodium iodoacetate, osteoarthritis*

Introduction

Osteoarthritis (OA) is the most common chronic joint disease diagnosed in the general population, a disease characterized by structural and functional alterations of the articular cartilage.[1] Although OA afflicts a large proportion of the population, there exist relatively few effective therapies which serve to alter or inhibit the actual patho-biologic course of the disease.[2] For many years, scientists have been searching for ways to inhibit the destructive process of the disease, or at least to slow the progressive and irreversible joint damage.[3] This is the driving force behind the numerous current and ongoing efforts to develop new tissue engineering-based strategies for the treatment of OA.[4] Exosomes (exos) are small extracellular membrane vesicles (30–100 nm in diameter) with a mechanism of cell-to-cell communication. Exos are the most extensive class of secreted membrane vesicles that carry proteins and RNAs for intercellular communication.[5-7] Due to their significant and dynamic role in the biology of a living organism, exo has been widely studied as both a biomarker and therapeutic agent.[8,9] Although exos derived from stem cells have therapeutic potential with regard to the curative treatment of many illnesses, the precise mechanism by which adipose-derived stem cell (ADSC)-derived exo (ADSCs-exo) affect the natural OA progression has not been widely or fully investigated. Gene expression profiling using microarray analysis has become a promising approach for identifying the changes underlying the initiation and progression of complex diseases such as OA, as well as for the discovery of "biomarkers" for diagnostic purposes, disease activity,

How to cite this article: Lee JC, Choe SY. Gene alterations after human adipose-derived stem cell-derived exosome injection in monosodium iodoacetate-induced osteoarthritis rats by microarray analysis. J Anat Soc India 2020;69:37-47.

Article Info

Received: 03 June 2019
Accepted: 16 January 2020
Available online: 11 April 2020

Address for correspondence:
Dr. Jae Chul Lee, Department of Plastic and Reconstructive Surgery, Seoul National University Bundang Hospital, 82, Gumi-ro 173 Beon-Gil, Bundang-Gu, Seongnam-si, Gyeonggi-do 463707, Korea.
E-mail: beas100@snu.ac.kr
Dr. Soo Young Choe, Department of Biology, Chungbuk National University, 52 Naesudong-ro, Heungdeok-gu, Cheongju 361-804, Korea.
E-mail: leejc@chungbuk.ac.kr

Access this article online

Website: www.jasi.org.in
DOI: 10.4103/JASI.JASI_67_19
Quick Response Code:

and response to treatment.[10] Therefore, in this study, we investigated the changes in gene expression and performed construction of the protein regulatory network by microarray analysis after the injection of human adipose-derived stem cells (hADSCs)-exo into monosodium iodoacetate (MIA)-induced OA rats.

Material and Methods

Animals and treatment

Six-week-old male Sprague-Dawley rats, weighing approximately 180–220 g each, were used for this study. All animal experiments conducted in accordance with the National Institutes of Health Guide for the Care Use of Laboratory Animals (NIH publication No. 86-23, revised in 1996). Knee tissue samples were immediately excised and submitted for microarray analysis.

Monosodium iodoacetate-induced osteoarthritis rat model

Under anesthesia, 50 μL of MIA, dissolved in phosphate-buffered saline (PBS) to yield a concentration of 10 mg/mL, was intra-articularly injected through the infrapatellar ligament of the right knee using a 26G needle. Exactly 1 week after MIA injection, rats in group #5 were administered an intra-articular injection of 200 μL human ADSCs-exo. Rats treated with PBS but not with MIA were used as the control group [Table 1].

Human adipose-derived stem cells culture

Subcutaneous adipose samples were obtained from normal humans who provided written informed consent to participate in the experiment. Adipose samples obtained from the patients were maintained in PBS containing antibiotics/antimycotics (Invitrogen, USA) and transported to our laboratory within a day. The ADSCs used for the generation of ADSCs-exo were at passage3–4.

Isolation and identification of exosome derived from adipose-derived stem cells-conditioned medium (CM)

To deplete bovine exos from the medium, the culture medium was centrifuged at 100,000 g for 15 h at 4°C and supernatant was used for ADSC culture.[11] Exo isolation, using Exo-Quick exo precipitation kit (System Biosciences, USA), was performed according to the manufacturer's specifications. The collected exosome morphologies were observed by 100 kv transmission electron microscopy (TEM) [Figure 1a and b].

Table 1: Differentially expressed genes between four groups

	Overexpression	Downexpression
MIA versus Control	1340* (489)†	1389* (502)†
ADSC versus MIA	1206* (500)†	1384* (441)†
ADSC-exo versus MIA	1923* (1017)†	1974* (664)†
ADSC-exo versus ADSC	1458* (560)†	1303* (450)†

Values are means±SD. *1.5-fold increase in the expression of genes, †2-fold increase in the expression of genes. Control: Control group, MIA: Monosodium iodoacetate group, ADSC: Human ADSCs group, ADSC-exo: Human ADSC-derived exosome, SD: Standard deviation

Quantification of exosome by CD81 ELISA

The concentration of exosome was determined by the amount of total immunoreactive exosome-associated CD81 (ExoELISA™, System Biosciences, Mountain View, CA). Briefly, 50 μl of exosome was immobilized in 96-well microtiter plates and incubated overnight at 37°C (binding step). Plates were washed three times for 5 min using a wash buffer solution and then incubated with primary antibody (CD81) at room temperature (RT) for 1 hr under agitation. Plates were washed and incubated with secondary antibody (1:5000) at RT 1 hr under agitation. Plates were washed and incubated with super-sensitive TMB ELISA substrate at RT for 45 min under agitation. The reaction was terminated using Stop Buffer solution. Absorbance was measured at 450 nm. The number of exosome particles/ml was obtained using an exosomal CD81 standard curve calibrated against number of exosome particles [Figure 1c].

Injection of adipose-derived stem cells-exo

ADSCs-exos were isolated from the adipose stem cells-culture medium 1 week after MIA injection, and cultured for 4–5 days, as described above. At 1 week post-MIA injection, ADSCs-exo (200 mg/ml) in 200 μL PBS were intra-articularly injected into the right knee using a 26G needle.

RNA extraction and cDNA synthesis

Total RNA was extracted from the right knee samples, which had been stored for 24 h at room temperature, and then refrigerated (−20°C) using a PAXgene knee RNA extraction kit according to the manufacturer's instructions.

Microarray analysis

Each total RNA sample (100 ng) was labeled and amplified using Low Input Quick Amp Labeling Kit (Agilent Technologies, CA, USA). The Cy3-labeled aRNAs were resuspended in 50 μl of hybridization solution (Agilent Technologies, CA, USA).

Statistical analysis

The arrays were analyzed using an Agilent scanner with associated software. Gene expression levels were calculated with Feature Extraction version 10.7.3.1 (Agilent Technologies, Santa Clara, CA, USA). Fold change filters included the requirement that the genes are present in at least 300% of controls for upregulated genes and lower than 300% of controls for downregulated genes.

Table 2: Upregulated genes expressed by over 500% between monosodium iodoacetate group and control group

Gene name	Gene ontology	Synonyms	GeneBank
Indian hedgehog	Angiogenesis	Ihh	NM_053384
Secretogranin II	Angiogenesis	Scg2	NM_022669
Fibroblast growth factor 10	Cell cycle	Fgf10	NM_012951
BMP/retinoic acid inducible neural specific 3	Cell cycle	Brinp3	NM_173121
MIS12, MIND kinetochore complex component, homolog (*Schizosaccharomyces pombe*)	Cell cycle	Mis12	NM_001047972
DMC1 dosage suppressor of mck1 homolog, meiosis-specific homologous recombination (yeast)	Cell cycle	Dmc1	NM_001130567
Folliculin interacting protein 2	Cell death	Fnip2	NM_001271167
Calcium-sensing receptor	Cell death	Casr	NM_016996
Salt-inducible kinase 1	Cell death	Sik1	NM_021693
Leucine-rich repeat kinase 2	Cell death	Lrrk2	NM_001191789
Transcription factor AP-2 beta	Cell death	Tfap2b	NM_001106896
Amyotrophic lateral sclerosis 2 (juvenile)	Cell death	Als2	NM_001013413
Collagen, type IX, alpha 1	Cell differentiation	Col9a1	NM_001100842
Collagen, type II, alpha 1	Cell differentiation	Col2a1	NM_012929
Glutamate receptor, ionotropic, delta 2 (Grid2) interacting protein	Cell differentiation	Grid2	NM_001105910
Forkhead box A2	Cell differentiation	Foxa2	NM_012743
Neural cell adhesion molecule 2	Cell differentiation	Ncam2	NM_203409
G protein-coupled receptor 157	Cell differentiation	Gpr157	NM_001012107
ELAV (embryonic lethal, abnormal vision, Drosophila)-like 4	Cell differentiation	Elavl4	NM_001077651
Nuclear receptor subfamily 2, group E, member 1	Cell differentiation	Nr2e1	NM_001113197
Oligodendrocyte transcription factor 3	Cell differentiation	Olig3	NM_001106269
Leucine-rich repeat and Ig domain containing 2	Cell differentiation	Lingo2	NM_001107926
Adhesion G protein-coupled receptor L3	Cell differentiation	Adgrl3	NM_130822
Paired box 5	Cell differentiation	Pax5	NM_001109261
Matrix metallopeptidase 8	Cell differentiation	Mmp8	NM_022221
The stimulator of chondrogenesis 1	Cell proliferation	Scrg1	NM_033499
POU class 3 homeobox 3	Cell proliferation	Pou3f3	NM_138837
Patched 1	Cell proliferation	Ptch1	NM_053566
Hedgehog interacting protein	Cell proliferation	Hhip	NM_001191817
RNA binding fox-1 homolog 3	RNA splicing	Rbfox3	NM_001134498
Muscleblind-like 1 (Drosophila)	RNA splicing	Mbnl1	NM_001191566
Complexin 2	Immune response	Cplx2	NM_053878
Zona pellucida glycoprotein 3 (sperm receptor)	Immune response	Zp3	NM_053762
Chemokine (C-C motif) ligand 25	Immune response	Ccl25	NM_001037203
Vesicle-associated membrane protein 7	Immune response	Vamp7	NM_053531
Ring finger protein 135	Immune response	Rnf135	NM_001012010
Complement component 4 binding protein, alpha	Immune response	C4bpa	NM_012516
Interferon regulatory factor 8	Immune response	Irf8	NM_001008722
Interleukin 17B	Inflammatory response	Il17b	NM_053789
Alpha-1-inhibitor III	Inflammatory response	A1i3	NM_001037975
Murinoglobulin 1	Inflammatory response	Mug1	NM_023103
Histone cluster 1, H2ba	Inflammatory response	Hist1h2ba	NM_022643
Leukotriene B4 receptor 2	Inflammatory response	Ltb4r	NM_053640
Phospholipase A2, group X	Secretion	Pla2g10	NM_017176
Protein tyrosine phosphatase, receptor type, N polypeptide 2	Secretion	Ptprn2	NM_031600
Endothelin 3	Secretion	Edn3	NM_001077650
Complexin 2	Secretion	Cplx2	NM_053878
Tectorin alpha	Extracellular matrix	Tecta	NM_001106814
Aggrecan	Extracellular matrix	Acan	NM_022190
Matrix metallopeptidase 20	Extracellular matrix	Mmp20	NM_001106800
Zona pellucida glycoprotein 2 (sperm receptor)	Extracellular matrix	Zp2	NM_031150
Matrilin 1, cartilage matrix protein	Extracellular matrix	Matn1	NM_001006979

Table 3: Down-regulated genes expressed by over 600% between monosodium iodoacetate group and the control group

Gene name	Gene ontology	Synonyms	GeneBank
Paired-like homeodomain 2	Angiogenesis	Pitx2	NM_019334
T-box 4	Angiogenesis	Tbx4	NM_001107034
Granzyme B (granzyme 2, cytotoxic T-lymphocyte-associated serine esterase 1)	Apoptotic process	Gzmb	NM_138517
Hypermethylated in cancer 1	Apoptotic process	Hic1	NM_001107021
Growth arrest-specific 2	Apoptotic process	Gas2	NM_001127504
2 ‘ -5 ‘ oligoadenylate synthetase 1K	Immune response	Oas1k	NM_001009489
2 ‘ -5 ‘ oligoadenylate synthetase 1H	Immune response	Oas1h	NM_001009491
SH2 domain containing 1A	Immune response	Sh2d1a	NM_001109313
2’-5’ oligoadenylate synthetase 1A	Immune response	Oas1a	NM_138913
Complement component 4 binding protein, beta	Immune response	C4bpb	NM_016995
Ubiquitin D	Inflammatory response	Ubd	NM_053299
Chemokine (C-X-C motif) ligand 2	Inflammatory response	Cxcl11	NM_053647
Chemokine (C-C motif) ligand 12	Inflammatory response	Ccl12	NM_001105822
Chemokine (C-X-C motif) ligand 10	Inflammatory response	Cxcl10	NM_139089
Chemokine (C-X-C motif) ligand 13	Inflammatory response	Cxcl13	NM_001017496
Chemokine (C-X-C motif) ligand 9	Inflammatory response	Cxcl9	NM_145672
Alpha-2-HS-glycoprotein	Inflammatory response	Ahsg	NM_012898
Carbonic anhydrase 9	Secretion	Car9	NM_001107956
Double C2, gamma	Secretion	Doc2g	NM_001011937
Activin A receptor, type IIB	Secretion	Acvr2b	NM_031554
Tetraspanin 14	Cell migration	Tspan1	NM_001169127
MAM domain-containing glycosylphosphatidylinositol anchor 1	Cell migration	Mdga1	NM_001107618
L1 cell adhesion molecule	Cell migration	L1cam	NM_017345
SRY (sex determining region Y)-box 18	Cell migration	Sox18	NM_001024781
Collagen-like tail subunit (single strand of homotrimer) of asymmetric acetylcholinesterase	Extracellular matrix	Colq	NM_019274
Leucine-rich repeat neuronal 1	Extracellular matrix	Lrrn1	NM_001037363
Matrix metallopeptidase 7	Extracellular matrix	Mmp7	NM_012864
Dentin sialophosphoprotein	Extracellular matrix	Dspp	NM_012790
LIM and cysteine-rich domains 1	Extracellular matrix	Lmcd1	NM_001008562

Results

Comparison of microarray analysis between the monosodium iodoacetate group and the control group

The expression levels of 2729 genes in the MIA treatment group were significantly different from those in the control group. In addition, no significant difference between the positive control and negative control (data not shown) genes was appreciated. The MIA treatment induced a 1.5-fold increase in the expression of 1340 genes (a two-fold increase in the expression of 489 genes) and a 1.5-fold decrease in the expression of 1389 genes (a two-fold decrease in the expression of 502 genes) compared to the control group [Table 1]. Among the upregulated genes [Table 2], two genes were related to angiogenesis, four genes to cell cycle, six genes to cell death, thirteen genes to cell differentiation, four genes to cell proliferation, two genes to RNA splicing, four genes to secretion, and five genes were related to the extracellular matrix. Seven genes were found to be related to the immune response, and five genes were found to be related to the inflammatory response. Twenty-nine genes were down-regulated in the MIA group compared with the control group [Table 3].

Comparison of microarray analysis of monosodium iodoacetate and adipose-derived stem cells treatment in monosodium iodoacetate-induced osteoarthritis rats

In microarray analysis, 500 genes showed more than two-fold upregulation of expression, while 441 genes were downregulated in the MIA treatment group compared with the ADSCs treatment group [Table 1]. The expressed genes which showed a six-fold increase are summarized in Table 4. One gene was related to angiogenesis, five genes to cell death, nineteen genes to cell differentiation, two genes to cell migration, ten genes to the immune response, and three genes were related to the inflammatory response. The genes which showed decreased expression levels are summarized in Table 5.

Comparison of microarray analysis of monosodium iodoacetate and adipose-derived stem cells-exo treatment in monosodium iodoacetate-induced osteoarthritis rats

In RNA-sequencing (Seq) analysis, 1017 genes showed

Table 4: Up-regulated genes expressed by over 600% between monosodium iodoacetate group and adipose-derived stem cell group

Gene name	Gene ontology	Synonyms	GeneBank
T-box 4	Angiogenesis	Tbx4	NM_001107034
Growth arrest-specific 2	Cell death	Gas2	NM_001127504
Ataxia, cerebellar, Cayman type	Cell death	Atcay	NM_001040190
Secreted frizzled-related protein 2	Cell death	Sfrp2	NM_001100700
SHC (Src homology 2 domain-containing) family, member 4	Cell death	Shc4	NM_001191065
Hypermethylated in cancer 1	Cell death	Hic1	NM_001107021
Myosin, light chain 2, regulatory, cardiac, slow	Cell differentiation	Myl2	NM_001035252
Myozenin 2	Cell differentiation	Myoz2	NM_001106469
Protocadherin related 15	Cell differentiation	Pcdh15	NM_001271377
BARX homeobox 1	Cell differentiation	Barx1	NM_001108880
Glutamate receptor interacting protein 1	Cell differentiation	Grip1	NM_032069
Solute carrier family 7 (anionic amino acid transporter light chain, xc- system), member 11	Cell differentiation	Slc7a11	NM_001107673
Sterile alpha and TIR motif-containing 1	Cell differentiation	Sarm1	NM_001105817
Glycoprotein m6b	Cell differentiation	Gpm6b	NM_138846
Ankyrin repeat domain 27 (VPS9 domain)	Cell differentiation	Ankrd2	NM_001271264
EPH receptor A5	Cell differentiation	Epha5	NM_024367
Solute carrier family 39 (zinc transporter), member 12	Cell differentiation	Slc39a12	NM_001106124
Neurofascin	Cell differentiation	Nfasc	NM_001160313
Myosin, heavy chain 11, smooth muscle	Cell differentiation	Myh11	NM_001170600
Smooth muscle alpha-actin	Cell differentiation	Acta2	NM_031004
Cysteine and glycine-rich protein 3 (cardiac LIM protein)	Cell differentiation	Csrp3	NM_057144
Early B-cell factor 2	Cell differentiation	Ebf2	NM_001108383
Myosin binding protein H	Cell differentiation	Mybph	NM_031813
Cell adhesion associated, oncogene regulated	Cell differentiation	Cdon	NM_017358
Biogenesis of lysosomal organelles complex-1, subunit 2	Cell differentiation	C1s	NM_001037349
Paired-like homeodomain 2	Cell migration	Pitx2	NM_019334
Glypican 3	Cell migration	Gpc3	NM_012774
Chemokine (C-X-C motif) ligand 11	Immune response	Cxcl11	NM_182952
RT1 class Ia, locus A2	Immune response	RT1-A2	NM_001008829
Complement factor B	Immune response	Cfb	NM_212466
Myxovirus (influenza virus) resistance 2	Immune response	Mx2	NM_134350
Chemokine (C-X-C motif) ligand 13	Immune response	Cxcl13	NM_001017496
Serine (or cysteine) peptidase inhibitor, clade A, member 3N	Immune response	Serpina3n	NM_031531
Chemokine (C-C motif) ligand 21	Immune response	Ccl21	NM_001008513
Complement component 1, s subcomponent	Immune response	C1s	NM_138900
C-type lectin domain family 4, member E	Immune response	Clec4e	NM_001005897
Granzyme B (granzyme 2, cytotoxic T-lymphocyte-associated serine esterase 1)	Immune response	Gzmb	NM_138517
Chemokine (C-X-C motif) ligand 10	Inflammation response	Cxcl10	NM_139089
Complement component 4B	Inflammation response	C4b	NM_001002805
Amine oxidase, copper containing 3 (vascular adhesion protein 1)	Inflammation response	Aoc3	NM_031582

more than two-fold upregulation of expression, while 664 genes were downregulated in the MIA treatment group compared with the ADSCs-exo treatment group [Table 1]. The expressed genes which showed a five-fold increase are summarized in Table 6. Two genes were related to angiogenesis, four genes to cell cycle, six genes to cell death, thirty-one genes to cell differentiation, four genes to cell proliferation, one gene to DNA repair, six genes to immune response, one gene to the inflammatory response, two genes to RNA splicing, and seven genes were found to be related to secretion. The genes which showed decreased expression levels are summarized in Table 7.

Total gene heat map

The expression prolifes from the MIA group, ADSCs group and ADSCs-exo group were compared with those of the reference C group. Gene heat maps were produced using the GenePattern genomic analysis platform. Red color indicates overexpression, while the green color indicates underexpression. Through microarray analysis, changes in

Table 5: Down-regulated genes expressed by over 600% between monosodium iodoacetate group and adipose-derived stem cell group

Gene name	Gene ontology	Synonyms	GeneBank
Indian hedgehog	Angiogenesis	Ihh	NM_053384
Fibroblast growth factor 10	Cell cycle	Fgf10	NM_012951
Fatty acid-binding protein 12	Cell cycle	Fabp1	NM_001134614
Cell division cycle 25 homolog C (*Schizosaccharomyces pombe*)	Cell cycle	Cdc25c	NM_001107396
Structural maintenance of chromosomes 1B	Cell cycle	Smc1b	NM_001130498
Gasdermin A	Cell death	Gsdma	NM_001108297
CD3 molecule, epsilon	Cell death	Cd3e	NM_001108140
Keratin 20	Cell death	Krt20	NM_173128
Tripartite motif-containing 69	Cell death	Trim69	NM_001013160
Distal-less homeobox 1	Cell differentiation	Dlx1	NM_001100531
Paired box 5	Cell differentiation	Pax5	NM_001109261
Phosphodiesterase 6C, cGMP specific, cone, alpha prime	Cell differentiation	Pde6c	NM_001108522
Mitogen-activated protein kinase 8 interacting protein 3	Cell differentiation	Mapk8ip3	NM_001100673
Scratch homolog 1, zinc finger protein (Drosophila)	Cell differentiation	Scrt1	NM_001130570
Calcium-binding protein 4	Cell differentiation	Cabp4	NM_001108926
RAB13, member RAS oncogene family	Cell differentiation	Rab13	NM_031092
Runt-related transcription factor 3	Cell differentiation	Runx3	NM_130425
Leukemia inhibitory factor receptor alpha	Cell differentiation	Lifr	NM_031048
Cadherin EGF LAG seven-pass G-type receptor 2	Cell differentiation	Celsr2	NM_001191110
Mannan-binding lectin serine peptidase 2	Immune response	Masp2	NM_172043
Defensin beta 36	Immune response	Defb36	NM_001037515
Fibrinogen beta chain	Immune response	Fgb	NM_020071
RT1 class I, locus CE12	Immune response	RT1-CE12	NM_001008835
Alpha-2-macroglobulin	Inflammation response	A2m	NM_012488
Chemokine (C-X-C motif) receptor 2	Inflammation response	Cxcr2	NM_017183
RNA binding fox-1 homolog 3	RNA splicing	Rbfox3	NM_001134498
Dopamine receptor D4	Secretion	Drd4	NM_012944
N-ethylmaleimide sensitive factor	Secretion	Nsf	NM_021748
Phospholipase A2, group X	Secretion	Pla2g10	NM_017176
Glutamate receptor, metabotropic 4	Secretion	Grm4	NM_022666
Synaptotagmin X	Secretion	Syt10	NM_031666

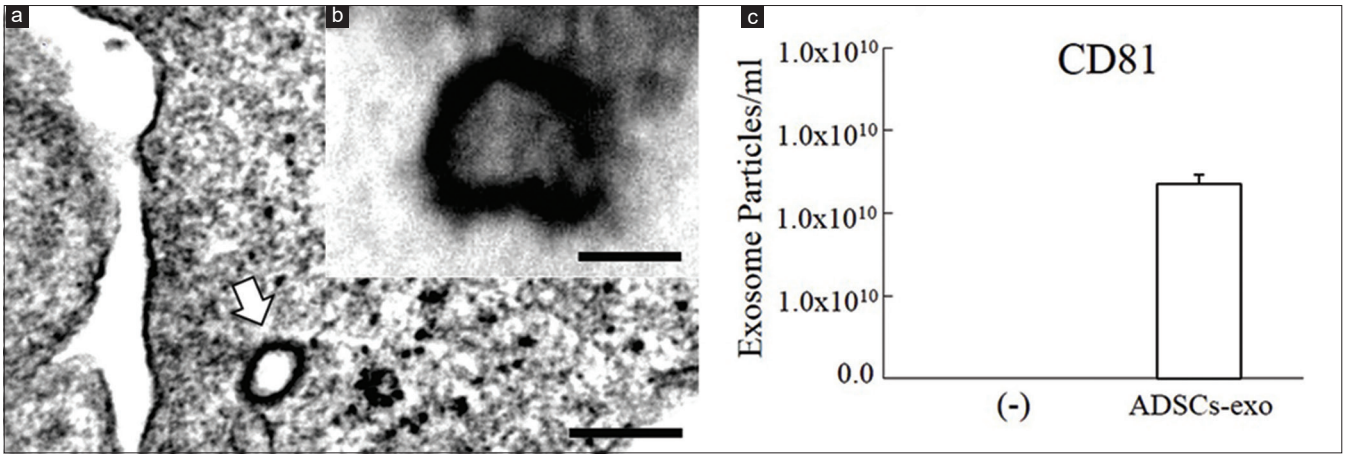

Figure 1: Characterization of adipose-derived stem cell-Exosome. (a) Morphologic analysis of adipose-derived stem cells-exo by transmission electron microscopy (*in vivo*, arrows). Scale bar = 200 nm. (b) Morphologic analysis of adipose-derived stem cells-exo by transmission electron microscopy (*in vitro*). Scale bar = 40 nm. (c) Detection of CD81 expression in exosome by Exo ELISA

the expression of genes associated with the cell death, cell differentiation, cell cycle, cell proliferation, inflammatory response, and immune response, were observed [Figure 2]. [12]

The construction of protein regulation network

The protein regulatory network is presented in Figure 3.

Table 6: Upregulated genes expressed by over 500% between monosodium iodoacetate group and adipose-derived stem cell-exo group

Gene name	Gene ontology	Synonyms	GeneBank
Paired-like homeodomain 2	Angiogenesis	Pitx2	NM_019334
SRY (sex determining region Y)-box 18	Angiogenesis	Sox18	NM_001024781
Fatty acid-binding protein 12	Cell cycle	Fabp1	NM_001134614
Stromal antigen 3	Cell cycle	Stag3	NM_053730
Myeloid leukemia factor 1	Cell cycle	Mlf1	NM_001107680
Adenylate kinase 1	Cell cycle	Ak1	NM_024349
Growth arrest-specific 2	Cell death	Gas2	NM_001127504
Hypermethylated in cancer 1	Cell death	Hic1	NM_001107021
Guanine nucleotide-binding protein (G protein), gamma transducing activity polypeptide 1	Cell death	Gngt1	NM_001135777
Crystallin, alpha B	Cell death	Cryab	NM_012935
Nuclear receptor subfamily 4, group A, member 1	Cell death	Nr4a1	NM_024388
BCL2/adenovirus E1B interacting protein 3	Cell death	Bnip3	NM_053420
Myozenin 2	Cell differentiation	Myoz2	NM_001106469
Myosin, light chain 2, regulatory, cardiac, slow	Cell differentiation	Myl2	NM_001035252
Ankyrin repeat domain 27 (VPS9 domain)	Cell differentiation	Ankrd2	NM_001271264
Cysteine and glycine-rich protein 3 (cardiac LIM protein)	Cell differentiation	Csrp3	NM_057144
Actin, alpha, cardiac muscle 1	Cell differentiation	Actc1	NM_019183
Netrin 4	Cell differentiation	Ntn4	NM_001106780
Myosin binding protein H	Cell differentiation	Mybph	NM_031813
Paired box 7	Cell differentiation	Pax7	NM_001191984
Leiomodin 2 (cardiac)	Cell differentiation	Lmod2	NM_001100964
MAM domain-containing glycosylphosphatidylinositol anchor 1	Cell differentiation	Mdga1	NM_001107618
Solute carrier family 7 (anionic amino acid transporter light chain, xc- system), member 11	Cell differentiation	Slc7a11	NM_001107673
SH3 and multiple ankyrin repeat domains 3	Cell differentiation	Shank3	NM_021676
Neurofascin	Cell differentiation	Nfasc	NM_001160313
Myogenic factor 6	Cell differentiation	Myf6	NM_013172
Actinin alpha 2	Cell differentiation	Actn2	NM_001170325
Transmembrane channel-like 1	Cell differentiation	Tmc1	NM_001108521
Myoglobin	Cell differentiation	Mb	NM_021588
Activin A receptor, type IIB	Cell differentiation	Acvr2b	NM_031554
Sarcoglycan, delta (dystrophin-associated glycoprotein)	Cell differentiation	Sgcd	NM_001109029
Solute carrier family 2 (facilitated glucose transporter), member 4	Cell differentiation	Slc2a4	NM_012751
Protocadherin related 15	Cell differentiation	Pcdh15	NM_001271377
Myelin-associated glycoprotein	Cell differentiation	Mag	NM_017190
Dihydropyrimidinase-like 5	Cell differentiation	Dpysl5	NM_023023
Usher syndrome 2A (autosomal recessive, mild)	Cell differentiation	Ush2a	NM_001302219
Four and a half LIM domains 1	Cell differentiation	Fhl1	NM_001271199
Kelch-like 40 (Drosophila)	Cell differentiation	Klhl40	NM_001108195
SH3 and cysteine-rich domain 3	Cell differentiation	Stac3	NM_001130558
Leucine-rich repeat neuronal 1	Cell differentiation	Lrrn1	NM_001037363
Tripartite motif-containing 54	Cell differentiation	Trim54	NM_001013217
C-mer proto-oncogene tyrosine kinase	Cell differentiation	Mertk	NM_022943
ATP-binding cassette, subfamily C (CFTR/MRP), member 8	Cell differentiation	Abcc8	NM_013039
Calsequestrin 2 (cardiac muscle)	Cell differentiation	Casq2	NM_017131
Homeo box D10	Cell differentiation	Hoxd10	NM_001107094
Tetraspanin 14	Cell proliferation	Tspan1	NM_001169127
Acyl-CoA synthetase long-chain family member 6	Cell proliferation	Acsl6	NM_130739
Glypican 3	Cell proliferation	Gpc3	NM_012774
Dual specificity phosphatase 13	Cell proliferation	Usp13	NM_001162408_1
FANCD2/FANCI-associated nuclease 1	DNA repair	Fan1	NM_001191633

Contd...

Table 6: Contd...

Gene name	Gene ontology	Synonyms	GeneBank
Serpin peptidase inhibitor, clade C (antithrombin), member 1	Immune response	Serpinc1	NM_001012027
RT1 class Ia, locus A2	Immune response	RT1-A2	NM_001008829
Vitronectin	Immune response	Vtn	NM_019156
Myosin light chain, phosphorylatable, fast skeletal muscle	Immune response	Mylpf	NM_012605
Aquaporin 4	Immune response	Aqp4	NM_001142366
Fibrinogen beta chain	Immune response	Fgb	NM_020071
Interleukin 5	Inflammatory response	Il5	NM_021834
Small nuclear ribonucleoprotein polypeptide N	RNA splicing	Snrpn	NM_031117
RNA binding motif protein 20	RNA splicing	Rbm20	NM_001107611
Fibrinogen gamma chain	Secretion	Fgg	NM_012559
Secernin 3	Secretion	Scrn3	NM_001013162
Group specific component	Secretion	Gc	NM_012564
Activin A receptor, type IIB	Secretion	Acvr2b	NM_031554
C-mer proto-oncogene tyrosine kinase	Secretion	Mertk	NM_022943
Phospholipase A2, group IIC	Secretion	Pla2g2c	NM_019202
Unc-13 homolog C (*Caenorhabditis elegans*)	Secretion	Unc13c	NM_173146

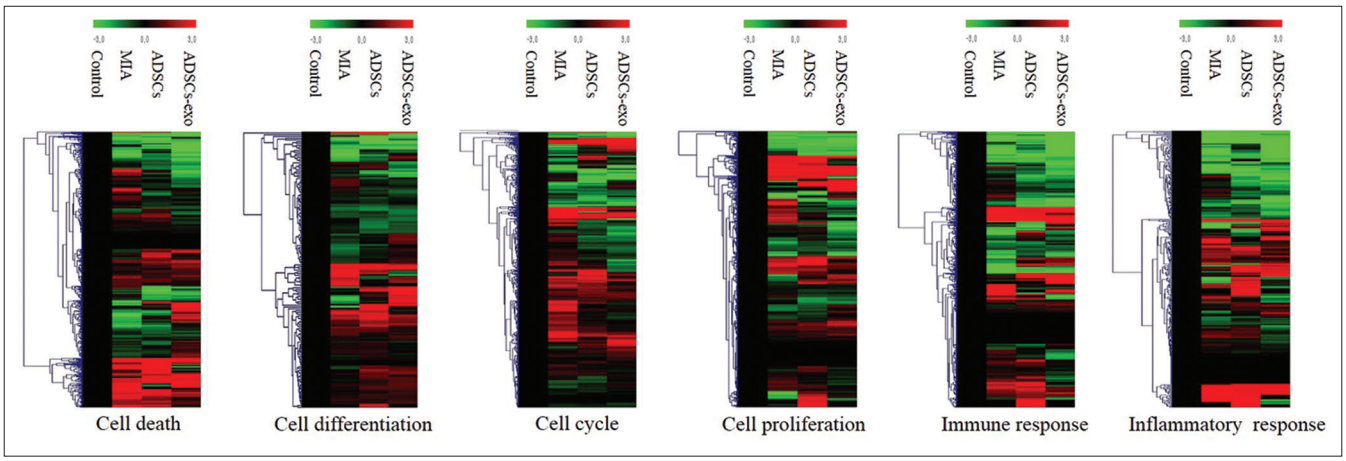

Figure 2: Gene heat map in monosodium iodoacetate-induced osteoarthritis rats and human adipose-derived stem cells-exo injection. The expression profiles of heat shock-activated genes were clustered hierarchically and are displayed using a red-green heat map. Heat map of genes upregulated and down-regulated ≥2 fold in monosodium iodoacetate-induced osteoarthritis rats and human adipose-derived stem cells-exo injection. Red color indicates over-expression, while the green color indicates under-expression. Control, control group; monosodium iodoacetate, monosodium iodoacetate group; adipose-derived stem cell, human AD-mesenchymal stem cells group; adipose-derived stem cells-exo, human adipose-derived stem cells-derived exosome group

The results revealed that there were several protein genes with differential expression in the control group compared to the MIA group [Figure 3a and b]. The change in network graph of several proteins was identified after the injection of human ADSCs [Figure 3c and d] and human ADSCs-exo [Figure 3e and f]. Furthermore, six protein networks were constructed [Figure 3]. The protein network consisted of 57 red nodes and 69 green nodes. The results revealed that the interactive relationships among proteins are relatively simple.

Discussion

In this study, it was demonstrated that hADSCs-exo, which were introduced through injection into the intra-articular space and through the infrapatellar ligament, were engrafted in the right knee tissues of MIA-induced OA rats. Adverse effects were not observed after the transfusion of hADSCs (2×10^6/mL/cm^2) and hADSCs-exo [Figure 1]. Recently, many papers reported that exos isolated from mouse bone marrow-derived mesenchymal stem cells (MSCs) and exo secreted by induced pluripotent stem cell-derived MSCs (iMSC-Exos) may represent a novel therapeutic effect on OA animal model.[13,14] However, most of these studies were limited to macroscopic and histological observations of the articular cartilage after stem cell-derived exo treatment. No information was obtained or provided with respect to the effects of these exos on the immune response and inflammatory processes in the synovial membrane and menisci, which occur secondary to OA. This study, using a rat model of OA, was designed to investigate the role of hADSCs-exo in the context of OA and their effect or influence on the inflammatory

Table 7: Down-regulated genes expressed by over 600% between monosodium iodoacetate group and adipose-derived stem cell-exo group

Gene name	Gene ontology	Synonyms	GeneBank
Forkhead box C2	Angiogenesis	Foxc2	NM_001101680
Fibroblast growth factor 10	Angiogenesis	Fgf10	NM_012951
Fibroblast activation protein, alpha	Cell cycle	Fap	NM_138850
HORMA domain containing 2	Cell cycle	Hormad2	NM_001017501
SH3 domain containing ring finger 1	Cell death	Sh3rf1	NM_198764
Metallothionein 3	Cell death	Mt3	NM_053968
Cartilage oligomeric matrix protein	Cell death	Comp	NM_012834
CD3e molecule, epsilon associated protein	Cell death	Cd3e	NM_001109416
Solute carrier family 25, member 27	Cell death	Slc25a27	NM_053500
Deleted in colorectal carcinoma	Cell death	Dcc	NM_012841
Collagen, type IX, alpha 1	Cell differentiation	Col9a1	NM_001100842
Collagen, type II, alpha 1	Cell differentiation	Col2a1	NM_012929
Aggrecan	Cell differentiation	Acan	NM_022190
Human immunodeficiency virus type I enhancer binding protein 3	Cell differentiation	Hivep3	NM_001107972
Forkhead box D1	Cell differentiation	Foxd1	NM_134337
Nephrosis 1, congenital, Finnish type (nephrin)	Cell differentiation	Nphs1	NM_022628
Nucleoporin 210-like	Cell differentiation	Nup210l	NM_001191900
Formin binding protein 1-like	Cell differentiation	Fnbp1	NM_001039609
Integrin, alpha M	Cell differentiation	Itgam	NM_012711
Numb homolog (Drosophila)	Cell differentiation	Numb	NM_133287
Runt-related transcription factor 3	Cell differentiation	Run×3	NM_130425
Frizzled-related protein	Cell differentiation	Frzb	NM_001100527
Ephrin B3	Cell differentiation	Efnb3	NM_001100980
Phosphodiesterase 6C, cGMP specific, cone, alpha prime	Cell differentiation	Pde6c	NM_001108522
Stimulator of chondrogenesis 1	Cell proliferation	Scrg1	NM_033499
Epidermal growth factor receptor	Cell proliferation	Egfr	NM_031507
Matrix metallopeptidase 16	Cell proliferation	Mmp16	NM_080776
Essential meiotic endonuclease 1 homolog 1 (*Schizosaccharomyces pombe*)	DNA repair	Eme1	NM_001105830
Pif1/Rrm3 DNA-helicase-like protein	DNA repair	Pif1	NM_001044253
Tripartite motif-containing 21	Immune response	Trim21	NM_001082572
Interleukin 12A	Immune response	Il12a	NM_053390
Secreted and transmembrane 1B	Immune response	Sectm1b	NM_199082
2'-5' oligoadenylate synthetase 2	Immune response	Oas2	NM_001009715
Killer cell lectin-like receptor subfamily K, member 1	Immune response	Klrk1	NM_133512
Killer cell lectin-like receptor, subfamily D, member 1	Immune response	Klrd1	NM_012745
Defensin beta 36	Immune response	Defb36	NM_001037515
Lactotransferrin	Immune response	Ltf	NM_001106864
Protein kinase D1	Immune response	Prkd1	NM_001276715
Fas ligand (TNF superfamily, member 6)	Immune response	Faslg	NM_012908
Interleukin 12 receptor, beta 1	Immune response	Il12rb1	NM_001170604
Tumor necrosis factor receptor superfamily, member 11a, NFKB activator	Immune response	Tnfrsf11a	NM_001271235
Interleukin 17B	Inflammatory response	Il17b	NM_053789
Serpin peptidase inhibitor, clade A (alpha-1 antiproteinase, antitrypsin), member 10	Inflammatory response	Serpina1	NM_133617
Histone cluster 1, H2ba	Inflammatory response	Hist1h2ba	NM_022643
Protein kinase C, zeta	Inflammatory response	Prkcz	NM_022507
RNA binding fox-1 homolog 3	RNA splicing	Rbfox3	NM_001134498
Synaptotagmin VI	Secretion	Syt6	NM_022191
Cerebellin 1 precursor	Secretion	Cbln1	NM_001109127
N-ethylmaleimide-sensitive factor	Secretion	Nsf	NM_021748

environment within the affected joint articulation. A more recent publication described that exo from embryonic stem cell-derived MSCs impeded cartilage destruction in the Destabilization of Medial Meniscus model.[15] This

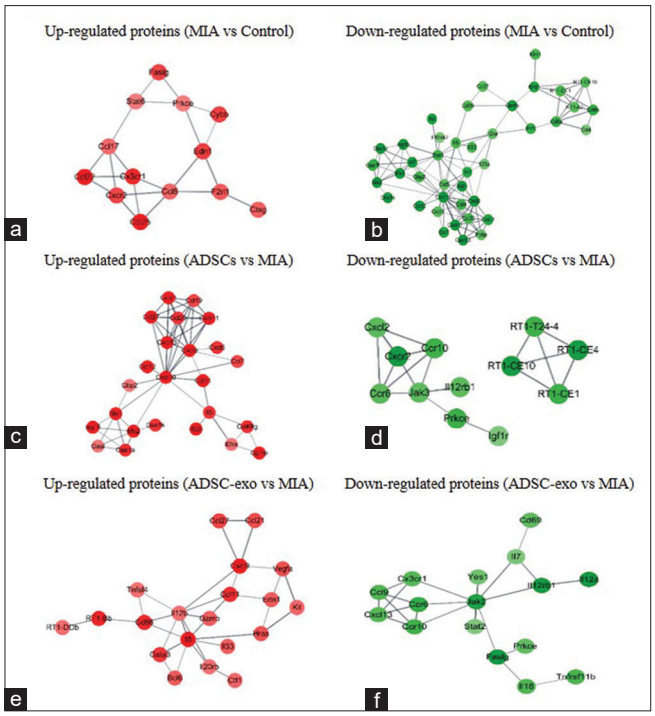

Figure 3: Protein-protein interaction network. (a-f) Protein network graphs of the biological processes based on Tables 2-7. Red nodes indicate upregulated proteins (a, c, e). Green nodes represent down-regulated proteins (b, d, f). (a) Faslg, Stat6, Prkce, Cybb, Ccl17, Edn1, Ccl22, Cx3cr1, Cxcr2, Ccl25, Ccl6, F2rl1, and Ctsg proteins. (b) Klrk1, Cd27, Klrd1, RT1-CE1, RT1-CE10, Cd69, Gzmb, RT1-A2, Cd8b, Kit, Cd8a, Eif2ak2, Il2ra, Prf1, Cd4, Oas1a, Isg15, Eif2ak2, Il5, Il33, Oas1, Irf7, Stat1, Il23a, Mx2, Oas1k, Mx1, Gbp2, Ccl12, Ccl5, Cxcl10, Tnf, Xcl1, Ccl4, Cxcl9, Cxcl1, Ccl7, Cxcl11, Ccl20, Cxcl13, Ccl27, and Ppbp proteins. (c) Ccl21, Ccl19, Ccl27, Ccl20, Cxcl11, Cxcl13, Cxcl9, Cxcl5, Ccl12, Ccl7, Gbp2, Cxcl10, Ccl11, Isg15, Mx1, Oasl, Oas1a, Mx2, Oas1k, Il5, Il33, Il2ra, Cd40lg, and Gzmb proteins (d) Cxxl2, Cxcr2, Ccr10, Ccr6, Jak3, Il12rb1, Prkce, Igf1r, RT1-T24-4, RT1-CE10, RT1-CE4, and RT1-CE1 proteins (e) Ccl27, Ccl21, Cxcl9, Vegfa, Tnfsf4, Ccl11, Edn1, Kit, RT1-Dob, RT1-Bb, Cd86, Il12b, Gzmb, Gata3, Bcl6, Il5, Il20rb, Ctf1, Il33, and Hras proteins. (f) Cd69, Il7, Ccl9, Cxcl13, Cx3cr1, Ccr6, Ccr10, Yes1, Jak2, Stat2, Faslg, Prkce, Il18, Tnfrsf11b, Il12rb1, and Il12a proteins. Control, control group; monosodium iodoacetate, monosodium iodoacetate group; adipose-derived stem cell, human AD-mesenchymal stem cells group; adipose-derived stem cells-exo, human adipose-derived stem cells-derived exosome group

concept is further corroborated by a recent study findings said to demonstrate evidence that IL1 β-pretreated MSCs could induce macrophage polarization toward an M2 phenotype more efficiently than naive MSCs, and that miR-146a-containing exo enhanced this effect.[16] In addition, the difference in gene expression levels after human ADSCs-exo therapy was compared in an effort to identify potential candidate genes which might potentially link the systemic immune response to the development of OA disease by examining the gene expression patterns between the MIA group and the ADSCs-exo group in an MIA-induced OA rat model. In the present study, many immunologic processes and genetic factors were thought to be implicated in the pathogenesis of OA. Immunologic abnormalities in the MIA group of OA rats reflected marked activation of the immune system, leading to increased cytokine production. The data indicated that there were several genes with differential expression in the ADSCs-exo group when the ADSCs-exo group was compared to the MIA group. The change in expression levels of several genes was confirmed after the injection of hADSCs-exo. These genes were related to the angiogenesis, inflammatory response, immune response, cell cycle, cell death, cell differentiation, cell proliferation, DNA repair, RNA splicing, and secretion. Despite the injection of hADSCs-exo into MIA-induced OA rats, relatively little is known about the relationship between OA and ADSCs-exo. Therefore, in the current study, it was our intention to more fully investigate the changes in gene expression by microarray analysis after the injection of hADSCs-exo into MIA-induced OA rats. Many studies have asserted, or at least theorized, that many patients do not respond to a single injection of hADSCs-exo. Furthermore, there is a greater risk of aneurysm formation in the unresponsive group than among those rats who defervesce completely after a single injection of hADSCs-exo. The limitations of the present study were as follows: the sample size was small, and further analysis with larger samples of other independent sets, as well as specific samples such as peripheral blood T cells, monocytes/macrophages, would be necessary to confirm the material effect of ahADSCs-exo injection.

Conclusion

The present study investigated the effects of hADSCs-exo on OA pathology, differential gene expression, and the level of related proteins in MIA-induced OA in rats. The interaction network consisted of 57 proteins encoded by upregulated genes. However, the interaction network also consisted of 69 proteins encoded by downregulated genes [Figure 3]. The changes in gene expression suggest the potential biological pathway that occurs in the angiogenesis, inflammatory response, immune response, cell cycle, cell death, cell differentiation, cell proliferation, DNA repair, RNA splicing, and secretion. In addition, understanding the processes driving hADSCs-exo recruitment could prove invaluable in the development of novel, targeted therapies to selectively inhibit pathological responses in OA.

Acknowledgments

This research was supported by Basic Science Research Program through the National Research Foundation of Korea funded by the Ministry of Education (2017R1D1A1B03028112).

Financial support and sponsorship

This research was supported by Basic Science Research Program through the National Research Foundation of Korea funded by the Ministry of Education (2017R1D1A1B03028112).

Conflicts of interest

There are no conflicts of interest.

References

1. Goldring SR. The role of bone in osteoarthritis pathogenesis. Rheum Dis Clin North Am 2008;34:561-71.
2. Roberts V, Lu B, Rajakumar S, Cowan PJ, Dwyer KM. The CD39-adenosinergic axis in the pathogenesis of renal ischemia-reperfusion injury. Purinergic Signal 2013;9:135-43.
3. Huang WC, Elkin EB, Levey AS, Jang TL, Russo P. Partial nephrectomy versus radical nephrectomy in patients with small renal tumors-is there a difference in mortality and cardiovascular outcomes? J Urol 2009;181:55-61.
4. Janetschek G. Laparoscopic partial nephrectomy for RCC: How can we avoid ischemic damage of the renal parenchyma? Eur Urol 2007;52:1303-5.
5. Bang C, Thum T. Exosomes: New players in cell-cell communication. Int J Biochem Cell Biol 2012;44:2060-4.
6. Camussi G, Deregibus MC, Bruno S, Cantaluppi V, Biancone L. Exosomes/microvesicles as a mechanism of cell-to-cell communication. Kidney Int 2010;78:838-48.
7. Schorey JS, Bhatnagar S. Exosome function: From tumor immunology to pathogen biology. Traffic 2008;9:871-81.
8. Gupta SK, Bang C, Thum T. Circulating microRNAs as biomarkers and potential paracrine mediators of cardiovascular disease. Circ Cardiovasc Genet 2010;3:484-8.
9. Michael A, Bajracharya SD, Yuen PS, Zhou H, Star RA, Illei GG, *et al*. Exosomes from human saliva as a source of microRNA biomarkers. Oral Dis 2010;16:34-8.
10. Häupl T, Stuhlmüller B, Grützkau A, Radbruch A, Burmester GR. Does gene expression analysis inform us in rheumatoid arthritis? Ann Rheum Dis 2010;69 Suppl 1:i37-42.
11. Lee HD, Kim YH, Koo BH, Kim DS. The ADAM15 ectodomain is shed from secretory exosomes. BMB Rep 2015;48:277-82.
12. Greenough TC, Straubhaar JR, Kamga L, Weiss ER, Brody RM, Mcmanus MM, *et al*. A gene expression signature that correlates with CD8+ T cell expansion in acute EBV infection. J Immunol 2015;195:4185-97.
13. Cosenza S, Ruiz M, Toupet K, Jorgensen C, Noël D. Mesenchymal stem cells derived exosomes and microparticles protect cartilage and bone from degradation in osteoarthritis. Sci Rep 2017;7:16214.
14. Zhu Y, Wang Y, Zhao B, Niu X, Hu B, Li Q, *et al*. Comparison of exosomes secreted by induced pluripotent stem cell-derived mesenchymal stem cells and synovial membrane-derived mesenchymal stem cells for the treatment of osteoarthritis. Stem Cell Res Ther 2017;8:64.
15. Wang Y, Yu D, Liu Z, Zhou F, Dai J, Wu B, *et al*. Exosomes from embryonic mesenchymal stem cells alleviate osteoarthritis through balancing synthesis and degradation of cartilage extracellular matrix. Stem Cell Res Ther 2017;8:189.
16. Song Y, Dou H, Li X, Zhao X, Li Y, Liu D, *et al*. Exosomal miR-146a Contributes to the Enhanced Therapeutic Efficacy of Interleukin-1β-Primed Mesenchymal Stem Cells Against Sepsis. Stem Cells 2017;35:1208-21.

Original Article

An Experimental Study on the Effect of Maternal Folate Diet on Microstructure of Some Vital Organs of Offspring

Lokadolalu Chandracharya Prasanna, N. Vinaykumar[1], Aswathi Ramesh

Department of Anatomy, Kasturba Medical College, Manipal Academy of Higher Education, Manipal, Karnataka, [1]Department of Anatomy, Government Medical College, Palakkad, Kerala, India

Abstract

Introduction: Folic acid (FA) deficiency or its supplementation during pregnancy affects fetal development at critical periods and can cause more potentially impaired organ development through epigenetic gene regulations. The present study aimed to analyze the effect of maternal FA deficiency and/or its supplementation in diet during gestation on offspring's few major fetal organs, including brain, liver, pancreas, and kidney. **Material and Methods:** This experimental study was done on 18 female Wistar rats to study the effects of dietary FA intake (absence/supplementation,/normal amount) during pregnancy on the development of offspring's liver, kidney, and pancreas development. **Results:** The present study revealed that with maternal FA supplementation, there was increase in the number of islets in pancreas, number of hepatic lobules, and renal glomeruli in offspring, which, in turn, correlates with increased risk of cardiovascular, renal, and metabolic diseases in their later life. **Discussion and Conclusion:** The findings in this study support the possible negative effects of higher FA supplementation during peri-conceptional and pregnancy phase on offspring and indicates long-term health hazards in their later life.

Keywords: *Development, folic acid, offspring, organ, pregnancy, supplementation*

Introduction

Folic acid (FA) has an important role in reducing the incidence of birth defects in offspring, and this fact has gained considerable attention in recent generation.[1] Prenatal supplementation of FA and its usage or consequence of long-term health hazards in offspring has remained debatable and unsettled.[2]

Due to a lack of epidemiological findings, the reference range for serum folate in women, especially during reproductive age, has not been mentioned.[3] In general, pregnancy demands high FA availability due to a greater need for the growth of the fetus and uteroplacental organs as well as the maternal excess FA urinary excretion.[4] Various studies have revealed that there is a positive correlation between the maternal plasma FA levels and the incidence of cardiovascular diseases,[5] structural brain changes/neurodegenerative conditions,[6-8] insulin resistance,[9] and childhood asthma[10] in offspring in the later period of life. Few clinical studies have reported on the incidence of decreased cognitive behavior,[11] glomerular sclerosis, systemic blood pressure,[12] and conotruncal defects[13] in the postnatal life.

The purpose of the present study was to evaluate the effect of maternal folate diet during gestation (either its absence or its supplementation) on the microstructure of their offspring's few vital organs (brain, liver, pancreas, and kidney). This would help us to correlate the risk of development of neurological, metabolic, and renal diseases in the offspring in their adult life.

Material and Methods

This experimental study was conducted from June 2017 to February 2018, after the approval letter was obtained by our institutional animal ethical committee. Eighteen female Wistar rats were obtained from the central animal research facility of our institution and their body weight was approximately 120 g.

Selection of groups

The female Wistar rats were divided randomly into three groups with six rats in each group. The first (control) group of animals was administered a diet containing a normal recommended dose of FA as provided

How to cite this article: Prasanna LC, Vinaykumar N, Ramesh A. An experimental study on the effect of maternal folate diet on microstructure of some vital organs of offspring. J Anat Soc India 2020;69:48-52.

Article Info

Received: 08 June 2019
Accepted: 04 February 2020
Available online: 11 April 2020

Address for correspondence:
Dr. Lokadolalu Chandracharya Prasanna, Kasturba Medical College, Manipal Academy of Higher Education, Manipal - 576 104, Karnataka, India.
E-mail: prasanna.lc@manipal.edu

Access this article online

Website: www.jasi.org.in
DOI: 10.4103/JASI.JASI_73_19
Quick Response Code:

by the central animal lab. The second group of animals was administered a diet with no FA content (purchased from Vinod Ramakrishna (VRK) Biotech Pvt Ltd, Miraj, Maharashtra, India. To ensure complete FA absence, we added 1% succinyl sulfathiazole to the diet with no FA. This reduces or inhibits the gut flora which is responsible for the synthesis of FA and also avoids coprophagy during gestation. The third group of animals was administered a diet with an excess amount of FA (4 mg/kg body weight, daily).

All rats were caged in separate polypropylene cages in the central animal research facility with (12 × 12 h light and dark cycle, 25°C, and 35% humidity) with free access to water. All rats were given diets specific to each group, 5 weeks before gestation, throughout the gestation, and 3 weeks after their delivery. The litter size, number, and weight of the pups were recorded after delivery. All the pups from each group were weaned on the 21st day, and then the male and female pups were separated and maintained in separate cages till adult age.

Collection of specimens

On the 75th day of birth, rats from each group were sacrificed. Upon dissecting the abdominal cavities, few organs (liver, pancreas, and kidneys) were carefully dissected, fixed in 10% formalin, and processed further for H and E staining. On microscopic examination, we studied three different fields of the same tissue, and the average was considered as the final value to avoid intraobserver variations.

Statistical analysis

Data were analyzed using the Statistical Package for the Social Sciences statistical software (version 6.0). The number of classical hepatic lobules and its hepatocytes, number of islets of Langerhans along with their cells, and the number of glomeruli were compared with each group. $P < 0.05$ was considered statistically significant.

Results

Microscopic details

Liver

Microscopic sections of the liver [Figure 1a] of the control group showed hepatocytes with

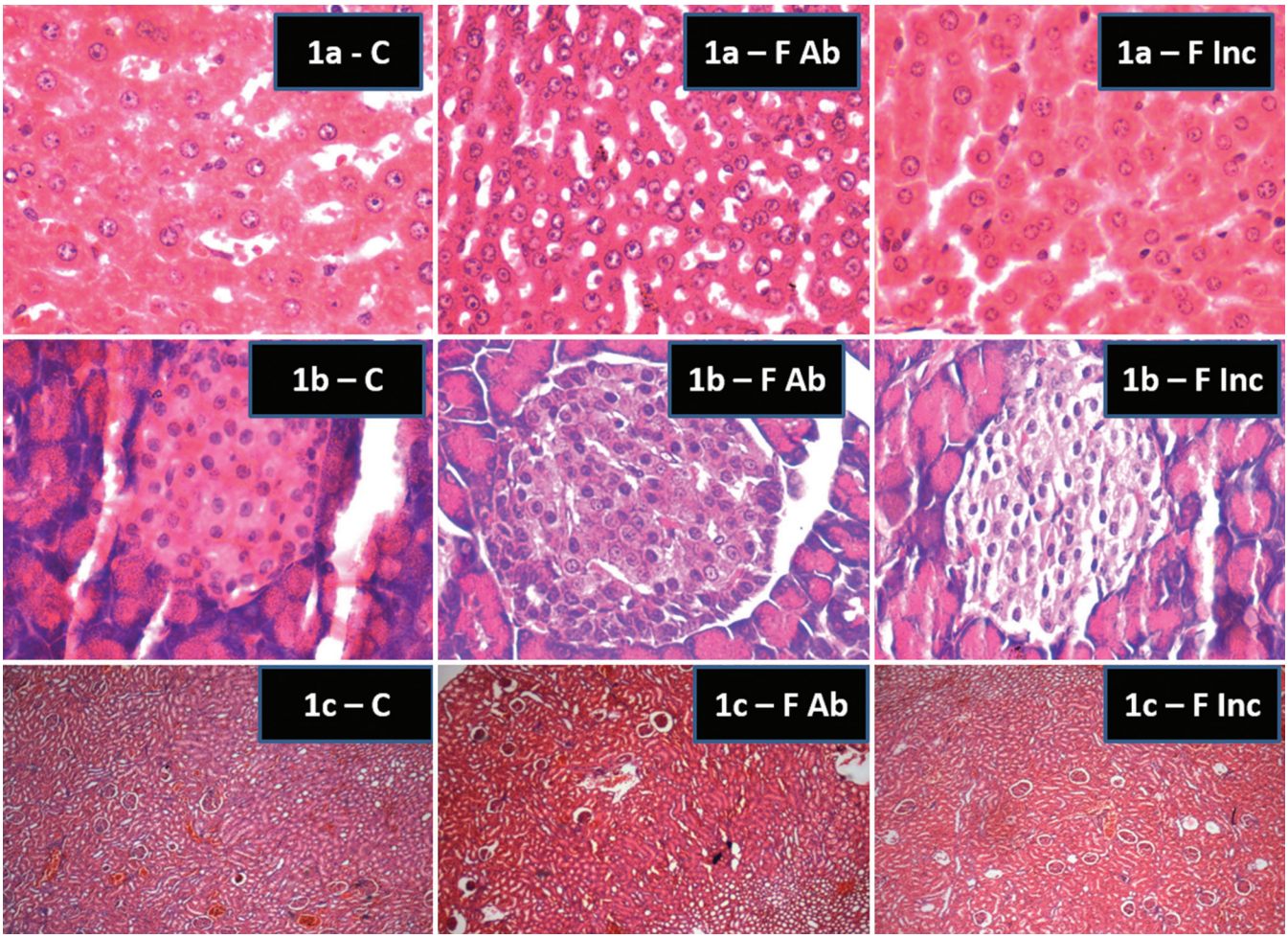

Figure 1: Photomicrograph of liver (a) at × 40, pancreas (b) at × 40, and kidney (c) at x10 magnification (C – Control group, F Ab: Folic acid-absent group, F Inc: Folic acid-supplemented group)

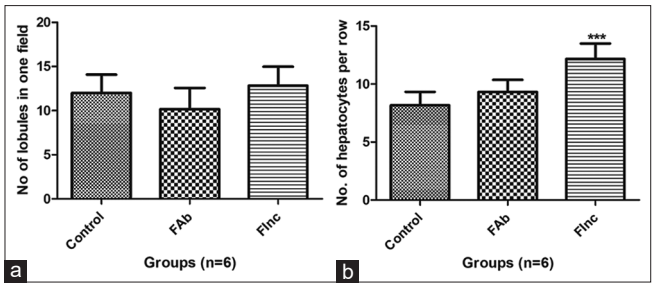

Graph 1: Effect of folic acid status during pregnancy and lactation on the (a) number of classical hepatic lobules (as evaluated by × 10 magnification) and (b) number of hepatocytes from the center to the periphery of each liver lobule in their fetuses (as evaluated by × 40 magnification). Each value represents mean ± standard deviation C: Control, F Ab: Folic acid absent, F Inc: Folic acid increased (Control vs. F Inc: ******P* < 0.001 as in b)

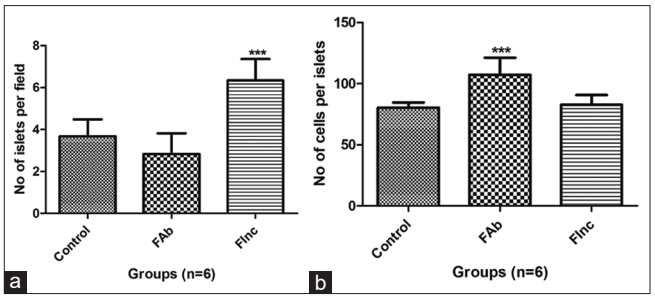

Graph 2: Effect of folic acid status during pregnancy and lactation on the (a) number of islets of Langerhans in their fetus pancreas (as evaluated by × 10 magnification) and (b) number of endocrine cells in each islet of Langerhans in their fetus pancreas (as evaluated by × 40 magnification). Each value represents mean ± standard deviation Control versus F Inc: * *P* < 0.001. C: Control, F Ab: Folic acid absent, F Inc: Folic acid increased (Control vs. F Ab: ******P* < 0.001 as in b)**

normal microstructure and prominent nucleoli. The number of classical hepatic lobules per field in low magnification (×10) was 12–13 and in each lobule [Graph 1a], the number of hepatocytes from central to peripheral zone as counted in higher magnification (×40) was found to be 8–9 [Graph 1b].

In FA-absent diet group sections, hepatocytes showed partial nucleomegaly with dispersed nucleoli, whereas in FA-supplemented group, hepatocytes showed heterogeneous nuclear changes with small and large few nuclei with prominent nucleoli. The classical hepatic lobule per field in FA-absent diet was 10–11, and the number of hepatocytes in each row increased to 9–10, whereas in the FA-supplemented group, the lobules increased to 16/field and the number of hepatocytes increased to 11–12 in each row.

Pancreas

Sections of the control group and the FA-supplemented group did not show any histological changes [Figure 1b, ×40]. In the control group, we found 3–4 islets per field in low magnification, i.e., ×10 [Graph 2a] and an average of 81–82 cells in each islet of Langerhans [Graph 2b].

Few exocrine acini of adult born to FA-absent diet group showed nucleomegaly with immature chromatin and single prominent nucleolus suggestive of megaloblastic changes. The islets were reduced to an average of 3, and the number of cells increased to 105/islet, whereas in the FA-supplemented group, we found the number of the islets to be between 6 and 7/field and 84–85 cells per islet.

Kidney

Histological sections of the kidney [Figure 1c, ×4) in the control group showed no significant changes and the number of glomeruli ranged between 20 and 21/field [Graph 3]. Adults born to mothers treated with absent FA diet showed large nuclei with prominent nucleoli (with average 25 glomeruli per field in × 10) and those born with FA-supplemented mothers showed heterogeneous nuclear changes, with small and large nuclei and prominent nucleoli. In addition, the number of glomeruli was found to be 30–31.

All the three groups maintained near-normal cytoarchitecture with minimal nuclear changes, and no inflammation and necrosis were identified.

Discussion

Alterations in the maternal micronutrients, especially FA in diet during gestation and/or lactation, are associated with an increased risk of cardiovascular, renal, and metabolic diseases in later life.[12,13] A research study recommended that higher dose of FA (5 mg) should be provided only in special cases such as history of neural tube defects in epileptic and diabetic mothers and patients with inconsistent birth control and recreational substance abuse in the form of alcohol, tobacco, and drugs.[14] Although FA supplementation to pregnant women demonstrates many benefits to their fetuses, concerns have been documented about the detrimental effects of the unmetabolized FA in their offspring.[15]

Accumulating evidence suggests that there is an association between the maternal plasma FA levels and the incidence of vascular diseases[12], structural brain changes and neurodegenerative conditions[15,16], insulin resistance[16], and childhood asthma[17] in their offspring in the later period of life. Few clinical studies implicate the incidence of decreased behaviour and cognitive behaviour[18], glomerular sclerosis, and systemic blood pressure, and conotruncal defects[19-21] in the postnatal life.

Lucock and Yates[22] claimed that excess FA use in pregnancy causes T allele of MTHFR in children, and such allele infants have a greater tendency of spontaneous abortion because of increased homocysteine levels in their mother. In addition, carriers of T allele are at greater risk of neurological disorders such as depression,[7] schizophrenia,[8] bipolar disorders,[7] neural tube defect,[23] and rarely

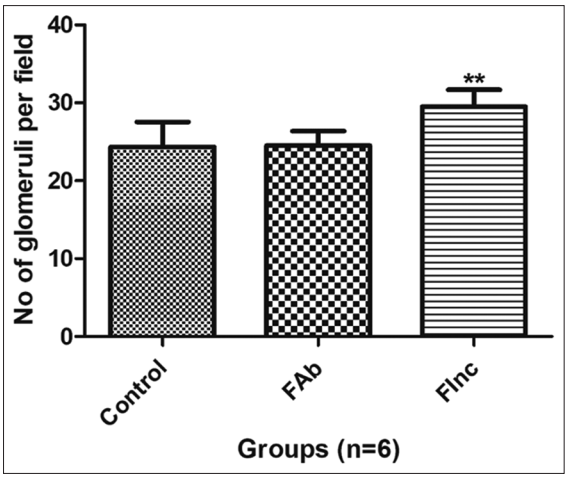

Graph 3: Effect of folic acid status during pregnancy and lactation on the number of glomeruli in their fetus kidney (as evaluated by × 4 magnification). Each value represents mean ± standard deviation. Control versus F Inc: ** Statistically highly significant *P* < 0.001. C: Control, F Ab: Folic acid absent, F Inc: Folic acid increased

Down's syndrome.[24,25] A cohort study by Valencia, as quoted by Valera-Gran *et. al*, (2014)[26] demonstrated that the excess maternal FA was associated with reduced fetal growth, which, in turn, reduces the infant's psychomotor development.

An experimental study of Wistar rats born to FA-supplemented mothers during their pregnancy showed no significant changes in liver microarchitecture.[27] Sections of the liver of rats born to mother given with excess/supplemented amount of FA showed enlarged hepatocytes with cytoplasmic vacuolations, consistent with hydropic degeneration or hepatic ballooning.[28] Roncalés *et al*.'s[29] study revealed a 17% increase in the number of hepatocytes as well as the size of the hepatocytes with FA supplementation. In another study, altered methylation promoters were found in livers of male fetuses born to mothers fed with FA-deficient diet.[11] Contrary to the earlier studies, we found that the number of classical hepatic lobules and the number of hepatocytes in each row increased in rats born to FA-supplemented mothers. In addition, hepatocytes showed heterogeneous nuclear changes with small and large few nuclei with prominent nucleoli.

Maternal FA deficiency can affect the offspring's pancreas and can cause a reduction in the β-cell area as well as a decrease in the number of cells per islet by 50% along with the increased risk of insulin resistance. This could be due to hormonal modification in both mother and fetus, alteration in epigenetic gene regulation, and limited fetal growth and development.[30] Chittiboyina *et al*.[30] found that there was a remarkable increase in the percentage of islets of Langerhans and decrease in the percentage of the number of acini in mouse embryo after supplementation of folate during gestation, concluding that administration of FA diet influences the development of the pancreas and its deficiency leads to histopathological alterations. In the present study, the number of islets decreased and numerous small and large islet cells were demonstrable in rats born to mothers fed with FA-absent diet and the number of islets increased in rats born to mothers fed with FA-excess diet with normal to a high number of cells per islet.

Maternal FA restriction results in a decrease in the number of nephrons, lower filtration surface area per glomerulus, electrolyte imbalance, an increase in glomerular pressure, glomerular sclerosis, and finally end up in systemic blood pressure and renal disease.[12,31] Black *et al*.[32] found that the reduced folate and Vitamin B12 concentrations with increased homocysteine levels in pregnancy can alter the nephrogenesis, leading to smaller kidney and reduced renal function in their offspring. However, few works of literature have stated that both kidney function and risk of metabolic syndrome were greatly benefited by supplementation of FA during pregnancy.[9] We found that there was an increase in the number of glomeruli as compared to other experimental groups.

Conclusion

The present study supports the possible negative effect of higher FA supplementation than recommended during periconceptional and throughout the pregnancy. However, it is hard to conclude conclusively due to the limitation of the small sample size in the present study. Further research is needed to evaluate the most folate-sensitive period of fetal organ development as well as the dose-dependent effects of folate during different periods of gestation (periconceptional, early gestation, mid-gestation, and during the last phase) on the development of vital organs and its association with the development of diseases in the later life.

Financial support and sponsorship

Nil.

Conflicts of interest

There are no conflicts of interest.

References

1. Barua S, Kuizon S, Junaid MA. Folic acid supplementation in pregnancy and implications in health and disease. J Biomed Sci 2014;21:77.
2. Prasanna LC, Punja R, Mamatha H, Konuri A, Kumar A. Role of folic acid supplementation during pregnancy on implantation of embryos. J Anat Soc India 2018;67:80-5. [DOI: 10.1016/j.jasi.2018.05.007].
3. McStay CL, Prescott SL, Bower C, Palmer DJ. Maternal folic acid supplementation during pregnancy and childhood allergic disease outcomes: A question of timing? Nutrients 2017;9:123.
4. Tamura T, Picciano MF. Folate and human reproduction. Am J Clin Nutr 2006;83:993-1016.
5. Clarke R, Halsey J, Lewington S, Lonn E, Armitage J, Manson JE, *et al*. Effects of lowering homocysteine levels with B vitamins on cardiovascular disease, cancer, and cause-specific

mortality: A meta-analysis of 8 randomized trials involving 37,485 individuals. Arch Intern Med 2010;170:1622-31.
6. Vermeer SE, van Dijk EJ, Koudstaal PJ, Oudkerk M, Hofman A, Clarke R, *et al*. Homocysteine, silent brain infarcts, and white matter lesions: The Rotterdam scan study. Ann Neurol 2002;51:285-9.
7. Gilbody S, Lewis S, Lightfoot T. Methylenetetrahydrofolate reductase (MTHFR) genetic polymorphisms and psychiatric disorders: A HuGE review. Am J Epidemiol 2007;165:1-13.
8. Muntjewerff JW, Kahn RS, Blom HJ, den Heijer M. Homocysteine, methylenetetrahydrofolate reductase and risk of schizophrenia: A meta-analysis. Mol Psychiatry 2006;11:143-9.
9. Christian P, Stewart CP. Maternal micronutrient deficiency, fetal development, and the risk of chronic disease. J Nutr 2010;140:437-45.
10. Kim JH, Jeong KS, Ha EH, Park H, Ha M, Hong YC, *et al*. Relationship between prenatal and postnatal exposures to folate and risks of allergic and respiratory diseases in early childhood. Pediatr Pulmonol 2015;50:155-63.
11. Steenweg-de Graaff J, Roza SJ, Steegers EA, Hofman A, Verhulst FC, Jaddoe VW, *et al*. Maternal folate status in early pregnancy and child emotional and behavioral problems: The Generation R study. Am J Clin Nutr 2012;95:1413-21.
12. Wood-Bradley RJ, Barrand S, Giot A, Armitage JA. Understanding the role of maternal diet on kidney development: An opportunity to improve cardiovascular and renal health for future generations. Nutrients 2015;7:1881-905.
13. Burgoon JM, Selhub J, Nadeau M, Sadler TW. Investigation of the effects of folate deficiency on embryonic development through the establishment of a folate deficient mouse model. Teratology 2002;65:219-27.
14. Wald NJ, Law MR, Morris JK, Wald DS. Quantifying the effect of folic acid. Lancet 2001;358:2069-73.
15. Greenberg JA, Bell SJ, Guan Y, Yu YH. Folic acid supplementation and pregnancy: More than just neural tube defect prevention. Rev Obstet Gynecol 2011;4:52-9.
16. Veena SR, Krishnaveni GV, Srinivasan K, Wills AK, Muthayya S, Kurpad AV, *et al.* Higher maternal plasma folate but not Vitamin B-12 concentrations during pregnancy are associated with better cognitive function scores in 9- to 10- year-old children in South India. J Nutr 2010;140:1014-22.
17. Baydas G, Koz ST, Tuzcu M, Nedzvetsky VS, Etem E. Effects of maternal hyperhomocysteinemia induced by high methionine diet on the learning and memory performance in offspring. Int J Dev Neurosci 2007;25:133-9.
18. Selhub J, Morris MS, Jacques PF, Rosenberg IH. Folate-vitamin B-12 interaction concerning cognitive impairment, anemia, and biochemical indicators of vitamin B-12 deficiency. Am J Clin Nutr 2009;89:S702-706.
19. Yajnik CS, Deshpande SS, Jackson AA, Refsum H, Rao S, Fisher DJ, *et al*. Vitamin B12 and folate concentrations during pregnancy and insulin resistance in the offspring: The Pune maternal nutrition study. Diabetologia 2008;51:29-38.
20. Bahous RH, Jadavji NM, Deng L, Cosín-Tomás M, Lu J, Malysheva O, *et al*. High dietary folate in pregnant mice leads to pseudo-MTHFR deficiency and altered methyl metabolism, with embryonic growth delay and short-term memory impairment in offspring. Hum Mol Genet 2017;26:888-900.
21. Vinaykumar N, Kumar A, Quadros LS, Prasanna LC. Determining the effect of folate diets during pregnancy and lactation on neurobehavioral changes in adult life of offspring. J Taibah Univ Med Sci 2019;14:523-30. [Doi: 10.1016/j.jtumed.2019.09.009].
22. Lucock M, Yates Z. Folic acid - vitamin and panacea or genetic time bomb? Nat Rev Genet 2005;6:235-40.
23. Christensen B, Arbour L, Tran P, Leclerc D, Sabbaghian N, Platt R, *et al*. Genetic polymorphisms in methylenetetrahydrofolate reductase and methionine synthase, folate levels in red blood cells, and risk of neural tube defects. Am J Med Genet 1999;84:151-7.
24. Rai AK, Singh S, Mehta S, Kumar A, Pandey LK, Raman R. MTHFR C677T and A1298C polymorphisms are risk factors for Down's syndrome in Indian mothers. J Hum Genet 2006;51:278-83.
25. Smith AD, Kim YI, Refsum H. Is folic acid good for everyone? Am J Clin Nutr 2008;87:517-33.
26. Valera-Gran D, García de la Hera M, Navarrete-Muñoz EM, Fernandez-Somoano A, Tardón A, Julvez J, *et al*. Folic acid supplements during pregnancy and child psychomotor development after the first year of life. JAMA Pediatr 2014;168:e142611.
27. Achón M, Alonso-Aperte E, Reyes L, Ubeda N, Varela-Moreiras G. High-dose folic acid supplementation in rats: Effects on gestation and the methionine cycle. Br J Nutr 2000;83:177-83.
28. Zhao Y, Huang G, Chen S, Gou Y, Dong Z, Zhang X. Folic acid deficiency increases brain cell injury via autophagy enhancement after focal cerebral ischemia. J Nutr Biochem 2016;38:41-9.
29. Roncalés M, Achón M, Manzarbeitia F, Maestro de las Casas C, Ramírez C, Varela-Moreiras G, *et al*. Folic acid supplementation for 4 weeks affects liver morphology in aged rats. J Nutr 2004;134:1130-3.
30. Chittiboyina S, Chen Z, Chiorean EG, Kamendulis LM, Hocevar BA. The role of the folate pathway in pancreatic cancer risk. PLoS One 2018;13:e0193298.
31. Cebrian C, Asai N, D'Agati V, Costantini F. The number of fetal nephron progenitor cells limits ureteric branching and adult nephron endowment. Cell Rep 2014;7:127-37.
32. Black MJ, Briscoe TA, Constantinou M, Kett MM, Bertram JF. Is there an association between level of adult blood pressure and nephron number or renal filtration surface area? Kidney Int 2004;65:582-8.

Review Article

Nervi Terminalis ("0" Pair of Cranial Nerve) Revisited from Fishes to Humans

Abstract

According to classical teaching in medical colleges and institutes, there are 12 pairs of cranial nerves, attached to the brain. They are numbered in Roman numerals from I to XII in the craniocaudal order of their attachment on the brain. In fact, there are 13 pairs of cranial nerves, the one which is not taught is the nervus terminalis (NT), i.e., "0" pair of cranial nerve. It is attached rostral to all other cranial nerves. Although it has been clearly identified as an additional nerve in the vertebrate species including humans for more than a century, its functional role is also understood to some extent. Still, it could not find its place in the standard textbooks of anatomy. It has also been given different names, viz., nerve of Pinkus, NT, cranial nerve "0," cranial nerve nulla, terminal nerve, and cranial nerve XIII.

Keywords: *Crania nerve XIII, cranial nerve "0," gonadotropin-releasing hormone, luteinizing hormone-releasing hormone, nervus terminalis, pheromones, reproductive behavior*

Rashi Singh, Gaurav Singh[1], Vishram Singh[2]

Department of Paedodontics and Preventive Dentistry, Santosh Dental College, Santosh Deemed to be University, NCR-Delhi, [1]Medicine and Life Sciences, Springer Nature, New Delhi, [2]Department of Anatomy KMC Manglore, MAHE Manipal, Karnataka, India

Introduction

The nervus terminalis (cranila nerve 0) is a tiny cranial nerve located rostral to the olfactory nerve. Its fibers are independent of those of septal nerve from vomeronasal organ and olfactory nerve from olfactory epithelium.

In lower vertebrates, it is made up of a single large bundle of nerve fibers, while in humans, it is made up of a plexus of nerve bindles lying on the gyrus rectus on the orbital surface of frontal lobe of cerebral hemisphere medial to olfactory bulb. It consists of unmyelinated fibers that arise from minute ganglia lying near the lamina terminalis. Anteriorly, the fibers of nervus terminalis (NT) pass through cribriform plate of ethmoid medial to the filaments of olfactory nerve to enter nasal cavity, where it ends in the nasal mucosa.

History

The NT was first described by a German scientist Fritsch G in 1878[1] in dogfish shark. They also showed it in labeled the drawing of the brain and labeled it as "uverzahliger nerve" [Figure 1]. This term stands for "supernumery nerve."

Later, it was described in detail by Pinkus in 1895[2] and was subsequently named as nerve of Pinkus.

Ten years later, Locy[3] described this nerve in detail in selachians and named it as NT.

It was first identified in human fetuses by Larsell in 1950[4] and in adult humans by Brookover and Johnston in 1914.[5,6]

In 1987, Demski and Schwanzel-Fukuda[7] named this nerve as cranial nerve zero because it was attached rostral to all other (12) cranial nerves. Since there is no numeral for "0" in the Roman numbering system; all the cranial nerves should be renumbered with NT, which has been done long back in the past.[8] In this way, NT will become cranial nerve I. Since the earlier numbering system is so well established that any change in it will not seem prudent to readers, and hence it was numbered as cranial XIII.

Further, there is no symbol for zero in the Roman numbering system, similar to that of Indian and Arabic zero. For this reason, the Vilensky[9] suggested that NT should be named as cranial nerve nulla (Latin word *null* = none to symbolize).

The NT was a common finding in adult humans Fuller GN and Burger PC, 1990[10] and Fields R.D., 2007[11]

How to cite this article: Singh R, Singh G, Singh V. Nervi terminalis ("0" pair of cranial nerve) revisited from fishes to humans. J Anat Soc India 2020;69:53-6.

Article Info

Received: 11 January 2020
Accepted: 18 February 2020
Available online: 11 April 2020

Address for correspondence:
Dr. Vishram Singh, OC-5/103, 1st Floor, Orange County Society, Ahinsa Khand-I, Indirapuram, Ghaziabad, Delhi - 201 014, India.
E-mail: drvishramsingh@gmail.com

Access this article online

Website: www.jasi.org.in
DOI: 10.4103/JASI.JASI_2_20
Quick Response Code:

Structure

The NT ("0" pair of cranial nerve) is present bilaterally as minute plexus of unmyelinated peripheral nerve bundles in the subarachnoid space on the orbital surface of the frontal lobe of the cerebral hemisphere lying on the gyrus rectus[11] [Figure 2]. These bundles consist of both unmyelinated autonomic and sensory nerve fibers. According to Pearson, 1941,[12] and Larsell, 1950,[4] the autonomic fibers reach the Bowman's glands and nasal blood vessels.

The fibers are NT that arises from minute ganglia lying on cribriform plate of ethmoid near the lamina terminalis. These ganglia give rise to both afferent and efferent fibers.

The fibers of NT pass anteriorly through foramina of cribriform plate, medial to fila of olfactory nerve to enter the nasal cavity, where it runs along the side of nasal septum with olfactory and nasopalatine nerves to supply the Bowman's glands and blood vessels within the nasal mucosa.

Posteriorly, the fibers of NT pass to the region of olfactory trigone, medial olfactory gyrus, and lamina terminalis.[3,11]

Embryology

From the beginning of the 20th century, numerous studies have been done regarding the origins and stages of olfactory structures in human beings.[12-16] According to these studies, the fibers of NT are of neural crest origin and migrate from the olfactory placode area to the nasal and cranial brain area.

These fibers of neural crest origin contribute to the gonadotropin-releasing hormone (GnRH)-secreting neurons. Further, the NT plays an important role in GnRH-I neuronal migration independent of olfactory and vomeronasal connections to the olfactory bulbs.[17,18] The origin of nerve fibers from neural crest cells was confirmed using immunoperoxidase staining for S-100 protein a marker. In 1980, the Schwanzel-Fukuda and Silverman[19] demonstrated immune reactive luteinizing hormone-releasing hormone (LHRH) in neurons in the ganglia of NT, but LHRH-like immunoreactivity was not found in the olfactory and vomernosal nerves. This clearly showed that LHRH (an analog of GnRH) containing neurons of NT belongs to separate system than that of olfactory system.

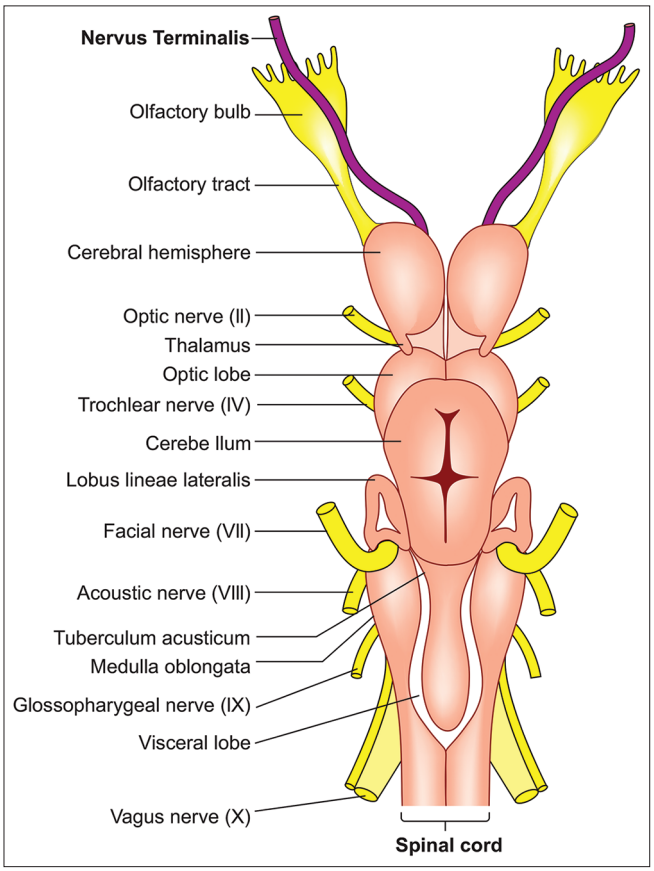

Figure 1: Nervus terminalis shown on the ventral aspect of a dogfish brain

Functions

In 1983, Demski and Northcutt[20] suggested that in dogfish, the NT is a primary chemosensory pathway for mediating a response to sexual pheromones.

In 1987, Wirsig and Leonard[21] stated that the transaction of NT in male hamsters decreases frequency of mating and increases the number of intromissions for ejaculation.

According to Whitlock,[17] the NT has a neuromodulatory role and modulates the pheromone-mediated sexual behavior. They further supported the view that the neuromodulatory cells of NT arise from neural crest cells. According to Fields, 2007,[10] this nerve is very important with regard to pheromones and sex behavior.

The NT also plays an important role in the development and maturation of hypothalamic–pituitary–gonadal axis.[11,22]

The NT releases LHRH or GnRH which causes the pituitary gland to secrete luteinizing hormone (LH) and follicle-stimulating hormone (FSH) in female and testosterone in males.[23,24]

It was also noted that if NT is interrupted, the changes are seen in the development of gonads and sexual behavior of the individual.

Discussion

According to the current standard textbooks of anatomy such as Gray's Anatomy,[25] Gray's Anatomy,[26] Gray's Anatomy for Students,[27] there are only 12 pairs of cranial nerves in human beings, but recently, a new cranial nerve called NT has been discovered by the scientists.

The NT provides a special chemosensory pathway of olfaction and affects the secretion of LH-releasing factor from the hypothalamus. The NT probably also plays an important role in smell (pheromones)-mediated sex

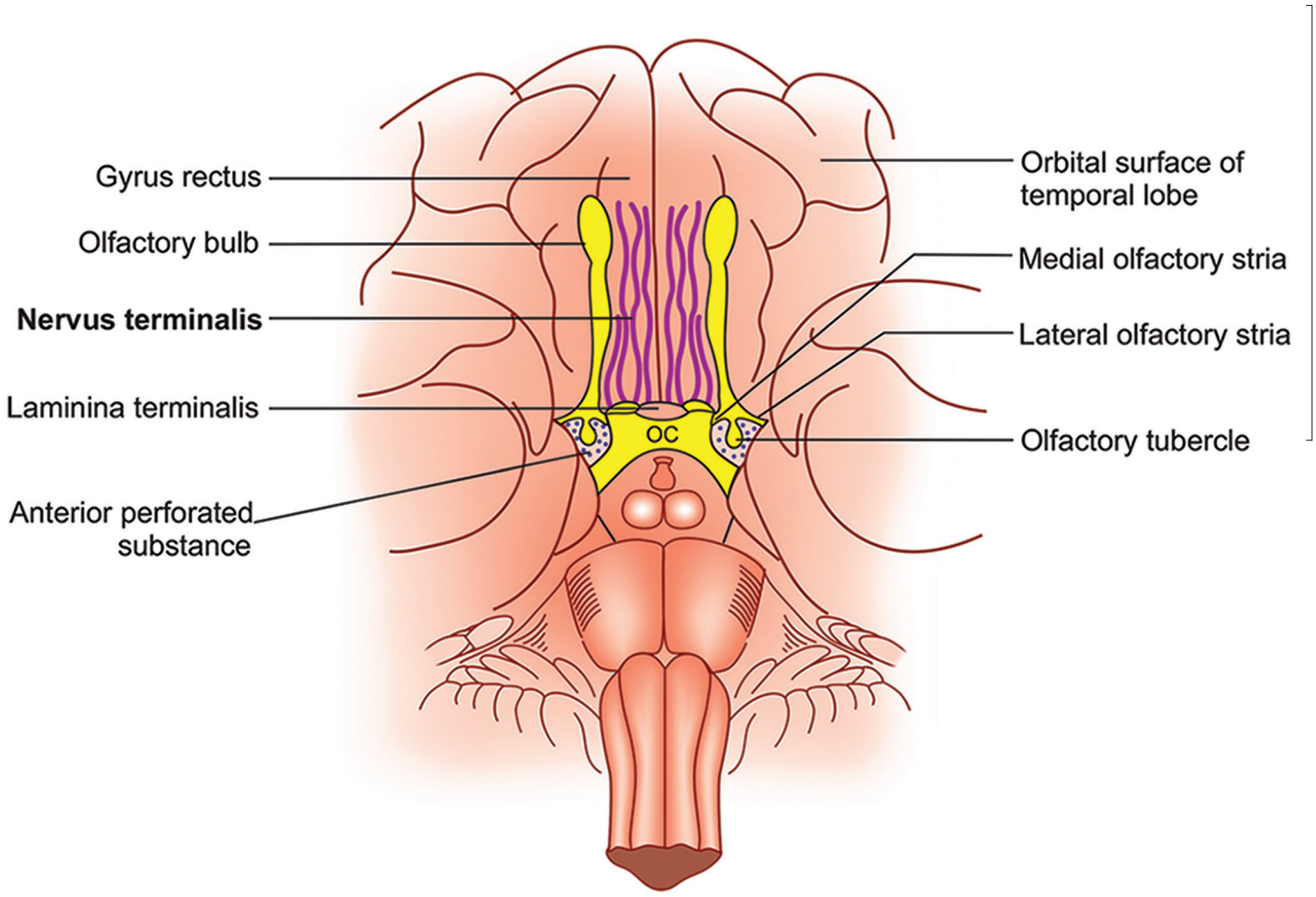

Figure 2: Bilateral plexus of nerve fascicles of nervus terminalis covering the gyrus rectus of the human brain

behavior.[28] The women's sense of smell is most acute when they are ovulating or when living together.[29] Since caudally, the fibers of NT project to the medial and lateral septal nuclei and preoptic areas. All these areas are known to be involved in regulating sexual behavior in mammals.[10]

Recently, it has been confirmed that an inconspicuous group of neurons called "kisspeptin (KP) neuronal network" is present in the above-mentioned areas.[30,31]

The "KP neuronal network" induces GnRH secretion from the hypothalamus which in turn regulates the secretion of LH and FSH. These hormones influence the synthesis and release of sex steroids from the gonads. This nerve provides a route through which pheromones are processed, i.e. play an important role in smell-mediated sexual behavior.[32] Further research work is required using newer techniques such as transmission electron microscopy and immunohistochemistry to further unfold the intricacies of its structure and function.

Clinical correlation

The nerve fibers of NT are extremely thin and hence torn inadvertently while exposing the brain.[14] Therefore, very careful dissection is required during surgery to visualize this nerve. This poses a big challenge to neurosurgeons and ENT surgeons during surgical procedures to avoid the laceration of NT. If NT is damaged during these procedures, it will lead to change in the reproductive behavior of an individual. Further, it may also cause GnRH deficiencies associated with Kallmann syndrome,[30] a clinical condition characterized by delayed puberty and an impaired sense of smell.

Conclusion

The NT is no more an enigmatic cranial nerve. It is present bilaterally in human beings. However, it is often not seen during routine classroom dissection by students, during autopsies by forensic experts, and during surgical procedures by surgeons because it is too thin and hence often torn with dura while exposing the brain.[33] The NT is involved in the release of GnRH from hypothalamus which plays an important role in the development of gonads and probably in smell-mediated sexual behavior of an individual.

Considering the presence and significance of NT in humans, this nerve deserves to be included in the standard textbooks of anatomy, neuroanatomy, and ENT and taught to the medical students.

Financial support and sponsorship

Nil.

Conflicts of interest

There are no conflicts of interest.

References

1. Fritsch G. Studies on the fieneren construction of the Fish brain with special consideration of homologies in other vertebrate classes. Berlin: Publishing house of the Gutmann'schen bookstore; 1878.
2. Pinkus F. The cranial nerves of the protopterus annectens. Morph Arb 1895;4:275-346.
3. Locy WA. On a newly recognized nerve connected with the forebrain of selachians. Anat Anz 1905;26:33-63.
4. Larsell O. The nervus terminalis. Ann Otol Rhinol Laryngol 1950;59:414-38.
5. Brookover C. The nervus terminalis in adult man. J Comp Neurol 1914:24:131-5.
6. Johnston JB. The nervus terminalis in man and mammals. Anat Rec 1914;8:185-98.
7. Demski LS, Schwanzel-Fukuda M. The terminal nerve (nervus terminalis): Structure, function, and evolution. Introduction. Ann N Y Acad Sci 1987;519:ix-xi.
8. Shaw JP. A history of the enumeration of the cranial nerves by European and British anatomists from the time of Galen to 1895, with comments on nomenclature. Clin Anat 1992:5:466-84.
9. Vilensky JA. The neglected cranial nerve: Nervus terminalis (cranial nerve N). Clin Anat 2014;27:46-53.
10. Fuller GN, Burger PC. Nervus terminalis (cranial nerve zero) in the adult human. Clin Neuropathol 1990;9:279-83.
11. Fields RD. Sex and the secret nerve. Sci Am Mind 2007;18:20-7.
12. Pearson AA. The development of the nervus terminalis in man. J Comp Neurol 1941;75:39-66.
13. Bossy J. Development of olfactory and related structures in staged human embryos. Anat Embryol (Berl) 1980;161:225-36.
14. Wirsig-Wiechmann CR, Wiechmann AF, Eisthen HL. What defines the nervus terminalis? Neurochemical, developmental, and anatomical criteria. Prog Brain Res 2002;141:45-58.
15. Müller F, O'Rahilly R. Olfactory structures in staged human embryos. Cells Tissues Organs 2004;178:93-116.
16. Whitlock KE, Wolf CD, Boyce ML. Gonadotropin-releasing hormone (GnRH) cells arise from cranial neural crest and adenohypophyseal regions of the neural plate in the zebrafish, Danio rerio. Dev Biol 2003;257:140-52.
17. Whitlock KE. Development of the nervus terminalis: Origin and migration. Microsc Res Tech 2004;65:2-12.
18. Taroc EZM, Prasad A, Lin JM, Forni PE. The terminal nerve plays a prominent role in GnRH-1 neuronal migration independent from proper olfactory and vomeronasal connections to the olfactory bulbs. Biol Open 2017;6:1552-68.
19. Schwanzel-Fukuda M, Silverman AJ. The nervus terminalis of the guinea pig: A new luteinizing hormone-releasing hormone (LHRH) neuronal system. J Comp Neurol 1980;191:213-25.
20. Demski LS, Northcutt RG. The terminal nerve: A new chemosensory system in vertebrates? Science 1983;220:435-7.
21. Wirsig CR, Leonard CM. Terminal nerve damage impairs the mating behavior of the male hamster. Brain Res 1987;417:293-303.
22. Wirsig-Wiechmann CR, Wiechmann AF. Vole retina is a target for gonadotropin-releasing hormone. Brain Res 2002;950:210-7.
23. Kiernan JA. Barr's The Human Nervous System: An Anatomical Viewpoint. 9th ed. Baltimore, MD: Lippincott Williams & Wilkins; 2009.
24. Sonne J, Lopez-Ojeda W. Neuroanatomy, Cranial Nerve O (Terminal Nerve). StatPearls: Publishing Treasure Island (FL); 2019.
25. Standring S. Gray's Anatomy: The Anatomical Basis of Clinical Practice. 41st ed. London: Elsevier; 2016.
26. Moore KL, Dalley AF, Agur AMR. Clinically Oriented Anatomy. 5th ed. Lippincott: Williams and Wilkins Baltimore; 2006.
27. Drake RL, Yogi AW, Mitchell AWN. Gray's Anatomy for Students. 2nd ed. Philadelphia: Churchill Livingstone, Elsevier; 2010.
28. Singh V. Textbook of Clinical Anatomy. 3rd ed. India: Elsevier, Relx India; 2016. p. 90.
29. Herz R. The Scent of Desire. New York: Harper Collins; 2007.
30. Mikkelsen JD, Simonneaux V. The neuroanatomy of the kisspeptin system in the mammalian brain. Peptides 2009;30:26-33.
31. Lehman MN, Hileman SM, Goodman RL. Neuroanatomy of the kisspeptin signaling system in mammals: Comparative and developmental aspects. Adv Exp Med Biol 2013;784:27-62.
32. Baum MJ, Bakker J. Roles of sex and gonadal steroids in mammalian pheromonal communication. Front Neuroendocrinol 2013;34:268-84.
33. Bordoni B, Zanier E. Cranial nerves XIII and XIV: Nerves in the shadows. J Multidiscip Healthc 2013;6:87-91.

The Editorial Process

A manuscript will be reviewed for possible publication with the understanding that it is being submitted to Journal of the Anatomical Society of India alone at that point in time and has not been published anywhere, simultaneously submitted, or already accepted for publication elsewhere. The journal expects that authors would authorize one of them to correspond with the Journal for all matters related to the manuscript. All manuscripts received are duly acknowledged. On submission, editors review all submitted manuscripts initially for suitability for formal review. Manuscripts with insufficient originality, serious scientific or technical flaws, or lack of a significant message are rejected before proceeding for formal peer-review. Manuscripts that are unlikely to be of interest to the Journal of the Anatomical Society of India readers are also liable to be rejected at this stage itself.

Manuscripts that are found suitable for publication in Journal of the Anatomical Society of India are sent to two or more expert reviewers. During submission, the contributor is requested to provide names of two or three qualified reviewers who have had experience in the subject of the submitted manuscript, but this is not mandatory. The reviewers should not be affiliated with the same institutes as the contributor/s. However, the selection of these reviewers is at the sole discretion of the editor. The journal follows a double-blind review process, wherein the reviewers and authors are unaware of each other's identity. Every manuscript is also assigned to a member of the editorial team, who based on the comments from the reviewers takes a final decision on the manuscript. The comments and suggestions (acceptance/ rejection/ amendments in manuscript) received from reviewers are conveyed to the corresponding author. If required, the author is requested to provide a point by point response to reviewers' comments and submit a revised version of the manuscript. This process is repeated till reviewers and editors are satisfied with the manuscript.

Manuscripts accepted for publication are copy edited for grammar, punctuation, print style, and format. Page proofs are sent to the corresponding author. The corresponding author is expected to return the corrected proofs within three days. It may not be possible to incorporate corrections received after that period. The whole process of submission of the manuscript to final decision and sending and receiving proofs is completed online. To achieve faster and greater dissemination of knowledge and information, the journal publishes articles online as 'Ahead of Print' immediately on acceptance.

Clinical trial registry

Journal of the Anatomical Society of India favors registration of clinical trials and is a signatory to the Statement on publishing clinical trials in Indian biomedical journals. Journal of the Anatomical Society of India would publish clinical trials that have been registered with a clinical trial registry that allows free online access to public. Registration in the following trial registers is acceptable: http://www.ctri.in/; http://www.actr.org.au/; http://www.clinicaltrials.gov/; http://isrctn.org/; http://www.trialregister.nl/trialreg/index.asp; and http://www.umin.ac.jp/ctr. This is applicable to clinical trials that have begun enrollment of subjects in or after June 2008. Clinical trials that have commenced enrollment of subjects prior to June 2008 would be considered for publication in Journal of the Anatomical Society of India only if they have been registered retrospectively with clinical trial registry that allows unhindered online access to public without charging any fees.

Authorship Criteria

Authorship credit should be based only on substantial contributions to each of the three components mentioned below:

1. Concept and design of study or acquisition of data or analysis and interpretation of data;
2. Drafting the article or revising it critically for important intellectual content; and
3. Final approval of the version to be published.

Participation solely in the acquisition of funding or the collection of data does not justify authorship. General supervision of the research group is not sufficient for authorship. Each contributor should have participated sufficiently in the work to take public responsibility for appropriate portions of the content of the manuscript. The order of naming the contributors should be based on the relative contribution of the contributor towards the study and writing the manuscript. Once submitted the order cannot be changed without written consent of all the contributors. The journal prescribes a maximum number of authors for manuscripts depending upon the type of manuscript, its scope and number of institutions involved (vide infra). The authors should provide a justification, if the number of authors exceeds these limits.

Contribution Details

Contributors should provide a description of contributions made by each of them towards the manuscript. Description should be divided in following categories, as applicable: concept, design, definition of intellectual content, literature search, clinical studies, experimental studies, data acquisition, data analysis, statistical analysis, manuscript preparation, manuscript editing and manuscript review. Authors' contributions will be printed along with the article. One or more author should take responsibility for the integrity of the work as a whole from inception to published article and should be designated as 'guarantor'.

Conflicts of Interest/ Competing Interests

All authors of must disclose any and all conflicts of interest they may have with publication of the manuscript or an institution or product that is mentioned in the manuscript and/or is important to the outcome of the study presented. Authors should also disclose conflict of interest with products that compete with those mentioned in their manuscript.

Submission of Manuscripts

All manuscripts must be submitted on-line through the website http://www.journalonweb.com/jasi. First time users will have to register at this site. Registration is free but mandatory. Registered authors can keep track of their articles after logging into the site using their user name and password.

- If you experience any problems, please contact the editorial office by e-mail at editor@jasi.org.in

The submitted manuscripts that are not as per the "Instructions to Authors" would be returned to the authors for technical correction, before they undergo editorial/ peer-review. Generally, the manuscript should be submitted in the form of two separate files:

[1] Title Page/First Page File/covering letter:

This file should provide

1. The type of manuscript (original article, case report, review article, Letter to editor, Images, etc.) title of the manuscript, running title, names of all authors/ contributors (with their highest academic degrees, designation and affiliations) and name(s) of department(s) and/ or institution(s) to which the work should be credited, . All information which can reveal your identity should be here. Use text/rtf/doc files. Do not zip the files.
2. The total number of pages, total number of photographs and word counts separately for abstract and for the text (excluding the references, tables and abstract), word counts for introduction + discussion in case of an original article;
3. Source(s) of support in the form of grants, equipment, drugs, or all of these;
4. Acknowledgement, if any. One or more statements should specify 1) contributions that need acknowledging but do not justify authorship, such as general support by a departmental chair; 2) acknowledgments of technical help; and 3) acknowledgments of financial and material support, which should specify the nature of the support. This should be included in the title page of the manuscript and not in the main article file.
5. If the manuscript was presented as part at a meeting, the organization, place, and exact date on which it was read. A full statement to the editor about all submissions and previous reports that might be regarded as redundant publication of the same or very similar work. Any such work should be referred to specifically, and referenced in the new paper. Copies of such material should be included with the submitted paper, to help the editor decide how to handle the matter.
6. Registration number in case of a clinical trial and where it is registered (name of the registry and its URL)
7. Conflicts of Interest of each author/ contributor. A statement of financial or other relationships that might lead to a conflict of interest, if that information is not included in the manuscript itself or in an authors' form
8. Criteria for inclusion in the authors'/ contributors' list
9. A statement that the manuscript has been read and approved by all the authors, that the requirements for authorship as stated earlier in this document have been met, and that each author believes that the manuscript represents honest work, if that information is not provided in another form (see below); and
10. The name, address, e-mail, and telephone number of the corresponding author, who is responsible for communicating with the other authors about revisions and final approval of the proofs, if that information is not included on the manuscript itself.

[2] Blinded Article file: The main text of the article, beginning from Abstract till References (including tables) should be in this file. The file must not contain any mention of the authors' names or initials or the institution at which the study was done or acknowledgements. Page headers/ running title can include the title but not the authors' names. Manuscripts not in compliance with the Journal's blinding policy will be returned to the corresponding author. Use rtf/doc files. Do not zip the files. **Limit the file size to 1 MB.** Do not incorporate images in the file. If file size is large, graphs can be submitted as images separately without incorporating them in the article file to reduce the size of the file. The pages should be numbered consecutively, beginning with the first page of the blinded article file.

[3] Images: Submit good quality color images. **Each image should be less than 2 MB in size.** Size of the image can be reduced by decreasing the actual height and width of the images (keep up to 1600 x 1200 pixels or 5-6 inches). Images can be submitted as jpeg files. Do not zip the files. Legends for the figures/images should be included at the end of the article file.

[4] The contributors' / copyright transfer form (template provided below) has to be submitted in original with the signatures of all the contributors within two weeks of submission via courier, fax or email as a scanned image. Print ready hard copies of the images (one set) or digital images should be sent to the journal office at the time of submitting revised manuscript. High resolution images (up to 5 MB each) can be sent by email.

Contributors' form / copyright transfer form can be submitted online from the authors' area on http://www.journalonweb.com/jasi.

Preparation of Manuscripts

Manuscripts must be prepared in accordance with "Uniform requirements for Manuscripts submitted to Biomedical Journals" developed by the International Committee of Medical Journal Editors (October 2008). The uniform requirements and specific requirement of Journal of the Anatomical Society of India are summarized below. Before submitting a manuscript, contributors are requested to check for the latest instructions available. Instructions are also available from the website of the journal (www.jasi.org.in) and from the manuscript submission site http://www.journalonweb.com/jasi).

Journal of the Anatomical Society of India accepts manuscripts written in American English.

Copies of any permission(s)

It is the responsibility of authors/ contributors to obtain permissions for reproducing any copyrighted material. A copy of the permission obtained must accompany the manuscript. Copies of any and all published articles or other manuscripts in preparation or submitted elsewhere that are related to the manuscript must also accompany the manuscript.

Types of Manuscripts

Original articles:

These include randomized controlled trials, intervention studies, studies of screening and diagnostic test, outcome studies, cost effectiveness analyses, case-control series, and surveys with high response rate. The text of original articles amounting to up to 3000 words (excluding Abstract, references and Tables) should be divided into sections with the headings Abstract, Key-words, Introduction, Material and Methods, Results, Discussion and Conclusion, References, Tables and Figure legends.

An abstract should be in a structured format under following heads: **Introduction, Material and Methods, Results,** and **Discussion and Conclusion.**

Introduction: State the purpose and summarize the rationale for the study or observation.

Material and Methods: It should include and describe the following aspects:

Ethics: When reporting studies on human beings, indicate whether the procedures followed were in accordance with the ethical standards of the responsible committee on human experimentation (institutional or regional) and with the Helsinki Declaration of 1975, as revised in 2000 (available at http://www.wma.net/e/policy/17-c_e.html). For prospective studies involving human participants, authors are expected to mention about approval of (regional/ national/ institutional or independent Ethics Committee or Review Board, obtaining informed consent from adult research participants and obtaining assent for children aged over 7 years participating in the trial. The age beyond which assent would be required could vary as per regional and/ or national guidelines. Ensure confidentiality of subjects by desisting from mentioning participants' names, initials or hospital numbers, especially in illustrative material. When reporting experiments on animals, indicate whether the institution's or a national research council's guide for, or any national law on the care and use of laboratory animals was followed. Evidence for approval by a local Ethics Committee (for both human as well as animal studies) must be supplied by the authors on demand. Animal experimental procedures should be as humane as possible and the details of anesthetics and analgesics used should be clearly stated. The ethical standards of experiments must be in accordance with the guidelines provided by the CPCSEA and World Medical Association Declaration of Helsinki on Ethical Principles for Medical Research Involving Humans for studies involving experimental animals and human beings, respectively). The journal will not consider any paper which is ethically unacceptable. A statement on ethics committee permission and ethical practices must be included in all research articles under the 'Materials and Methods' section.

Study design:

Selection and Description of Participants: Describe your selection of the observational or experimental participants (patients or laboratory animals, including controls) clearly, including eligibility and exclusion criteria and a description of the source population. *Technical information*: Identify the methods, apparatus (give the manufacturer›s name and address in parentheses), and procedures in sufficient detail to allow other workers to reproduce the results. Give references to established methods, including statistical methods (see below); provide references and brief descriptions for methods that have been published but are not well known; describe new or substantially modified methods, give reasons for using them, and evaluate their limitations. Identify precisely all drugs and chemicals used, including generic name(s), dose(s), and route(s) of administration.

Reports of randomized clinical trials should present information on all major study elements, including the protocol, assignment of interventions (methods of randomization, concealment of allocation to treatment groups), and the method of masking (blinding), based on the CONSORT Statement (http://www.consort-statement.org).

Reporting Guidelines for Specific Study Designs

Initiative	Type of Study	Source
CONSORT	Randomized controlled trials	http://www.consort-statement.org
STARD	Studies of diagnostic accuracy	http://www.consort-statement.org/stardstatement.htm
QUOROM	Systematic reviews and meta-analyses	http://www.consort- statement.org/Initiatives/MOOSE/moose.pdf statement.org/Initiatives/MOOSE/moose.pdf
STROBE	Observational studies in epidemiology	http://www.strobe-statement.org
MOOSE	Meta-analyses of observational studies in epidemiology	http://www.consort- statement.org/Initiatives/MOOSE/moose.pdf

Statistics: Whenever possible quantify findings and present them with appropriate indicators of measurement error or uncertainty (such as confidence intervals). Authors should report losses to observation (such as, dropouts from a clinical trial). When data are summarized in the Results section, specify the statistical methods used to analyze them. Avoid non-technical uses of technical terms in statistics, such as 'random' (which implies a randomizing device), 'normal', 'significant', 'correlations', and 'sample'. Define statistical terms, abbreviations, and most symbols. Specify the computer software used. Use upper italics (*P* 0.048). For all *P* values include the exact value and not less than 0.05 or 0.001. Mean differences in continuous variables, proportions in categorical variables and relative risks including odds ratios and hazard ratios should be accompanied by their confidence intervals.

Results: Present your results in a logical sequence in the text, tables, and illustrations, giving the main or most important findings first. Do not repeat in the text all the data in the tables or illustrations; emphasize or summarize only important observations. Extra- or supplementary materials and technical detail can be placed in an appendix where it will be accessible but will not interrupt the flow of the text; alternatively, it can be published only in the electronic version of the journal.

When data are summarized in the Results section, give numeric results not only as derivatives (for example, percentages) but also as the absolute numbers from which the derivatives were calculated, and specify the statistical methods used to analyze them. Restrict tables and figures to those needed to explain the argument of the paper and to assess its support. Use graphs as an alternative to tables with many entries; do not duplicate data in graphs and tables. Where scientifically appropriate, analyses of the data by variables such as age and sex should be included.

Discussion: Include summary of *key findings* (primary outcome measures, secondary outcome measures, results as they relate to a prior hypothesis); *Strengths and limitations* of the study (study question, study design, data collection, analysis and interpretation); *Interpretation and implications* in the context of the totality of evidence (is there a systematic review to refer to, if not, could one be reasonably done here and now?, what this study adds to the available evidence, effects on patient care and health policy, possible mechanisms); *Controversies* raised by this study; and *Future research directions* (for this particular research collaboration, underlying mechanisms, clinical research).

Do not repeat in detail data or other material given in the Introduction or the Results section. In particular, contributors should avoid making statements on economic benefits and costs unless their manuscript includes economic data and analyses. Avoid claiming priority and alluding to work that has not been completed. New hypotheses may be stated if needed, however they should be clearly labeled as such. About 30 references can be included. These articles generally should not have more than six authors.

Review Articles:

These are comprehensive review articles on topics related to various fields of Anatomy. The entire manuscript should not exceed 7000 words with no more than 50 references and two authors. Following types of articles can be submitted under this category:

- Newer techniques of dissection and histology
- New methodology in Medical Education
- Review of a current concept

Please note that generally review articles are by invitation only. But unsolicited review articles will be considered for publication on merit basis.

Case reports:

New, interesting and rare cases can be reported. They should be unique, describing a great diagnostic or therapeutic challenge and providing a learning point for the readers. Cases with clinical significance or implications will be given priority. These communications could be of up to 1000 words (excluding Abstract and references) and should have the following headings: Abstract (unstructured), Key-words, Introduction, Case report, Discussion and Conclusion, Reference, Tables and Legends in that order.

The manuscript could be of up to 1000 words (excluding references and abstract) and could be supported with up to 10 references. Case Reports could be authored by up to four authors.

Letter to the Editor:

These should be short and decisive observations. They should preferably be related to articles previously published in the Journal or views expressed in the journal. They

should not be preliminary observations that need a later paper for validation. The letter could have up to 500 words and 5 references. It could be generally authored by not more than four authors.

Book Review: This consists of a critical appraisal of selected books on Anatomy. Potential authors or publishers may submit books, as well as a list of suggested reviewers, to the editorial office. The author/publisher has to pay INR 10,000 per book review.

Other:

Editorial, Guest Editorial, Commentary and Opinion are solicited by the editorial board.

References

References should be *numbered* consecutively in the order in which they are first mentioned in the text (not in alphabetic order). Identify references *in text*, tables, and legends by Arabic numerals in superscript with square bracket after the punctuation *marks. References cited only* in tables or figure legends should be numbered in accordance with the sequence established by the first identification in the text of the particular table or figure. Use the style of the examples below, which are based on the formats used by the NLM *in Index Medicus*. The titles of journals *should be abbreviated* according to the style used in Index Medicus. Use complete name of the journal for non-indexed journals. Avoid using abstracts as references. Information from manuscripts submitted but not accepted should be cited in the text as "unpublished observations" with written permission from the source. Avoid citing a "personal communication" unless it provides essential information not available from a public source, in which case the name of the person and date of communication should be cited in parentheses in the text. The commonly cited types of references are shown here, for other types of references such as newspaper items please refer to ICMJE Guidelines (http://www.icmje.org or http://www.nlm.nih.gov/bsd/uniform_requirements.html).

Articles in Journals

1. Standard journal article (for up to six authors): Parija S C, Ravinder PT, Shariff M. Detection of hydatid antigen in the fluid samples from hydatid cysts by co-agglutination. Trans. R.Soc. Trop. Med. Hyg.1996; 90:255–256.
2. Standard journal article (for more than six authors): List the first six contributors followed by *et al*.

Roddy P, Goiri J, Flevaud L, Palma PP, Morote S, Lima N. *et al*., Field Evaluation of a Rapid Immunochromatographic Assay for Detection of Trypanosoma cruzi Infection by Use of Whole Blood. J. Clin. Microbiol. 2008; 46: 2022-2027.

3. Volume with supplement: Otranto D, Capelli G, Genchi C: Changing distribution patterns of canine vector borne diseases in Italy: leishmaniosis vs. dirofilariosis. Parasites & Vectors 2009; Suppl 1:S2.

Books and Other Monographs

1. Personal author(s): Parija SC. Textbook of Medical Parasitology. 3rd ed. All India Publishers and Distributors. 2008.
2. Editor(s), compiler(s) as author: Garcia LS, Filarial Nematodes In: Garcia LS (editor) Diagnostic Medical Parasitology ASM press Washington DC 2007: pp 319-356.
3. Chapter in a book: Nesheim M C. Ascariasis and human nutrition. In Ascariasis and its prevention and control, D. W. T. Crompton, M. C. Nesbemi, and Z. S. Pawlowski (eds.). Taylor and Francis,London, U.K.1989, pp. 87–100.

Electronic Sources as reference

Journal article on the Internet: Parija SC, Khairnar K. Detection of excretory *Entamoeba histolytica* DNA in the urine, and detection of *E. histolytica* DNA and lectin antigen in the liver abscess pus for the diagnosis of amoebic liver abscess. *BMC Microbiology* 2007, **7**:41. doi:10.1186/1471-2180-7-41. http://www.biomedcentral.com/1471-2180/7/41

Tables

- Tables should be self-explanatory and should not duplicate textual material.
- Tables with more than 10 columns and 25 rows are not acceptable.
- Number tables, in Arabic numerals, consecutively in the order of their first citation in the text and supply a brief title for each.
- Place explanatory matter in footnotes, not in the heading.
- Explain in footnotes all non-standard abbreviations that are used in each table.
- Obtain permission for all fully borrowed, adapted, and modified tables and provide a credit line in the footnote.
- For footnotes use the following symbols, in this sequence: *, †, ‡, §, ‖,¶ , **, ††, ‡‡
- Tables with their legends should be provided at the end of the text after the references. The tables along with their number should be cited at the relevant place in the text

Illustrations (Figures)

- Upload the images in JPEG format. The file size should be within 1024 kb in size while uploading.
- Figures should be numbered consecutively according to the order in which they have been first cited in the text.
- Labels, numbers, and symbols should be clear and of uniform size. The lettering for figures should be large enough to be legible after reduction to fit the width of a printed column.

- Symbols, arrows, or letters used in photomicrographs should contrast with the background and should be marked neatly with transfer type or by tissue overlay and not by pen.
- Titles and detailed explanations belong in the legends for illustrations not on the illustrations themselves.
- When graphs, scatter-grams or histograms are submitted the numerical data on which they are based should also be supplied.
- The photographs and figures should be trimmed to remove all the unwanted areas.
- If photographs of individuals are used, their pictures must be accompanied by written permission to use the photograph.
- If a figure has been published elsewhere, acknowledge the original source and submit written permission from the copyright holder to reproduce the material. A credit line should appear in the legend for such figures.
- Legends for illustrations: Type or print out legends (maximum 40 words, excluding the credit line) for illustrations using double spacing, with Arabic numerals corresponding to the illustrations. When symbols, arrows, numbers, or letters are used to identify parts of the illustrations, identify and explain each one in the legend. Explain the internal scale (magnification) and identify the method of staining in photomicrographs.
- Final figures for print production: Send sharp, glossy, un-mounted, color photographic prints, with height of 4 inches and width of 6 inches at the time of submitting the revised manuscript. Print outs of digital photographs are not acceptable. If digital images are the only source of images, ensure that the image has minimum resolution of 300 dpi or 1800 x 1600 pixels in TIFF format. Send the images on a CD. Each figure should have a label pasted (avoid use of liquid gum for pasting) on its back indicating the number of the figure, the running title, top of the figure and the legends of the figure. Do not write the contributor/s' name/s. Do not write on the back of figures, scratch, or mark them by using paper clips.
- The Journal reserves the right to crop, rotate, reduce, or enlarge the photographs to an acceptable size.

Protection of Patients' Rights to Privacy

Identifying information should not be published in written descriptions, photographs, sonograms, CT scans, etc., and pedigrees unless the information is essential for scientific purposes and the patient (or parent or guardian, wherever applicable) gives informed consent for publication. Authors should remove patients' names from figures unless they have obtained informed consent from the patients. The journal abides by ICMJE guidelines:

1. Authors, not the journals nor the publisher, need to obtain the patient consent form before the publication and have the form properly archived. The consent forms are not to be uploaded with the cover letter or sent through email to editorial or publisher offices.
2. If the manuscript contains patient images that preclude anonymity, or a description that has obvious indication to the identity of the patient, a statement about obtaining informed patient consent should be indicated in the manuscript.

Sending a revised manuscript

The revised version of the manuscript should be submitted online in a manner similar to that used for submission of the manuscript for the first time. However, there is no need to submit the "First Page" or "Covering Letter" file while submitting a revised version. When submitting a revised manuscript, contributors are requested to include, the 'referees' remarks along with point to point clarification at the beginning in the revised file itself. In addition, they are expected to mark the changes as underlined or colored text in the article.

Reprints and proofs

Journal provides no free printed reprints. Authors can purchase reprints, payment for which should be done at the time of submitting the proofs.

Publication schedule

The journal publishes articles on its website immediately on acceptance and follows a 'continuous publication' schedule. Articles are compiled in issues for 'print on demand' quarterly.

Copyrights

Checklist

Covering letter

- Signed by all contributors
- Previous publication / presentations mentioned
- Source of funding mentioned
- Conflicts of interest disclosed

Authors

- Last name and given name provided along with Middle name initials (where applicable)
- Author for correspondence, with e-mail address provided
- Number of contributors restricted as per the instructions
- Identity not revealed in paper except title page (e.g. name of the institute in Methods, citing previous study as 'our study', names on figure labels, name of institute in photographs, etc.)

Presentation and format

- Double spacing
- Margins 2.5 cm from all four sides
- Page numbers included at bottom
- Title page contains all the desired information
- Running title provided (not more than 50 characters)
- Abstract page contains the full title of the manuscript
- Abstract provided (structured abstract of 250 words for original articles, unstructured abstracts of about 150 words for all other manuscripts excluding letters to the Editor)
- Key words provided (three or more)
- Introduction of 75-100 words
- Headings in title case (not ALL CAPITALS)
- The references cited in the text should be after punctuation marks, in superscript with square bracket.
- References according to the journal's instructions, punctuation marks checked
- Send the article file without 'Track Changes'

Language and grammar

- Uniformly American English
- Write the full term for each abbreviation at its first use in the title, abstract, keywords and text separately unless it is a standard unit of measure. Numerals from 1 to 10 spelt out
- Numerals at the beginning of the sentence spelt out
- Check the manuscript for spelling, grammar and punctuation errors
- If a brand name is cited, supply the manufacturer's name and address (city and state/country).
- Species names should be in italics

Tables and figures

- No repetition of data in tables and graphs and in text
- Actual numbers from which graphs drawn, provided
- Figures necessary and of good quality (colour)
- Table and figure numbers in Arabic letters (not Roman)
- Labels pasted on back of the photographs (no names written)
- Figure legends provided (not more than 40 words)
- Patients' privacy maintained (if not permission taken)
- Credit note for borrowed figures/tables provided
- Write the full term for each abbreviation used in the table as a footnote

Journal of
The Anatomical Society of India

Salient Features:

- Publishes research articles related to all aspects of Anatomy and Allied medical/surgical sciences.
- Pre-Publication Peer Review and Post-Publication Peer Review
- Online Manuscript Submission System
- Selection of articles on the basis of MRS system
- Eminent academicians across the globe as the Editorial board members
- Electronic Table of Contents alerts
- Available in both online and print form.

The journal is registered with the following abstracting partners:
Baidu Scholar, CNKI (China National Knowledge Infrastructure), EBSCO Publishing's Electronic Databases, Ex Libris – Primo Central, Google Scholar, Hinari, Infotrieve, Netherlands ISSN center, ProQuest, TdNet, Wanfang Data

The journal is indexed with, or included in, the following:
SCOPUS, Science Citation Index Expanded, IndMed, MedInd, Scimago Journal Ranking, Emerging Sources Citation Index.

Impact Factor® as reported in the 2018 Journal Citation Reports® (Clarivate Analytics, 2019): 0.168

Editorial Office:
Dr. Vishram Singh, Editor-in-Chief, JASI
OC-5/103, 1st floor, Orange County Society,
Ahinsa Khand-I, Indirapuram, Ghaziabad,
Delhi, NCR- 201014.
Email: editorjasi@gmail.com
(O) | Website: www.asiindia.in

The journal is owned and run by The Anatomical Society of India